BIOBASED CHEMICALS

from

POLYHYDROXYBUTYRATE

Jurjen Spekreijse

Thesis committee

Promotor
Prof. Dr J.P.M. Sanders
Emeritus Professor of Valorization of Plant Production Chains
Wageningen University

Co-promotors
Dr E.L. Scott
Assistant professor, Biobased Chemistry and Technology Group
Wageningen University

Prof. Dr J.H. Bitter
Professor of Biobased Chemistry and Technology
Wageningen University

Other members
Prof. Dr M.H.M. Eppink, Wageningen University
Prof. Dr J. Gascon, Delft University of Technology
Dr P.P. Pescarmona, University of Groningen
Dr R.A. Rozendal, Paques BV, Balk

BIOBASED CHEMICALS
from
POLYHYDROXYBUTYRATE

Jurjen Spekreijse

Table of contents

Introduction

1.1 Fossil dependency of the world

Our current society is built on fossil feedstocks as most of our energy requirements are fulfilled by fossil resources such as coal, oil and natural gas. These fossil resources are generally converted to CO_2 after use. For example, the primary use of fossil feedstock is to burn it to CO_2 and to use the released energy for transportation or electricity. Another use is to convert the oil into materials, plastics and chemicals. In an optimal scenario where plastics do not end up in oceans and landfills, they are reused and recycled until no more use can be found. At this stage, they are burned to CO_2 to recover energy.[1] In short, fossil resources are converted to CO_2 in various ways for our energy and product needs. This conversion of fossil feedstock has several drawbacks.

1.1.1 GLOBAL WARMING

The most important issue associated with the use of fossil feedstocks as a finite resource is global warming. The conversion of fossil feedstocks to CO_2, which is released into the atmosphere, is the main cause for global warming.[2] Global warming can be accurately quantified and the average surface air temperature (SAT) has increased by 0.64 °C to 0.69 °C between 1980 and 1999. The prediction for future increase of SAT is between 2 °C to 4.5 °C, however, values above 4.5 °C cannot be excluded.[3] On the 21st Conference of the Parties of the United Nations in 2015 it was agreed to aim at a temperature rise below 2 °C, preferably below 1.5 °C.[4]

A rise in global temperature causes a wide range of global issues ranging from extreme weather conditions to sea level rising by ice melting and water expansion. There are also effects whose consequences are not yet well understood such as the expected acidification of oceans by a pH decrease between 0.14 and 0.35 in the 21st century.[3]

1.2 Alternatives for fossil feedstocks

Alternatives to these outdated fossil resource technologies must be developed. To replace fossil feedstock for the generation of energy, there are several possible alternatives. For example, energy can be generated from sunlight, wind, waterpower, geothermal energy or from burning biomass. A combination of these resources will most likely be the optimal solution.[5]

For the production of chemicals there are fewer options, since carbon cannot be obtained from energy sources such as sunlight and wind. Since chemicals are converted to CO_2 at their end of use, CO_2 should be the starting point of a sustainable process to obtain chemicals, where a fast conversion of CO_2 to chemicals is required. Therefore, sustainable chemical production can either be achieved by direct conversion of CO_2 to chemicals or the indirect conversion of

CO_2 to biomass, which can subsequently be converted to chemicals. In contrast to chemicals obtained from fossil feedstocks, this will lead to a closed carbon cycle and prevents the global issues associated with the use of fossil feedstocks (Figure 1.1).
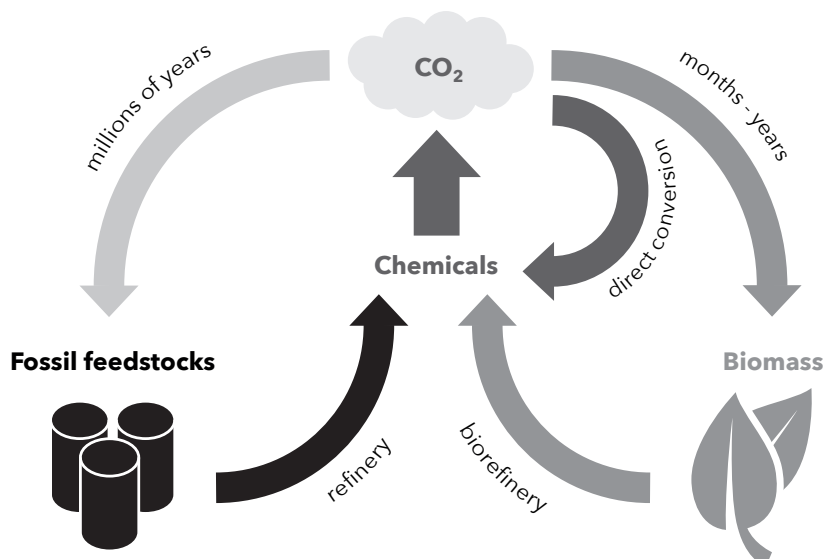

Figure 1.1. Conversion of CO2 to chemicals via biomass in years or via fossil feedstocks in millions of years.

Conversion of CO_2 to chemicals is an interesting field of chemistry and many routes have been explored. These include incorporation of CO_2 into organic molecules, copolymerisation and binding CO_2 to metal centres.[2] Some of these processes have reached commercial scale. As an example, fermentation of glucose with an incorporation of CO_2 produces succinic acid. This conversion can be performed by numerous microorganisms and to date, four companies have commercialised this process.[6]

At present, biomass is used to obtain a range of products, such as cotton, paper, wood and wool. However, to become independent from fossil resources, all polymeric materials and chemical building blocks need to be obtained from biomass. There is an argument that the use of biomass for energy and fuels would decrease food production and thereby cause an increase in food prices, which is called the food versus fuel debate.[7] However, the economics of food crops is more complicated and a simple correlation between the 400% increase in biofuel production and the price of food crops does not exist. Instead, food crop prices are directly influenced by oil prices.[8] For the production of chemicals and materials, the food versus fuel debate becomes irrelevant due to the difference in production volume. The current world plastics production is estimated at 300 million ton per year.[9] This is only 7.3% of the global production of biomass

on cultivated land (4.1 gigaton per year).[10] It should be noted that the cultivated land does not include forestry and that only a fraction of the biomass from cultivated land is suitable for consumption.

The biobased streams that can be utilised for chemical production can be divided in several categories: dedicated biobased plantations, agricultural residues, logging residues, process residues and organic wastes. Dedicated biobased plantations include switchgrass and eucalyptus plantations. Suitable land should be chosen with minimal land use change and with careful planning. Grasslands are often seen as suitable locations.[8] Agricultural residues are the remaining biomass after crop harvest, such as stalks and leaves. Logging residues consists of the unsellable branches and residues from pruning. Part of the agricultural and logging residues has to remain on the land to prevent corrosion and maintain soil organic carbon. The exact amount is dependent on the soil type and climate, but constitutes around 33% of these waste streams. Another 33% is currently used for traditional fuel and livestock feed and the other 33% currently has no use and is left on the fields. Process residues are the waste streams from agricultural and forestry industry such as husks and sawmill residues.[11] Finally, organic wastes include discarded food products, demolition wood and discarded wood products.[8] The value of these biomass streams can be improved when they are used as a feedstock for polymers and chemicals as well.

1.3 Biorefinery approach

To obtain optimal value from biomass, it is important to separate and use every part of biomass. Therefore, just as oil is refined into several fractions that all have their own range of applications, biomass could also be refined to obtain specialised fractions in a biorefinery approach. By these means, biomass can be separated in fractions that are used for chemicals, food, fuels and energy. When fossil feedstock is used, the introduction of functional groups costs large amounts of energy. In a biorefinery, this can be avoided by using the functionality already present in biomass.[12]

An example of a biorefinery is the use of distillers dried grains with solubles (DDGS), a by-product from fermentation processes in the bioethanol or alcohol beverage industries.[13] DDGS is currently used as a feed for livestock. However, using a biorefinery the components of DDGS could be used more efficiently. The carbohydrates and proteins could be separated and converted in a range of products, which includes biofuels, biopolymers, platform chemicals and packaging materials.[13] The biorefinery concept can be applied to the food and agricultural industry where the current waste streams from food production are used as feed for chemical production, which is a good starting point for the production of biobased chemicals.

1.3.1 BIOBASED CHEMICALS FROM WASTE STREAMS

Not all by-products can be as easily used for feed as DDGS. These by-products, or waste streams, are often dilute or contain poisonous components. The dilute and complex nature of these waste streams poses a challenge for a biorefinery. For example, the waste stream from pulp and paper industry contains a chemical oxygen demand (COD) from 0.8 g/L [14] to 11 g/L,[15] consisting of multiple components such as carbohydrates, lignin, resin acids and chlorinated organic molecules.[14] A method to overcome both the diverse and dilute nature of this stream is the use of microorganisms. Microorganisms are able to take up a range of carbon sources and convert them into a well-defined product. For example, cyanobacteria can convert an amino acid rich waste stream into a polypeptide consisting of aspartic acid and arginine. The polypeptide is insoluble in water and therefore the two well-defined products can be isolated from a heterogeneous and dilute mixture. The amino acids can then be used to produce nitrogen containing chemicals.[16] Another example of microorganisms converting a range of carbon sources to a well-defined product is the production of polyhydroxyalkanoate (PHA).

1.4 Polyhydroxyalkanoate

Polyhydroxyalkanoates (PHAs) are polyesters that are produced by microorganisms as means of carbon storage. These microorganisms can produce PHAs when carbon is abundant and also possess enzymes to break down the PHA to make use of the stored carbon. The abundance of bacteria that produce PHA hydrolases and PHA depolymerases is the reason that PHA is a biodegradable polymer.[17]

Polyhydroxybutyrate (PHB)   Polyhydroxyvalerate (PHV)
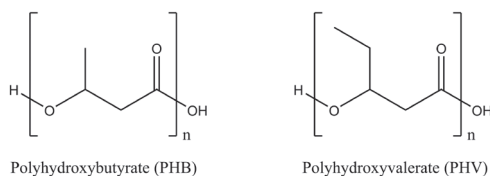
Figure 1.2. Structure of polyhydroxyalkanoates (PHAs) with on the left polyhydroxybutyrate (PHB) and on the right polyhydroxyvalerate (PHV).

PHA is a polyester that exists as a copolymer of monomers with varying alkyl side chain lengths. These side chains vary in length depending on the monomer, for example polyhydroxybutyrate (PHB, 3-hydroxybutyrate) and polyhydroxyvalerate (PHV, 3-hydroxyvalerate) (Figure 1.2). PHA is not toxic, often highly crystalline, insoluble in water, and has an isotactic structure. Due to these properties PHA was seen as a biodegradable competitor for fossil based polypropylene and first applications were aimed at packaging, coatings and disposable products.[18] These applications shifted to more high end applications in the form of medical implants and drug release carriers.[9]

Starting in the 1980s, and with research effort fluctuating with oil price, companies have produced PHAs on pilot and larger scale. Most efforts were oriented towards applications as packaging and raw materials with glucose, sucrose, fatty acids or lauric acid as starting material. The main drawbacks of PHA production from these pure starting materials are the costs involved in sterilisation of the reactors and the use of pure cultures.[19] The main advantage of a pure culture is the option to use metabolic engineering, which can enhance the production efficiency and open the pathway to alternative copolymers.[20]

1.4.1 PHA FROM WASTEWATER

To enable PHA production from wastewater, a feast-famine approach can be used (Figure 1.3). In this approach a mixed culture is treated with an abundance of nutrients in a feast phase. During this phase all microorganisms can grow. After a feast phase, a limitation in nutrients is applied during a famine phase. In the famine phase only the microorganisms that stored nutrients, in the form of PHA, can survive. Using a sequence of feast and famine phases, a selective pressure is applied for PHA producing microorganisms. This removes the need for sterile conditions and makes it possible to produce PHA from wastewater.[21] Due to the flexibility of the feast-famine approach, PHA can be generated from many different wastewater streams. Some examples include municipal wastewater, [22] wastewater from paper mills[23] and from a chocolate factory.[24]
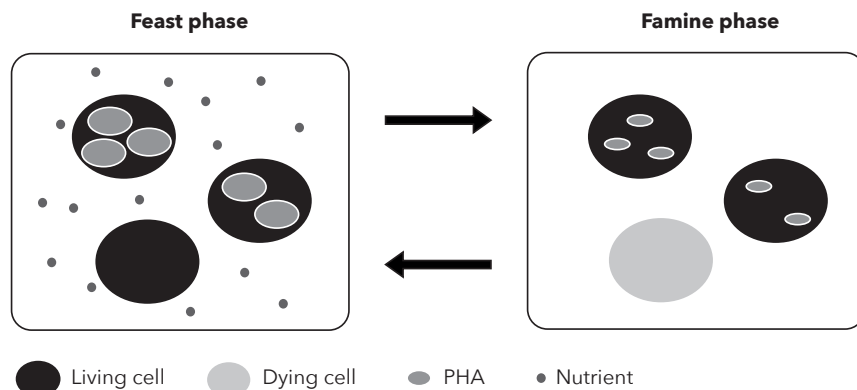
Figure 1.3. Feast-famine approach using a mixed culture with a selective pressure for PHA producing microorganisms.

Next to microorganisms, genetically engineered plants can also be a source of PHA and many plants have been shown to be capable of growing PHA and high PHA accumulation has been achieved in *Arabidopsis*. However, *Arabidopsis* has no monetary value on its own. PHA accumulation in other plants such as switchgrass (6% PHA in dry weight of the plant) and

tobacco (8.8% PHA in dry weight of the plant) did not reach the target to get an economically feasible PHA production, which is calculated to be 7.5% to 15% PHA in dry weight of the plant, without a significant reduction in biomass production. [25]

Municipal wastewater in Brussels was used for a pilot plant test for 22 months. In this experiment, the COD was converted to volatile fatty acids (VFA) in a fermentation, followed by a conversion of VFA to PHAs using the feast-famine approach. This lead to 60% to 70% removal of the COD and producing 0.4 g PHA per gram volatile suspended solids (VSS). The authors believe a production of 0.5 g PHA/g VSS is realistically achievable from Belgian municipal wastewater.[22]

A PHA production pilot plant at a chocolate factory has been shown to convert VFA into PHA using a feast-famine process. The culture was enriched with *P. acidivorans* and an average PHA content of 0.7 g PHA/g VSS was obtained. Similar experiments at lab scale would reach 0.9 g PHA/g VSS and the difference can be explained by the presence of carbon material that are not VFAs and the presence of other solids in the wastewater.[24]

Finally, wastewater from paper industry is also a suitable substrate for PHA production. With a fermentation 74% of the soluble COD in wastewater from a paper mill can be converted to VFAs. Following this pre-treatment, a feast-famine system produces PHA from the VFAs leading up to 53% PHA per VSS and removing 95% of the carbon waste from the water stream. Therefore, this system is able to produce 0.11 kg PHA per kg COD while cleaning the paper mill wastewater stream.[23]

1.4.2 PHA AVAILABILITY

To get insight in the availability of PHA with a production of 0.11 kg PHA per kg COD, an estimation can be made on the potential world production of PHAs from paper and pulp wastewater streams. The total world production of paper was 403 million ton worldwide in 2013.[26] Every ton of paper or pulp produced generates 60 m^3 of wastewater, which leads to 24,180 million m^3 wastewater, or 24.2×10^{12} L wastewater produced worldwide per year for the production of pulp and paper. Wastewater from pulp and paper contains a varying amount of carbon. Numbers range from 0.8 g/L COD[14] to 11 g/L.[15] Using these numbers, there is a total COD of 21.36×10^{12} to 292.6×10^{12} g available for the production of PHAs. For every kg COD in pulp and paper wastewater 0.11 kg PHA can be produced.[23] This means the total world production of PHA from paper and pulp ranges from 2.1 to 29 million ton per year. This is sufficient to replace up to 10% of the current world's plastic consumption using only carbon from pulp and paper wastewater streams. It is worth noting that if pulp and paper processes were to be optimised and less wastewater becomes available, a similar amount of hemicellulose will still be available for the production of PHAs. It could be advantageous to remove the hemicellulose before the paper production in order to optimise both processes.

1.4.3 ECONOMIC FEASIBILITY OF PHA

Next to their biobased nature, the success of PHA production on a commercial scale is also dependent on the economic aspect of the production process. Current commercialised PHA productions are based on pure culture fermentations, which have a high costs for the feedstock and working under sterile conditions. The cost of the carbon source contributes to 40% to 50% of the production cost of PHA.[27] This causes the prices to be in the range of 2 to 3 €/kg PHA.[28] This is significantly higher compared to fossil based polyesters such as PET, which had a market price of 1.3 €/kg in 2013.[29]

By using wastewater as a carbon source and a feast-famine approach, there is no longer a need for sterile conditions. Moreover, by purifying wastewater during the production process, wastewater treatment is avoided and can be subtracted from the production cost. These factors lead to an estimated cost of 1.4 to 2.0 €/kg PHA. This is still higher than current plastics used for applications such as packaging, however, where production processes of current plastics have been optimised for many years, the PHA production from wastewater is still a young process and further optimisation could lead to more competitive prices. These optimisations will be most effective in the downstream processing of PHA, which contributes to 70% of the total production cost. Most of the costs are due to utilities, which take up 50% to 74% of the total production cost, depending on the purification method.[30]

1.4.4 PHA IMPLEMENTATION CHALLENGES

After harvesting the microorganisms, the PHA has to be isolated from the biomass. Since the PHA is grown inside the cells in granules, the cell needs to be disrupted before the PHA can be isolated, which results in a costly process. Several types of pre-treatment have been explored for cell disruption using chemical, physical or biological breakage of the cells and care has to be taken that these methods do not negatively impact the PHA properties. Notable methods are solvent extraction, which uses the basis that PHA is water insoluble, but does dissolve in a number of organic solvents. Chemical disruption can also be used and breaks down cell matter selectively without breaking down PHA.[31] In an economic and environmental assessment it has been shown that a chemical method using sodium hydroxide and sodium dodecyl sulphate (SDS) is the most promising method for the isolation of PHA from wastewater.[30]

Moreover, there are also drawbacks when PHAs are made from waste streams using mixed cultures regarding PHA implementation. An important drawback is that waste streams have a fluctuating composition over time. Since the properties of PHAs, such as the valerate composition, depend on the composition of the waste stream, the properties of waste based PHA will not be identical from day to day. For example, the ratio of valerate to butyrate was found to vary up to 10% at pilot scale.[24] Since consistent properties are crucial in the processing and applications of polymers, such a variation causes challenges in the implementation of waste based PHA as a material. Other implementation challenges of PHA come in the form of undesired material properties. The material is stiff, brittle and does not age well. For example, the elongation at break is less than 15%, where polypropylene has an elongation at break of 400%.[32] Another

implementation issue of PHA as a polymeric material is the observed decrease in molecular weight at temperatures of 170 °C to 200 °C, which is between the melting point of PHA and the temperature at which volatile degradation can be observed.[33] These properties need to be overcome by the use of additives or polymer blends before PHAs can be processed as a material.[32]

To circumvent the challenges of the implementation of PHA from wastewater, PHA could instead be seen as an intermediate, rather than a final product. This would still benefit from the advantages of PHA production, such as the purification of wastewater, isolating the carbon for reuse and obtaining a biobased material. However, the drawbacks of PHAs, such as the fluctuating properties and implementation challenges, are circumvented. In this perspective, generating PHA is an elegant way to isolate and homogenise carbon rich waste streams for the production of biobased chemicals. Often PHB is used, since it is the most abundant form of PHA.

1.4.5 CONVERSION OF PHB TO CHEMICALS

Pyrolysis of PHB leads to the formation of crotonic acid (CA) as its major product,[34] which can be used as an intermediate to obtain chemicals from PHB. Using concentrated sulphuric acid at 100 °C leads to a CA yield of 90%. Using base lead to 3-hydroxy butyrate (3HB) to be formed as a by-product.[35] A milder catalyst in the form of magnesium hydroxide needs a higher temperature of 260 to 320 °C to obtain high yields of CA (84%).[36] The pyrolysis of PHB to CA has the advantage that it can directly be applied to biomass without prior isolation of PHB, thereby reducing the costs of downstream processing (DSP). This formation of CA from PHB has been optimised and using 310 °C 63% CA could be obtained from the pyrolysis of PHB that was not isolated from the cells.[37]

A further conversion of CA to butanol can be achieved by a reduction with hydrogen over a CuO catalyst, which leads up to 90% yield at 200 °C.[38] The conversion of CA to form both propylene and acrylic acid in a single step using ethylene and a ruthenium based metathesis catalyst has also been investigated, though lead to low turnover numbers (TONs) of 300 to 500.[39]

Isolation and purification of CA remains a challenge. Industrial processes use a distillation and crystallisation from water, which causes low yields due to the high solubility of CA in water.[40] To circumvent these purification issues, we aim at the conversion of PHB to MC, which is immiscible with water and therefore easier to purify.

1.5 Aim of this thesis: Conversion of PHB towards methyl acrylate and propylene

The aim of this thesis is to enable an economically attractive conversion of PHA to biobased chemicals by understanding the chemistry behind the conversion. PHB was chosen as it is the most abundant form of PHA produced at the pilot plant at the chocolate factory.[24] Instead of a pyrolysis to CA, we use a direct conversion of PHA to MC. MC has the advantage that it is insoluble in water, which will ease its separation from aqueous biomass streams. MC could subsequently be converted to propylene and methyl acrylate (Figure 1.4), two important monomers for the polymer industry.
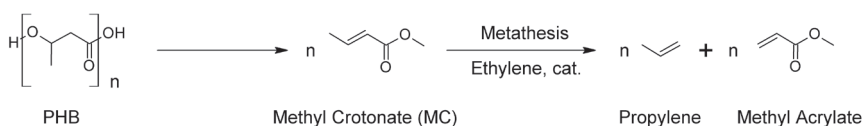

Figure 1.4. Conversion of PHB to propylene and methyl acrylate (MA) via the formation of methyl crotonate (MC).

1.5.1 THESIS OUTLINE

In chapter 2 we describe the results of a mechanistic study of the conversion of PHB (PHA with 2% 3-hydroxyvalerate monomers) to methyl crotonate. The reaction pathway was elucidated and using this knowledge, the reaction was optimised. These optimised conditions were then applied directly to un-purified biomass from a PHA pilot plant in chapter 3. Using unpurified PHA circumvents the need for expensive DSP.

In chapter 3, the influence of water, fermentation salts and the presence of valerate monomers on the chemical pathway was investigated. Understanding the influence of these factors, the extent to which the DSP can be avoided becomes evident.

MC obtained from PHA could be used directly or it could be further converted into methyl acrylate (MA) and propylene. For the conversion of MC to MA and propylene an ethenolysis is required. This is a catalytic conversion using ethylene and an expensive homogeneous ruthenium catalyst. For this method to become economically feasible, the catalyst should be recyclable. **In chapter 4** an immobilisation technique for this catalyst in metal organic frameworks (MOFs) is described to enable the reuse of the catalyst. A unique method of mechanochemical immobilisation is obtained and a mechanochemical conversion of MOFs is discovered. This conversion has however a significant influence on the activity of the catalyst.

In chapter 5, the current state of ethenolysis in literature is investigated and the bottlenecks for applying this reaction on biobased chemicals are identified. Purity of substrates appear to be crucial in order to reach economically feasible TONs.

Finally, **in chapter 6** the results and conclusions of the thesis are summarised and discussed. The implementation and application of the findings in this thesis are evaluated and an outlook for further research directions is given.

1.6 References

1. Hopewell, J.; Dvorak, R.; Kosior, E. *Philosophical transactions of the Royal Society of London. Series B, Biological sciences* **2009,** 364, (1526), 2115-26.

2. Joshi, P. B. *Int J Chem Sci* **2014,** 12, (4), 1208-1220.

3. Meehl, G. A.; Stocker, T. F.; W.D., C.; Friedlingstein, P.; Gaye, A. T.; Gregory, J. M.; Kitoh, A.; Knutti, R.; Murphy, J. M.; Noda, A.; Raper, S. C. B.; Watterson, I. G.; Weaver, A. J.; Zhao, Z. C. *Climate Change* **2007**.

4. Nations, U. *21st Conference of the Parties, Paris* **2015**.

5. Turner, J. A. *Science* **1999,** 285, 687-689.

6. Choi, S.; Song, C. W.; Shin, J. H.; Lee, S. Y. *Metabolic engineering* **2015,** 28, 223-39.

7. Searchinger, T.; Edwards, R.; Mulligan, D.; Heimlich, R.; Plevin, R. *Science* **2015,** 347, (6229), 1420-1422.

8. Rosillo-Calle, F. *Journal of Chemical Technology & Biotechnology* **2016**, n/a-n/a.

9. Chen, G. Q.; Patel, M. K. *Chemical reviews* **2012,** 112, (4), 2082-99.

10. Klass, D. L. *Biomass for Renewable Energy, Fuels, and Chemicals* **1998,** 2, 29-50.

11. Daioglou, V.; Stehfest, E.; Wicke, B.; Faaij, A.; van Vuuren, D. P. *GCB Bioenergy* **2016,** 8, (2), 456-470.

12. Scott, E.; Peter, F.; Sanders, J. *Applied microbiology and biotechnology* **2007,** 75, (4), 751-62.

13. Chatzifragkou, A.; Kosik, O.; Prabhakumari, P. C.; Lovegrove, A.; Frazier, R. A.; Shewry, P. R.; Charalampopoulos, D. *Process Biochemistry* **2015,** 50, (12), 2194-2207.

14. Lin, C.-J.; Zhang, P.; Pongprueksa, P.; Liu, J.; Evers, S. A.; Hart, P. *Environmental Progress & Sustainable Energy* **2014,** 33, (2), 359-368.

15. Thompson, G.; Swain, J.; Kay, M.; Forster, C. F. *Bioresource technology* **2001,** 77, 275-286.

16. Könst, P. M.; Scott, E. L.; Franssen, M. C. R.; Sanders, J. P. M. *Journal of Biobased Materials and Bioenergy* **2011,** 5, (1), 102-108.

17. Madison, L. L.; Huisman, G. W. *Microbiology and Molecular Biology Reviews* **1999,** 63, (1), 21-53.

18. Reddy, C. S. K.; Ghai, R.; Rashmi; Kalia, V. C. *Bioresource technology* **2003,** 87, 137-146.

19. Chen, G. Q. *Chemical Society reviews* **2009,** 38, (8), 2434-46.

20. Laycock, B.; Halley, P.; Pratt, S.; Werker, A.; Lant, P. *Progress in Polymer Science* **2013,** 38, 536-583.

21. Kleerebezem, R.; van Loosdrecht, M. C. *Current opinion in biotechnology* **2007,** 18, (3), 207-12.

22. Morgan-Sagastume, F.; Hjort, M.; Cirne, D.; Gerardin, F.; Lacroix, S.; Gaval, G.; Karabegovic, L.; Alexandersson, T.; Johansson, P.; Karlsson, A.; Bengtsson, S.; Arcos-Hernandez, M. V.; Magnusson, P.; Werker, A. *Bioresource technology* **2015,** 181C, 78-89.

23. Bengtsson, S.; Werker, A.; Christensson, M.; Welander, T. *Bioresource technology* **2008,** 99, (3), 509-16.

24. Tamis, J.; Luzkov, K.; Jiang, Y.; Loosdrecht, M. C.; Kleerebezem, R. *Journal of biotechnology* **2014,** 192PA, 161-169.

25. Somleva, M. N.; Peoples, O. P.; Snell, K. D. *Plant biotechnology journal* **2013,** 11, (2), 233-52.

26. Industrierna, S. http://www.forestindustries.se/documentation/statistics_ppt_files/international/global-paper-production-by-region **2016**.

27. Choi, J.; Lee, S. Y. *Applied microbiology and biotechnology* **1999,** 51, 13-21.

28. Jacquel, N.; Lo, C.-W.; Wei, Y.-H.; Wu, H.-S.; Wang, S. S. *Biochemical Engineering Journal* **2008,** 39, (1), 15-27.

29. Packham, I. *ICIS Chemical Bussiness,* http://www.icis.com/resources/news/2014/03/07/9760473/special-report-r-pet-uptake-is-taking-off/ **2014**.

30. Fernandez-Dacosta, C.; Posada, J. A.; Kleerebezem, R.; Cuellar, M. C.; Ramirez, A. *Bioresource technology* **2015,** 185, 368-77.

31. Madkour, M. H.; Heinrich, D.; Alghamdi, M. A.; Shabbaj, II; Steinbuchel, A. *Biomacromolecules* **2013,** 14, (9), 2963-72.

32. Bugnicourt, E. *Express Polymer Letters* **2014,** 8, (11), 791-808.

33. Grassie, N.; Murray, E. J.; Holmes, P. A. *Polymer Degradation and Stability* **1984,** 6, 95-103.

34. Grassie, N.; Murray, E. J.; Holmes, P. A. *Polymer Degradation and Stability* **1984,** 6, 47-61.

35. Chen, L. X. L.; Yu, J. *Macromolecular Symposia* **2005,** 224, (1), 35-46.

36. Ariffin, H.; Nishida, H.; Shirai, Y.; Hassan, M. A. *Polymer Degradation and Stability* **2010,** 95, (8), 1375-1381.

37. Zakaria Mamat, M. R.; Ariffin, H.; Hassan, M. A.; Mohd Zahari, M. A. K. *Journal of Cleaner Production* **2014,** 83, 463-472.

38. Schweitzer, D.; Mullen, C. A.; Boateng, A. A.; Snell, K. D. *Organic Process Research & Development* **2014,** DOI: 10.1021/op500156b.

39. Schweitzer, D.; Snell, K. D. *Organic Process Research & Development* **2014**, 141124132601002.

40. Farid, N. F. S. M.; Ariffin, H.; Mamat, M. R. Z.; Mohd Zahari, M. A. K.; Hassan, M. A. *RSC Adv.* **2015,** 5, (42), 33546-33553.
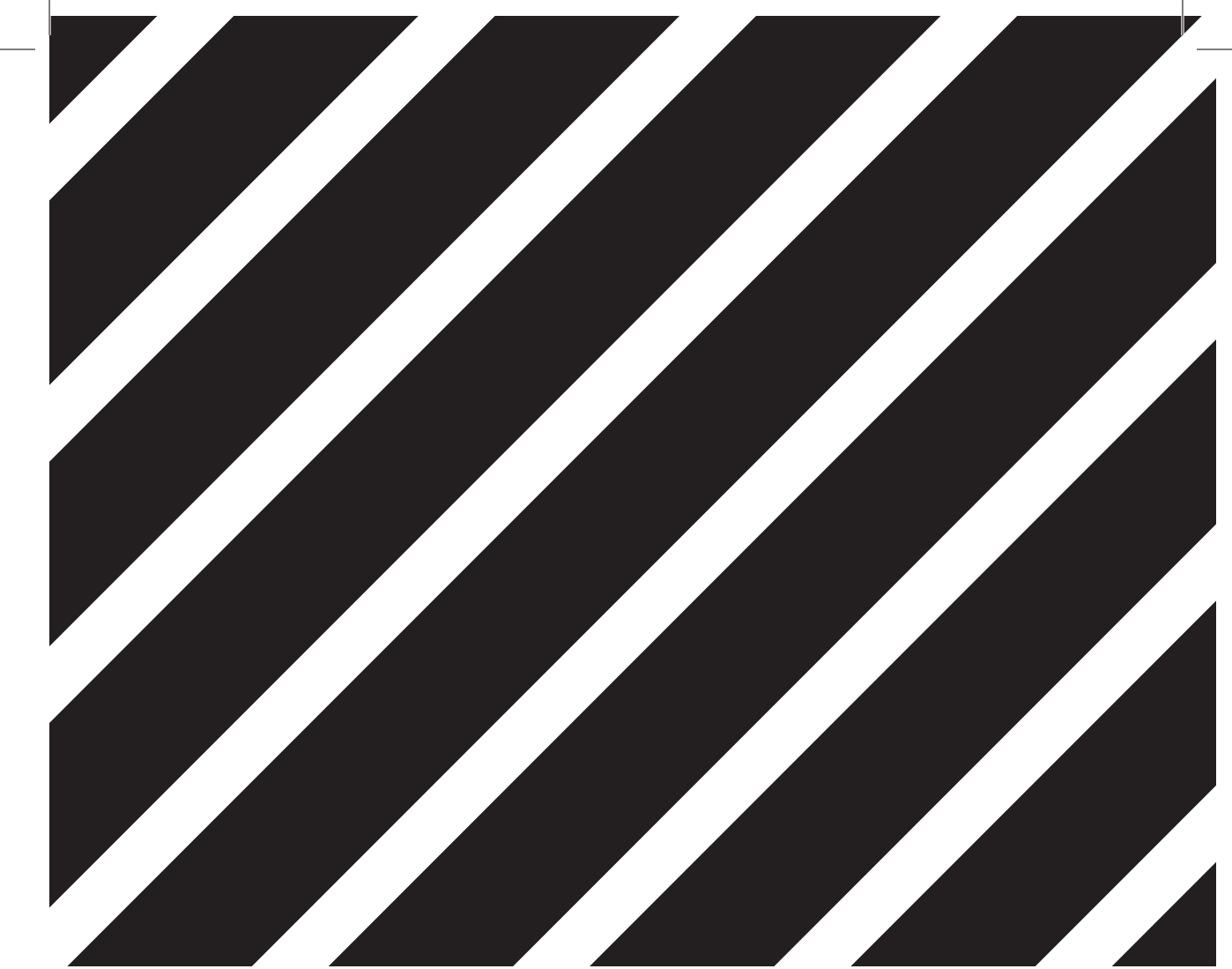
Conversion of polyhydroxybutyrate (PHB) to methyl crotonate for the production of biobased monomers

Abstract

Within the concept of the replacement of fossil with biobased resources, bacterial polyhydroxy-butyrate (PHB) can be obtained from volatile fatty acids (VFAs) from agro-food waste streams and used as an intermediate towards attractive chemicals. Here we address a crucial step in this process, the conversion of PHB to methyl crotonate (MC), which can be converted *via* cross metathesis with ethylene to methyl acrylate and propylene, two important monomers for the plastics industry. The conversion of PHB to MC proceeds *via* a thermolysis of PHB to crotonic acid (CA), followed by an esterification to MC. At pressures below 18 bar the thermolysis of PHB to CA is the rate determining step, where above 18 bar, the esterification of CA to MC becomes rate limiting. At 200 °C and 18 bar a full conversion and 60% selectivity to MC is obtained. This conversion circumvents processing and application issues of PHB as a polymer and allows PHB to be used as an intermediate to produce biobased chemicals.

2.1 Introduction

A search for a sustainable alternative for fossil based chemistry is needed due to depleting fossil resources, geopolitical instability and global warming. Biomass as a feedstock offers an alternative with a closed carbon cycle. There are two challenges to overcome when using biomass as a feedstock. The first is the heterogeneous nature of biomass, which makes it difficult to isolate desired chemicals. The second is that many biomass streams are dilute, where small amounts of valuable compounds are present in large quantities of water. To overcome these two challenges, microorganisms can be used to uniform a diverse biomass stream by making insoluble polymers. An example is cyanophycin producing bacteria, which can be used to obtain aspartic acid and ornithine, precursors of biobased acrylamide and 1,4-diaminobutane, from amino acid rich waste streams from agro industries.[1] Another example to uniform biomass streams using microorganisms is polyhydroxyalkanoates (PHA), and more specifically polyhydroxybutyrate (PHB). It has been shown that PHB originating from plants can be converted into crotonic acid (CA)[2, 3], which can be used as a precursor for biobased propylene and acrylic acid.[2] In both examples biomass is converted to drop-in chemicals, which are biobased versions of currently used chemicals that can replace their fossil based counterpart, preventing the need for developing new materials.

PHB can be obtained in several ways, since many different groups of bacteria can store carbon from biomass feedstocks to produce PHB.[4] All metabolizable carbon, ranging from CO_2[5] to crude glycerol[6], which can be used as a carbon source and PHB can also be produced in plants.[7] On a pilot and large scale, the production of PHB mainly uses glucose, sucrose, fatty acids and lauric acid as carbon sources[8] and aims to produce materials for packaging, disposables and biomedical applications. The current global production is 100.000 to 130.000 tons per year and is expected to grow 10 to 30% per year.[9] Commercialisation of PHB, however, is difficult due to high production costs originating from using pure cultures and often pure substrates and the necessity to work under sterile conditions.[10, 11]

To lower production costs, wastewater containing volatile fatty acids (VFAs) from several industries (i.e. agricultural, food, paper) can be treated in a mixed culture fermentation to generate PHB and simultaneously clean wastewater. Using wastewater as a feed lowers production costs by removing the costs for starting material and using a mixed culture removes the need for a sterilization.[10, 12, 13] An added benefit is the removal of VFAs from wastewater, removing the need for further wastewater treatment facilities. Enrichment of the culture based on natural and ecological selection results in a culture dominated by *Plasticicumulans acidivorans* with a PHB production of over 80% dry weight.[14, 15] PHB originating from a fluctuating wastewater feed, however, will result in PHB materials with varying properties, which creates challenges in creating markets for these materials. Moreover, the processing conditions of PHB (ca. 170 °C) are close to the temperature where degradation of PHB can be observed (170 to 200 °C).[16] A conversion of PHB to chemicals has been proposed by Metabolix, where PHB is converted to crotonic acid (CA) *via* pyrolysis at 200 °C using $Ca(OH)_2$ as a catalyst. The CA produced could be further converted into drop-in chemicals such as n-butanol[17], maleic anhydride and propylene.[2, 3] Converting PHB to chemicals can also be applied at the end of life of PHB products.

PHB is unsuitable for landfills where it produces methane and therefore has to be collected separately. Instead of composting the waste PHB, it can potentially generate more added value when it is converted to monomers as means of a tertiary recycling process.[18]

The pyrolysis or thermal degradation of PHB to CA has been thoroughly explored to investigate the stability of PHB. It has been shown that PHB will degrade at 170 to 200 °C [16] and above 250 °C CA and oligomers have been observed.[19, 20] Little attention, however, has been given to optimise this conversion for the preparative production of CA from PHB. Formation of CA from PHB has been shown[2, 21-23] and high conversion and selectivity can be reached when $Mg(OH)_2$ (84% of PHB converted to CA at 260 to 320 °C)[23] or concentrated acid is used (90% of PHB converted to CA at 100 °C)[21]. Without the addition of a catalyst, 63% CA can be obtained from pyrolysis at 310°C.[20]

Another well-known conversion of PHB is a transesterification of PHB in acidic methanol or butanol to form 3-hydroxybutyrates, which can be detected by mass spectrometry in order to quantify PHB, *i.e.* for quantifying PHB production in cells.[24-26] When base or more than 60% acid is used for the assay, crotonates are formed from methyl 3-hydroxybutyrate (M3HB)[24, 27] A quantitative transesterification as means to produce methyl crotonate (MC) from PHB is unknown so far.

After a conversion of PHB to CA, CA can be converted into drop-in chemicals. We previously showed that CA can be converted to acrylic acid and propylene *via* metathesis with ethylene. Metathesis on crotonates may appear to be a challenging reaction due to the near vicinity of an electron withdrawing carboxylic acid group. However, 45% to 50% conversion has been obtained under non-optimized conditions.[28, 29] The products of these reactions, acrylic acid (4.5 million ton produced worldwide per year)[30] and propylene (global demand of 50 million tons per year)[9], are important commodity chemicals for the plastics industry. Current methods to produce biobased acrylates are from the conversion of 3-hydroxypropionic acid, which can be obtained by fermentation, or from the conversion of glycerol to acrylic acid.[9] There are several pathways towards biobased acrylates that include a metathesis step. The metathesis of fumaric acid with ethylene to acrylic acid is patented, but gives low yields.[31] In a patent from Metabolix biobased acrylates are obtained from crotonates by a metathesis with propylene.[2] Moreover, microbially-derived muconic acid can be converted into biobased 1,3-butene and acrylic acid by metathesis with ethylene and has been patented by Amyris.[32] Finally, a reaction of ethylene with cinnamic acid, which could be obtained from rest streams of bioethanol production yields styrene and acrylic acid.[33] Biobased propylene can be obtained from several potential routes and commercialization of biobased propylene produced from sugarcane bioethanol has just begun with Braskem, who built a plant in 2013 with a capacity of 30.000 tons per year.[34]

Inspired by the observations of crotonate formation in the transesterification of PHB, we report the investigation of the preparative conversion of PHB to MC, which can act as a biobased substrate for the metathesis to biobased propylene and methyl acrylate (Scheme 2.1). MC production was performed in methanol in a single step, without the use of additives or a catalyst. The reaction pathway was clarified in order to optimise conversion and selectivity by varying pressure, temperature and reaction time. Converting PHB from VFA (and sugar) rich wastewater

into drop-in chemicals circumvents process and quality issues associated with PHB from waste-water. Potentially, it could also be applied as a post-use treatment of PHB, circumventing end of life challenges. Moreover, this conversion opens the route to biobased propylene and methyl acrylate, two important monomers for the plastics industry.
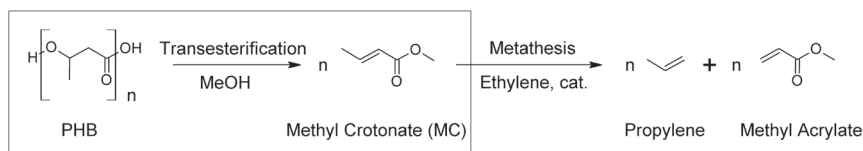
Scheme 2.1. Conversion of PHB to methyl crotonate (MC) as precursor for the productions of biobased propylene and acrylates.

2.2 Experimental

All experiments were performed in duplicate in 75 mL Parr pressure reactors (Parr multiple reactor system series 5000, 6 x 75 mL, Hastelloy C-276) equipped with glass liners and glass-coated stirring bars. Gas samples were collected from the pressure reactors with 1L PVF Tedlar Sample Bags. Nitrogen gas (Nitrogen 3.0, purity ≥99.9%) was supplied by Linde Gas Benelux. Anhydrous methanol (99.8%), crotonic acid (98%), methyl crotonate (98%), methyl (R)-(-)-3-hydroxybutyrate (99%) and DL-3-hydroxybutyric acid (as sodium salt) were purchased from Sigma-Aldrich, methyl 3-methoxybutanoate was purchased from Ambinter, and PHB was kindly provided by Technical University Eindhoven (2 mol% Polyhydroxy valerate (PHV), Mn = 450 kDa and Mw/Mn = 1.3). All chemicals were used as received.

0.6 g of starting material was loaded in a glass liner with a glass-coated stirring bar. The liner was placed in a Parr reactor and the atmosphere was purged with argon. Dry methanol was then added using a syringe while keeping the reactor under an argon flow. The reactor was closed and flushed with nitrogen and pressurised with nitrogen to the desired pressure at room temperature and heating was applied. The heating caused the pressure in the closed reactor to increase to the reported 'pressure build-up'. Typical heating times up to 200 °C took place in 20 to 30 minutes. The reaction time started when the temperature reached 200 °C. After the allocated reaction time, the reactor was allowed to cool to room temperature before being opened. The crude mixture was worked-up as follows: when solids were present, the suspension was filtered with a Büchner filter and weighed. The clear solution was passed through a 0.20 µm single use filter unit and analysed by HPLC.

2.3 Results and discussion

Thermolysis or thermal degradation of PHB to crotonic acid (CA) without the presence of methanol has been fully investigated and several mechanisms have been proposed. Grassie *et al.* were the first to propose a chain scission mechanism (CS) in which the ester bond breaks *via* an intramolecular six membered ring intermediate.[16] Kawalec *et al.* introduced the possibility of an E1cB mechanism where carboxylate end groups act as a base[35] and Ariffin *et al.* concluded that thermolysis of PHB to CA follows a combination of both mechanisms.[36] These studies were performed on degradation of dry PHB, where in our study we investigated the conversion of PHB in the presence of methanol. The addition of methanol adds an esterification step to the pathway (Scheme 2.2, route A), resulting in the formation of methyl crotonate (MC). Moreover, the presence of methanol introduces a transesterification pathway, which gives rise to the formation of methyl 3-hydroxybutyrate (M3HB), followed by a dehydration reaction to form MC (Scheme 2.2, route B). This results in two theoretical reaction pathways from PHB to MC.
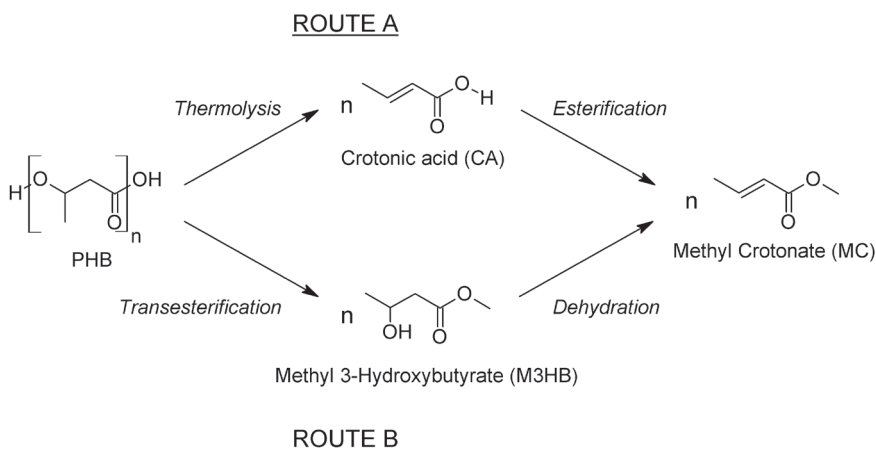
Scheme 2.2. Two possible pathways from PHB to MC.

To get insight in the influence of reactor to methanol volume ratio on the conversion of PHB to MC, initial experiments were performed with a varying amount of methanol. The amount of PHB was varied, while the ratio of PHB to methanol was kept constant (Figure 2.1). In a closed reactor, liquid methanol at 200 °C has a vapour pressure 39 bar and under these conditions, the ideal gas law predicts that ca. 3 mL methanol will be in vapour phase in a reactor volume of 75 mL. This results in a different gas to liquid ratio when various amounts of methanol are present in the reactor. Since the reactor head is cooled to 25 °C, the methanol is able to condense and flow back down to the heated part of the reactor. When the amount of methanol is reduced to 10 mL, there is not sufficient methanol present to flow down to the bottom of the reactor and a system where the methanol refluxes in the reactor head is created. In this system 3 mL methanol is in gaseous state and the remaining 7 mL is present as liquid in the dead volume of the reactor head. The highest temperature at which liquid methanol is present

determines the vapour pressure and therefor the pressure in the system reaches only 7 bar. In order to circumvent this lowering of the pressure, nitrogen can be added at the beginning of the reaction. Additional nitrogen results in a system where 10 mL of methanol can be used and liquid methanol is present at 200 °C, which results in a pressure of 39 bar. Pressure versus temperature data can be found in Figure A1, appendix A.
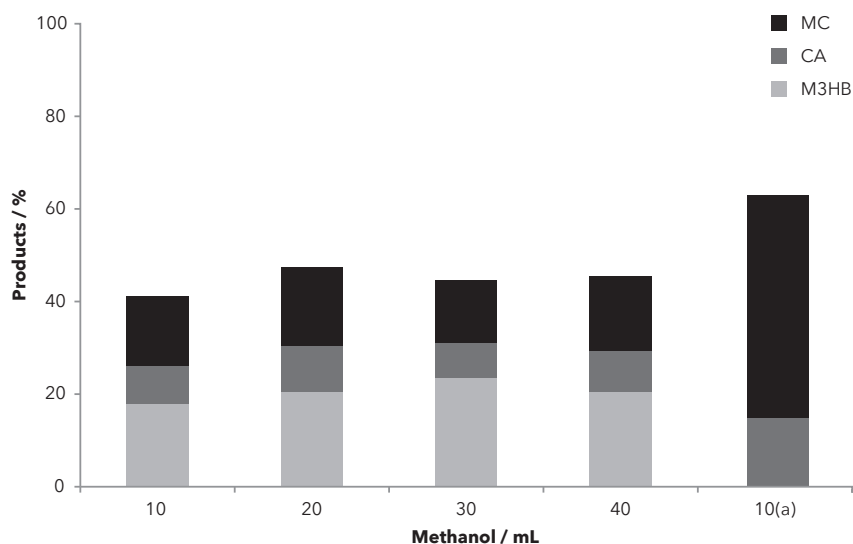
Figure 2.1. Conversion of PHB in methanol with varying amounts of methanol. Reaction conditions: 0.6 g PHB per 10 mL MeOH, t = 6 hours, pressure build-up of up to 39 bar, for 10 and 20 mL nitrogen gas was added to reach 39 bar. Average of duplicate experiments. a) p = 7 bar.

The conversion of PHB to MC is independent on the volume of methanol used, reaching 15% MC in all reactions at 39 bar (Figure 2.1). However, when 10 mL of methanol is used without added pressure and the methanol is present only in the reactor head, less M3HB is observed and the conversion to MC becomes three times higher, rising from 15% to 48%, which indicates that the pathway via M3HB (scheme 2.2, route B) is unfavourable. Based on the high conversion of PHB to MC at 10 mL methanol without added nitrogen, these conditions were further investigated.

To investigate the possibility of a catalyst free esterification step, which is necessary for formation of MC from PHB in methanol *via* the thermolysis route (Scheme 2.2, route A), CA was reacted in a closed reactor in methanol at various temperatures (Figure 2.2). The reactors were closed at an atmospheric pressure of nitrogen, which resulted in a pressure of 7 to 9 bar at the reaction temperature, this build-up of pressure is from now referred to as pressure build-up.
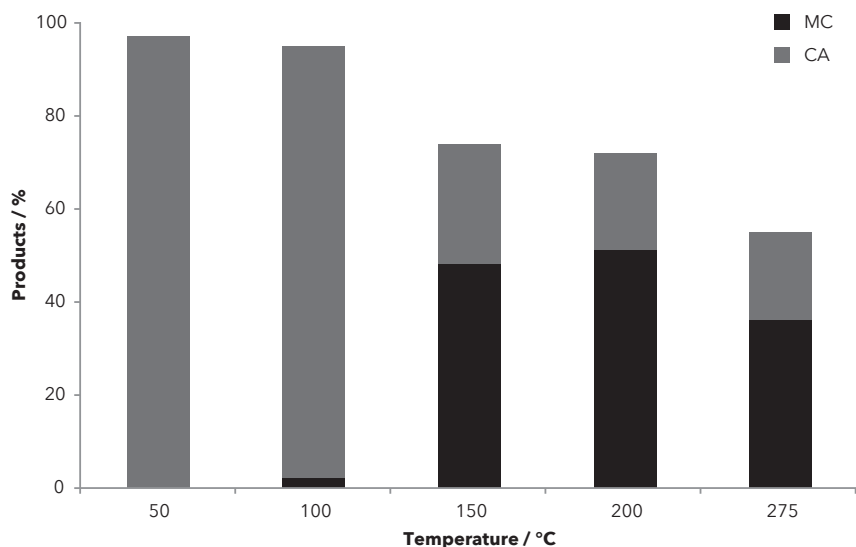
Figure 2.2. Catalyst free esterification of 0.6 g CA in 10 mL methanol at various temperatures for 6 hours, reactors closed at atmospheric pressure (pressure build up to 7-9 bar). Average of duplicate experiments.

Figure 2.2 shows that CA does not undergo esterification below 100 °C. At 150 °C a conversion to MC was observed, but increasing the temperature further had little effect on the conversion. The catalyst free esterification of CA has not been reported in literature so far. However, the catalyst free reaction of free fatty acids to esters in vegetable oils has been reported at temperatures of 200 °C [37], which is in the same temperature range of the current findings. Next to the conversion to MC, about 30% of mass was unaccounted for by HPLC. This mass can most likely be contributed to gaseous products such as propylene and CO_2 originating from the decarboxylation reaction of CA, which has already been reported to take place at 310 °C.[38] Further discussion of such degradation reactions are addressed later (Figure 2.5). To investigate the possibility of a transesterification-dehydration reaction pathway (Scheme 2.2, route B), M3HB was also subjected to the same reaction conditions (Figure 2.3).
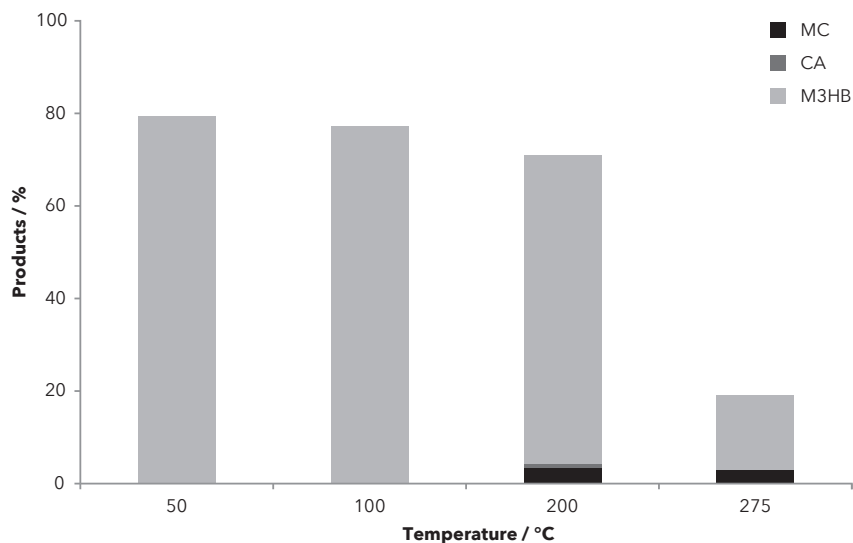
Figure 2.3. Reactivity of 0.6 g M3HB in 10 mL methanol at various temperatures for 6 hours, pressure build-up of 7-9 bar. Average of duplicate experiments.

Figure 2.3 shows that conversion of M3HB to MC or CA under these conditions is less than 5% and therefore can be neglected. The only significant conversion occurring is the degradation of M3HB to gaseous compounds, especially above 200 °C. At 50 °C, about 80% of the M3HB is recovered and at 275 °C only 16% of the M3HB could be recovered and still less than 5% crotonates are formed. The fact that no significant amounts of CA or MC can be formed from M3HB has been observed before in experiments with M3HB in gaseous form[39] and in a solution of *m*-xylene[40]. Degradation of M3HB follows a six membered ring intermediate which leads to the formation of C_2 species instead of MC.[40] Our observation that also no crotonates are formed in methanol suggests that conversion of PHB to MC cannot take place *via* a transesterification-dehydration route and therefore that the conversion of PHB to MC has to occur *via* a thermal conversion of PHB to CA followed by a catalyst free esterification to MC.

With the pathway known, the conversion of PHB to MC can be optimised. From the reactivity of CA in Figure 2.2 it is clear that no esterification takes place below a temperature of 150 °C, therefore the investigation of the temperature dependence takes place from 150 °C, which was performed in methanol in a closed reactor without additional inert gasses (Figure 2.4).
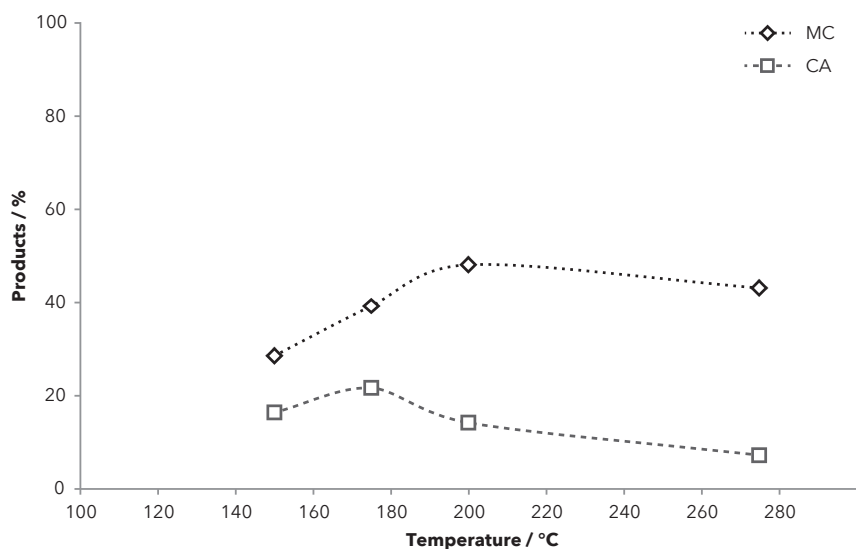
Figure 2.4. Temperature dependence of the conversion of PHB to CA and MC. Reaction conditions: 0.6 g PHB, 10 mL MeOH, pressure build-up of up to 8 bar, t = 6 hours. Average of duplicate experiments.

In Figure 2.4, it is shown that conversion of PHB starts at temperatures as low as 150 °C, a clear trend can be observed where formation of MC increases with rising temperatures up to 200 °C. Reactions at temperatures above 200 °C, however, showed a lower product formation.

The observed starting temperature of conversion (150 °C) is much lower than the minimum temperature of 270 °C reported for pyrolysis.[20] Conversions of PHB at low temperature can be achieved in watery systems with a concentrated acid or dilute base. With acid, a full conversion to CA has been observed, where base leads to a mixture of 3HB and CA.[41] In methanol the conversion of PHB has been performed at −18 °C to −24 °C using NaOH, which results in PHB oligomers.[42] However, no conversion of PHB has been reported below 190 °C without the use of an acid or base, although a lowering of the average molecular weight has been observed at these temperatures.[16] Our lower thermolysis temperature could be an effect of the higher pressure (8 bar) or the presence of methanol, since a lowering of the degradation temperature has been reported at atmospheric pressure in the presence of glycerol.[43] The lowering of degradation temperature in the presence of glycerol is explained by an alcoholysis, which is unlikely in our system due to the low amounts of M3HB formed (10%).

The rising of the conversion between 150 °C and 200 °C indicates a higher conversion of oligomeric PHB to MC and CA at higher temperatures, where the decrease in conversion above 200 °C can be explained by an increasing rate of decarboxylation of monomeric PHB fragments into gaseous compounds.

No insoluble PHB was observed after the reactions, which indicates that all PHB has been converted into small, soluble organic molecules and oligomers. At the optimal temperature of 200 °C, no oligomers were observed by the analysis of the reaction mixture with HPLC with MS and MALDI-TOF, where no oligomers were found (see appendix A). As a reference, a reaction of PHB in methanol at 100 °C for 67 hours showed a PHB conversion of 15.5% to oligomers consisting of up to 15 monomer units (see MALDI-TOF in appendix A). In a GC-MS analysis of gas recovered from the reactor head after reaction, propylene and ethylene were found, which are typical degradation products of PHB.[19] Most likely, these products are formed from decarboxylation of crotonates, which is known to be the dominant degradation pathway for CA[38] Control experiments with MC as substrate in methanol (Figure 2.5) also showed mass losses, especially at higher temperatures, which is in confirmation with the hypothesis of decarboxylation products.
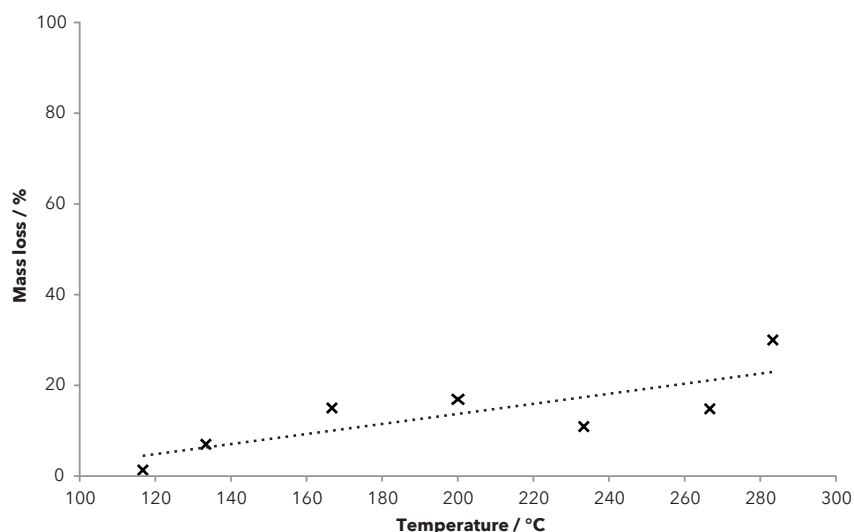
Figure 2.5. Control reaction of MC stability in methanol with a pressure build-up of 1-8 bar at different temperatures. Reaction conditions: 0.6 g MC, 10 mL MeOH, t = 6 hours. Average of duplicate experiments.

To investigate the hypothesis of decarboxylation of MC causing mass loss in the conversion of PHB, MC was exposed to the same experimental conditions as PHB. At 25 °C MC is stable and a full recovery is observed (Figure 2.5). When the temperature is increased to 50 °C, less than ten per cent of the initial mass is lost. This amount slowly increases with increasing temperature to 30% at 275 °C. These values are slightly higher than the reported literature values, where roughly 30% MC is decomposed without the presence of methanol at 480 °C after 40 minutes.[44] In comparison to the mass loss of PHB, the mass loss of MC is slightly lower (28% for PHB and 15% for MC at 200 °C). It is important to notice that CA and M3HB can also undergo decarboxylation and we observe mass loss to gaseous products for these compounds as well, which can explain this difference. (see Figure 2.2 and 2.3). A side reaction of methanol

with MC to form methyl 3-methoxybutanoate *via* a Michael addition could explain the faster loss of MC in methanol than the observed literature value without the presence of methanol.[44] The catalytic Michael addition of methanol to MC has been previously observed[45] and there are indications that at 125 to 175 °C CA can form a dimer *via* a Michael addition.[46] However, this side reaction is excluded, since this product was not detected by HPLC.

In order to determine the effect of reaction time on the conversion of PHB in methanol, *via* CA to MC, a series of experiments were performed at 200 °C and 8 bar. Figure 2.6 shows that in the first 2 hours more monomeric compounds are formed from oligomeric PHB as the sum of crotonates increases.
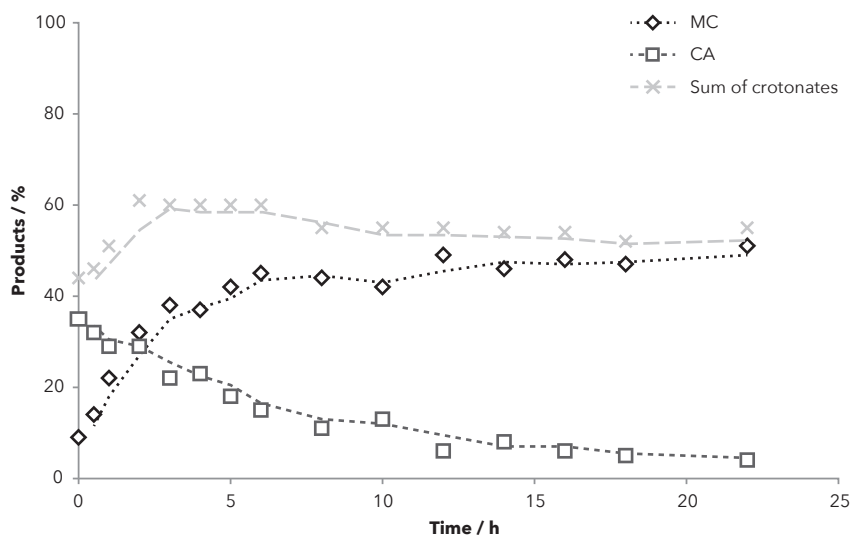
Figure 2.6. Reaction of PHB to MC at 200 °C and 8 bar of pressure build-up performed at different reaction times. The reaction at t = 0 hours was heated to 200 °C and immediately cooled to room temperature. Average of duplicate experiments.

At 8 bar, the sum of crotonates reaches a maximum of 60%, from where it slowly goes down to reach 55% after 22 hours. Figure 2.6 also shows that CA is initially formed and is converted into MC over time. Initially there is 35% CA, which goes down to 4% after 22 hours.

To study the mechanism of the conversion of PHB to MC in more detail, the reaction was run at 200 °C for 6 hours at several different pressures (Figure 2.7).
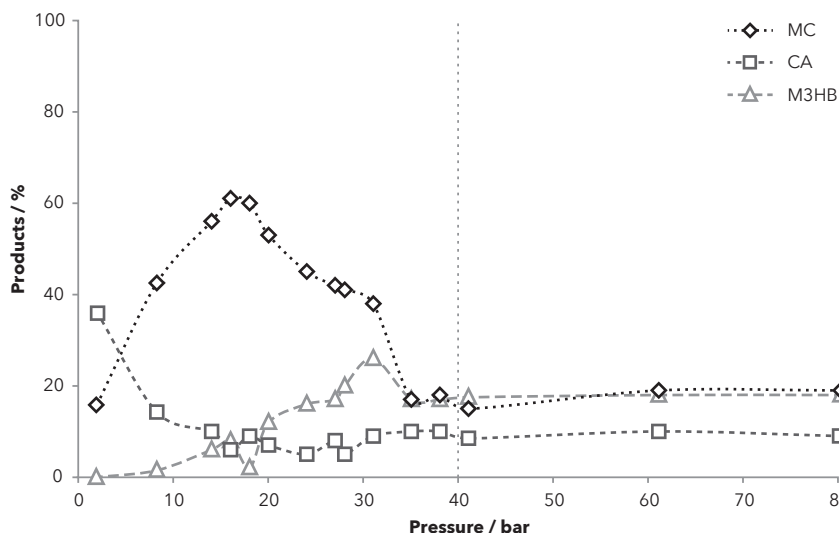
Figure 2.7. Selectivity towards MC at 200 °C at different pressures. Reaction conditions: 0.6 g PHB, 10 mL MeOH, t = 6 h. Pressure indicates the pressure build-up at the reaction temperature. The dotted line represents the vapour pressure of methanol at 200 °C. Average of duplicate experiments.

In Figure 2.7, the reaction at 2 bar of pressure build-up was obtained by putting the reactor under vacuum after cooling in an ethanol/liquid nitrogen bath to avoid methanol evaporation, followed by applying the reaction conditions. A trend can be observed where selectivity towards MC rises to a maximum of 60% at 18 bar before going down when pressure is further increased to 30 bar, and then drops rapidly to 20% above 30 bar. The rapid drop above 30 bar matches the vapour pressure of methanol at 200 °C, which means the methanol reaches the bottom of the reactor. When methanol is present in dead volumes and refluxing at the reactor head, the reaction has a higher selectivity than when methanol is reaching the PHB at the bottom of the reactor in the liquid phase.

Up to 18 bar, more MC is formed with increasing pressure, while formation of CA slowly decreases. This indicates that esterification of CA is the rate determining step (RDS) and that this step speeds up with increasing pressure. At 18 bar a sudden change in the trend is observed, where the formation of MC declines with increasing pressure, which implies that the esterification is now sufficiently fast to overtake the thermolysis, which makes the thermolysis step the RDS above 18 bar. The thermolysis slows down with increasing pressure, resulting in a lower selectivity towards MC with further increasing pressure. At higher pressures, the methanol is forced lower into the reactor and therefore more reactions between methanol and PHB takes place increasing the M3HB formation. This effect can be explained by the reaction pathway, where the transesterification of PHB to M3HB competes with the productive conversion of PHB to CA (Scheme 2.2).

To verify the hypothesis that rate determining steps depend on pressure applied during the reaction, CA was used as substrate and subjected to the same conditions (Figure 2.8).
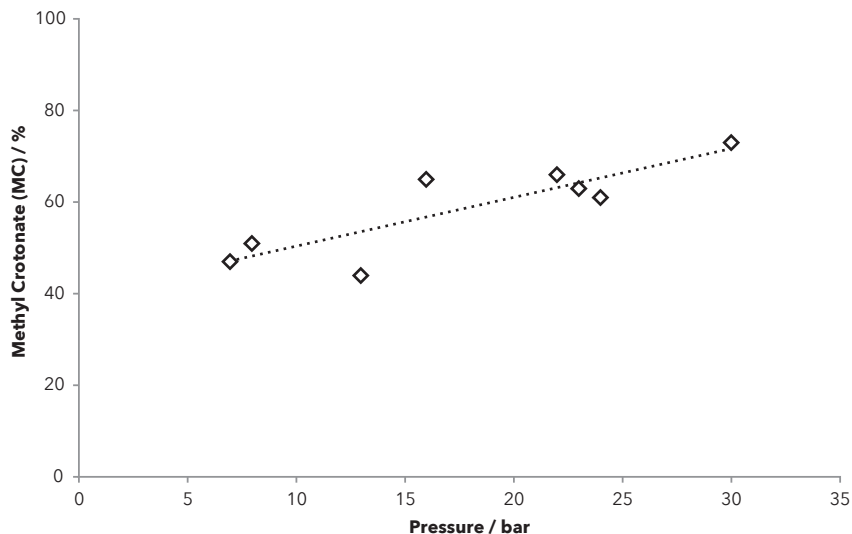
Figure 2.8. Conversion of CA to MC at various pressures. Reaction time = 6 hours, temperature = 200 °C. Pressure indicates the pressure build-up at the reaction temperature. Average of duplicate experiments.

In Figure 2.8 there is a clear trend where a higher pressure leads to more esterification product formed, with 50% conversion of CA to MC at 8 bar and 70% at 30 bar. This is in agreement with the hypothesis of a switching RDS.

To further prove our hypothesis, conversion of PHB to MC was performed at 200 °C with three set pressures of 8, 26 and 55 bar and stopped at different times, where t = 0 hours stands for a reaction that was heated up and immediately cooled down. The results of these experiments are presented in Figures 2.9a, 2.9b and 2.9c.
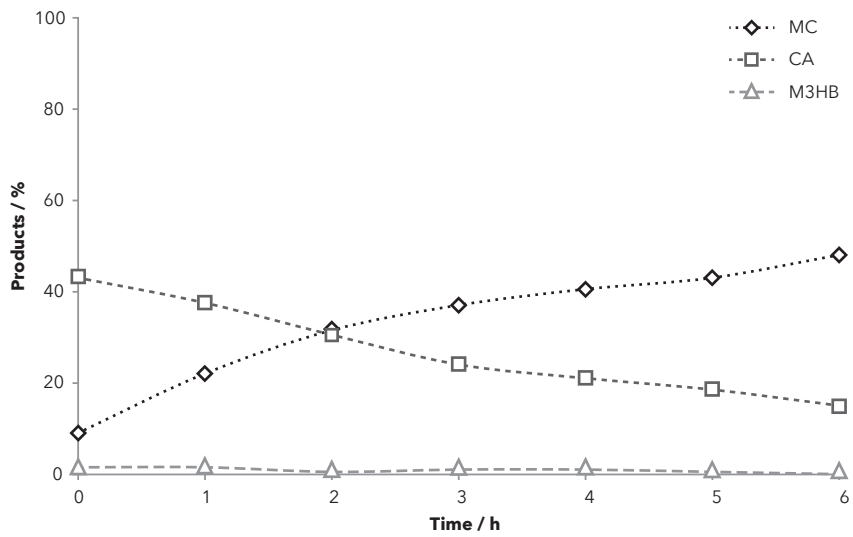
Figure 2.9a. Conversion of PHB to MC at 200 °C, 8 bar of pressure build-up at various reaction times. Average of duplicate experiments.
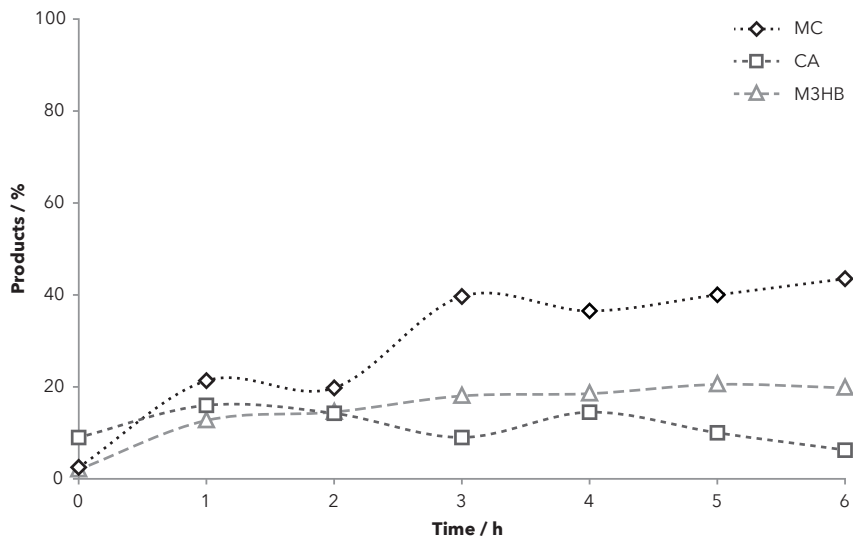
Figure 2.9b. Conversion of PHB to MC at 200 °C, 26 bar of pressure build-up at various reaction times. Average of duplicate experiments.
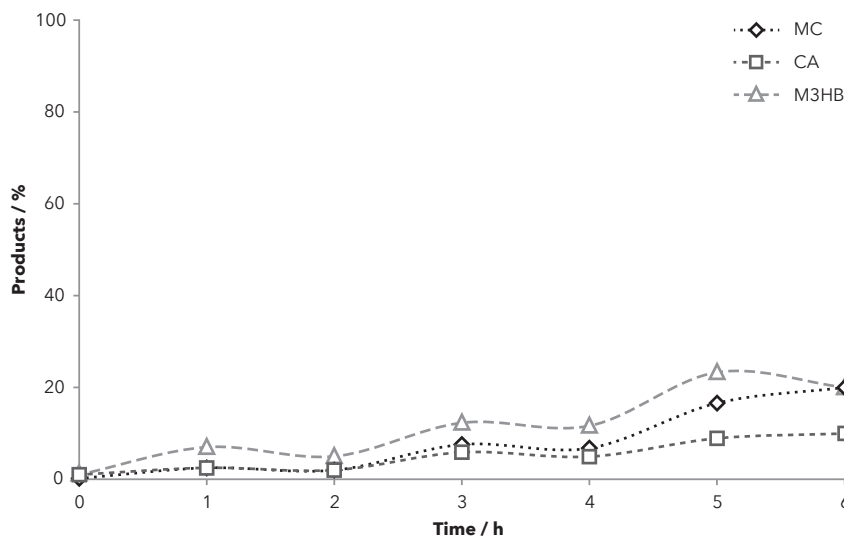
Figure 2.9c. Conversion of PHB to MC at 200 °C, 55 bar of pressure build-up at various reaction times. Average of duplicate experiments.

In Figure 2.9a with 8 bar of pressure build-up, a fast thermolysis to CA and a slow esterification to MC is observed. This leads to an immediate formation of a large amount of CA (43%), while only 9% of PHB is subsequently converted to MC. Over time, the CA is converted into MC, resulting in 48% MC and 15% CA after 6 hours.

In Figure 2.9b with 26 bar of pressure build-up, the thermolysis step slows down and initial formation of CA was lower than the initial CA formation observed at 8 bar (9% versus 35%) and only 3% was already converted into MC at t = 0 hours. The esterification step, however, speeds up and after 6 hours only 6% CA remains against 15% at 8 bar. The slower thermolysis gives rise to a competing transesterification pathway forming 20% M3HB after 6 hours, limiting the formation of total crotonates to 50% at 26 bar compared to 63% at 8 bar.

In Figure 2.9c, with 55 bar of pressure build-up and methanol reaching the bottom of the reactor, thermolysis is slowed down sufficiently for the competing transesterification reaction to become the predominant pathway, resulting in 20% M3HB formation after 6 hours. This lowers the formation of CA and MC at 55 bars to a total of 30% crotonates formed.

From Figures 2.7, 2.8 and 2.9a, b and c it can be concluded that the thermolysis step favours low pressures when the methanol reaches the PHB in the bottom part of the reactor, transesterification takes place, which competes with the thermolysis. and the esterification step favours higher pressures. This makes the esterification step the RDS at pressures below 18 bar and the thermolysis step the RDS at pressures above 18 bar. The switching RDS creates

an optimum pressure for MC production from PHB at 18 bar. Moreover, at higher pressures a transesterification pathway competes with the slowed down thermolysis step, resulting in the formation of more M3HB and less crotonates.

Where transesterification reactions applied to biomass generally use catalysts, either homogeneous or heterogeneous, we show that PHB can undergo transesterification in methanol without the use of a catalyst. Moreover, when catalyst free transesterifications are performed, supercritical conditions or use of co-solvents are often applied.[47] When PHB undergoes pyrolysis to CA, similar conversions of 63% CA are reached compared to 60% MC in our system. With pyrolysis, however, higher temperatures are needed (310 °C compared to 200 °C) and the obtained product has to undergo an addition esterification to obtain MC. In our system there is no need for harsh conditions or additional compounds. Using methanol to convert PHB to MC instead of CA does not only prevent the use of $Mg(OH)_2$[23] or concentrated H_2SO_4[21], it also gives direct access to MC, which makes an additional esterification step obsolete. Methanol used for the conversion of PHB to MC can also be obtained from biobased sources, for example from syngas obtained from straw.[9] This results in a fully biobased conversion of PHB to chemicals, where no fossil based compounds or catalysts are required.

2.4 Conclusion

We showed that PHB can be directly converted into methyl crotonate (MC) at elevated temperatures in methanol without the use of an additional catalyst and below supercritical conditions. Using a temperature profile over the reactor, a system was created with methanol refluxing in the reactor head, creating optimal conditions for the conversion of PHB to MC. At 200 °C, 18 bar and 6 hours, PHB was fully converted with a 70% selectivity towards crotonates. Based on our mechanistic study we propose that the reaction follows a thermolysis pathway to crotonic acid (CA), followed by a catalyst free esterification to form MC. The rate determining step (RDS) is dependent on the reaction pressure and changes at 18 bar. Below 18 bar, esterification of CA to MC is the RDS, while above 18 bar, the thermal conversion of PHB to CA is the RDS. The direct production of MC, a suitable substrate for a further metathesis reaction generating propylene and methyl acrylate, makes it possible to obtain fully biobased monomers for the plastics industry from PHB, circumventing processing and quality issues that PHB currently faces when used as a material. Larger scale reactions, as well as downstream processing, are currently investigated in our laboratory.

2.5 References

1. Könst, P. M.; Scott, E. L.; Franssen, M. C. R.; Sanders, J. P. M. *Journal of Biobased Materials and Bioenergy* **2011,** 5, (1), 102-108.

2. Van Walsem, J.; Anderson, E.; Licata, J.; Sparks, K. A.; Mirley, C.; Sivasubramanian, M. S. *WO 2011/100608 A1* **2011**.

3. Somleva, M. N.; Peoples, O. P.; Snell, K. D. *Plant biotechnology journal* **2013,** 11, (2), 233-52.

4. Jiang, Y.; Marang, L.; Kleerebezem, R.; Muyzer, G.; van Loosdrecht, M. C. *Biotechnology and bioengineering* **2011,** 108, (9), 2022-35.

5. Wang, B.; Pugh, S.; Nielsen, D. R.; Zhang, W.; Meldrum, D. R. *Metabolic engineering* **2013,** 16, 68-77.

6. Hu, S.; McDonald, A. G.; Coats, E. R. *Journal of Applied Polymer Science* **2013**, 1314-1321.

7. Gumel, A. M.; Annuar, M. S. M.; Chisti, Y. *Journal of Polymers and the Environment* **2012,** 21, (2), 580-605.

8. Chen, G. Q. *Chemical Society reviews* **2009,** 38, (8), 2434-46.

9. de Jong, E.; Higson, A.; Walsh, P.; Wellisch, M. *Biofuels, Bioproducts and Biorefining* **2012**, (6), 606-624.

10. Bengtsson, S.; Hallquist, J.; Werker, A.; Welander, T. *Biochemical Engineering Journal* **2008,** 40, (3), 492-499.

11. Koller, M.; Gasser, I.; Schmid, F.; Berg, G. *Engineering in Life Sciences* **2011,** 11, (3), 222-237.

12. Bengtsson, S.; Werker, A.; Christensson, M.; Welander, T. *Bioresource technology* **2008,** 99, (3), 509-16.

13. Laycock, B.; Halley, P.; Pratt, S.; Werker, A.; Lant, P. *Progress in Polymer Science* **2013,** 38, 536-583.

14. Kleerebezem, R.; van Loosdrecht, M. C. *Current opinion in biotechnology* **2007,** 18, (3), 207-12.

15. Marang, L.; Jiang, Y.; van Loosdrecht, M. C.; Kleerebezem, R. *Bioresource technology* **2013,** 142C, 232-239.

16. Grassie, N.; Murray, E. J.; Holmes, P. A. *Polymer Degradation and Stability* **1984,** 6, 95-103.

17. Schweitzer, D.; Mullen, C. A.; Boateng, A. A.; Snell, K. D. *Organic Process Research & Development* **2014,** DOI: 10.1021/op500156b.

18. Song, J. H.; Murphy, R. J.; Narayan, R.; Davies, G. B. *Philosophical transactions of the Royal Society of London. Series B, Biological sciences* **2009,** 364, (1526), 2127-39.

19. Grassie, N.; Murray, E. J.; Holmes, P. A. *Polymer Degradation and Stability* **1984,** 6, 47-61.

20. Zakaria Mamat, M. R.; Ariffin, H.; Hassan, M. A.; Mohd Zahari, M. A. K. *Journal of Cleaner Production* **2014,** 83, 463-472.

21. Chen, L. X. L.; Yu, J. *Macromolecular Symposia* **2005,** 224, (1), 35-46.

22. Ariffin, H.; Nishida, H.; Shirai, Y.; Hassan, M. A. *Polymer Degradation and Stability* **2010,** 95, (8), 1375-1381.

23. Ariffin, H.; Nishida, H.; Hassan, M. A.; Shirai, Y. *Biotechnology journal* **2010,** 5, (5), 484-92.

24. Huijberts, G. N. M.; Van der Wal, H.; Wilkinson, C.; Eggink, G. *Biotechnology Techniques* **1994,** 8, (3), 187-192.

25. Furrer, P.; Hany, R.; Rentsch, D.; Grubelnik, A.; Ruth, K.; Panke, S.; Zinn, M. *Journal of chromatography. A* **2007,** 1143, (1-2), 199-206.

26. Werker, A.; Lind, P.; Bengtsson, S.; Nordstrom, F. *Water research* **2008,** 42, (10-11), 2517-26.

27. Hesselmann, R. P. X.; Fleischmann, T.; Hany, R.; Zehnder, A. J. B. *Journal of Microbiological Methods* **1999,** 35, 111-119.

28. Bosma, R. H. A.; Aardweg, G. C. N. V. d.; Mol, J. C. *Journal of Organometallic Chemistry* **1983,** 255, 159-171.

29. Sanders, J. P. M.; Van Haveren, J.; Scott, E.; Van Es, D. S.; Le Nôtre, J.; Spekreijse, J. *US 2012/0178961 A1* **2012**.

30. Straathof, A. J. *Chemical reviews* **2013,** 114, (3), 1871-1908.

31. Burk, M. J.; Pharkya, P.; Dien, S. v.; Burgard, A. P.; Schilling, C. H. *WO 2009/045637 A2* **2009**.

32. Schofer, S.; Safir, A.; Vazquez, R. *WO 2013/082264 A1* **2013**.

33. Spekreijse, J.; Le Nôtre, J.; van Haveren, J.; Scott, E. L.; Sanders, J. P. M. *Green Chemistry* **2012,** 14, 2747-2751.

34. Chen, G. Q.; Patel, M. K. *Chemical reviews* **2012,** 112, (4), 2082-99.

35. Kawalec, M.; Adamus, G.; Kurcok, P.; Kowalczuk, M.; Foltran, I.; Focarete, M. L.; Scandola, M. *Biomacromolecules* **2007,** 8, (4), 1053-1058.

36. Ariffin, H.; Nishida, H.; Shirai, Y.; Hassan, M. A. *Polymer Degradation and Stability* **2008,** 93, (8), 1433-1439.

37. De, B. K. *Journal of the American Oil Chemists' Society* **2006,** 83, (5), 443-448.

38. Bigley, D. B.; Clarke, M. J. *J.C.S. Perkin II* **1982**, 1-6.

39. August, R.; McEwen, I.; Taylor, R. *J. Chem. Soc., Perkin Trans. II* **1987**, 1683-1689.

40. Zapata, E.; Gaviria, J.; Quijano, J. *International Journal of Chemical Kinetics* **2007,** 39, (2), 92-96.

41. Yu, J.; Plackett, D.; Chen, L. X. L. *Polymer Degradation and Stability* **2005,** 89, (2), 289-299.

42. Yu, G.-e.; Marchessault, R. H. *Polymer* **2000,** 41, 1087-1098.

43. Janigová, I.; Lacík, I.; Chodák, I. *Polymer Degradation and Stability* **2002,** 77, 35-41.

44. Butler, J. N.; Small, G. J. *Can. J. Chem.* **1963,** 41, 2492-2499.

45. Stewart, I. C.; Bergman, R. G.; Toste, F. D. *Journal of the American Chemical Society* **2003,** 125, 8696-8697.

46. Skau, E. L.; Saxton, B. *Journal of the American Chemical Society* **1930,** 52, (1), 335-341.

47. Talebian-Kiakalaieh, A.; Amin, N. A. S.; Mazaheri, H. *Applied Energy* **2013,** 104, 683-710.
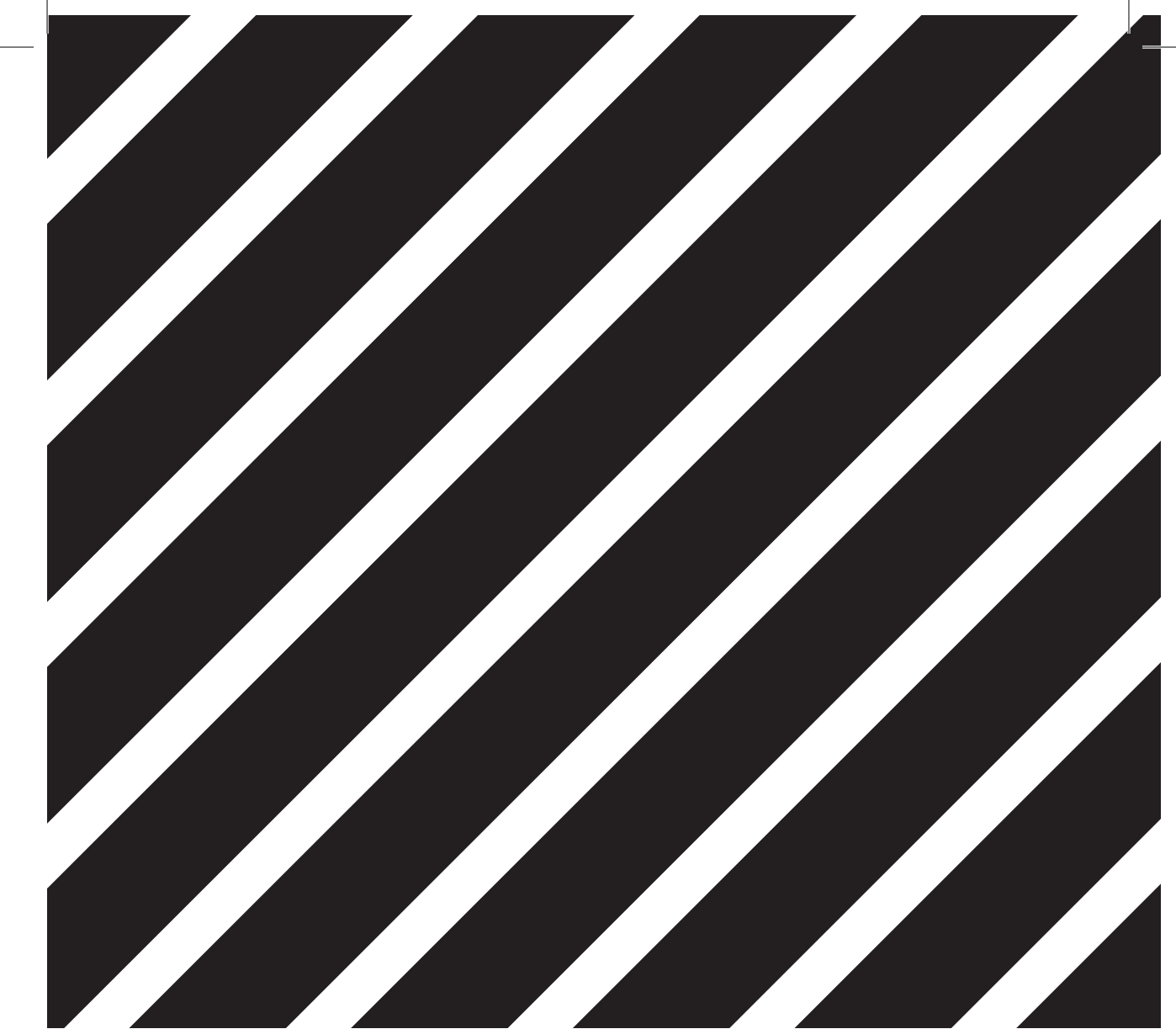
2

Conversion of polyhydroxyalkanoates to methyl crotonate using whole cells

Abstract

Isolated polyhydroxyalkanoates (PHA) can be used to produce biobased bulk chemicals. However, isolation is complex and costly. To circumvent this, whole cells containing PHA may be used. Here, PHA containing 3-hydroxybutyrate and small amounts of 3-hydroxyvalerate was produced from wastewater and used in the conversion of the 3-hydroxybutyrate monomer to methyl crotonate. Due to increased complexity of the reaction mixture the effect of 3-hydroxyvalerate content, magnesium salts and water was studied in order to evaluate the need for downstream processing. A water content up to 20% and the presence of 3-hydroxyvalerate have no influence on the conversion of the 3-hydroxybutyrate to methyl crotonate. The presence of Mg^{2+}-ions resulted either in an increased yield or in byproduct formation depending on the counterion. Overall, it is possible to bypass a major part of the downstream processing of PHA for the production of biobased chemicals.

3.1 Introduction

The use of fossil feedstocks has a number of drawbacks relating to depleting reserves, fluctuating costs, global warming and security of supply. Biomass is an attractive alternative, especially for the production of chemicals and materials. To prevent the "food versus fuel" debate[1] utilisation of biomass feedstocks that are currently treated as waste streams is of crucial importance. However, these feedstocks are often dilute and heterogeneous in nature which presents a challenge in the isolation of specific products. An elegant way to address this is the use of microorganisms that unify and isolate carbon based molecules from these waste streams. One example is the use of microorganisms to produce polyhydroxyalkanoates (PHAs) in media that are rich in volatile fatty acids and sugars. PHAs are polyesters that can contain various monomers and comonomers such as 3-hydroxybutyrate and 3-hydroxyvalerate.

PHA can be produced by using pure cultures, which enables optimisation by metabolic engineering. This leads towards an efficient PHA production and the possibility to obtain PHA with functionalised monomers.[2] Another approach for PHA production is the use of a feast-famine process on waste streams, where during a feast phase the microorganisms produce PHA and during a famine phase only productive species survive.[3] While productivity is lower, such an approach prevents the use of expensive equipment and sterilisation.[4, 5] Carbon sources range from municipal waste, where 0.4 g PHA per gram volatile suspended solids (VSS) is obtained[6] to outlets from agro-food industry with 0.7 g PHA/g VSS.[7]

Downstream processing of PHA from the fermentation broth is an energy intensive and costly procedure, where especially the removal of PHA from within the cells is seen as challenging and expensive.[8] An economic and environmental assessment shows that it accounts for 70% of the total cost of PHA production from wastewater.[9] Next to the challenges of purification, PHA originating from waste streams will have fluctuating properties,[10] such as variable amounts of 3-hydroxybutyrate and 3-hydroxyvalerate. This makes it difficult to compete with products of consistent quality generated from petro-chemistry and other alternatives such as high purity lactic acid.[11] Finally, PHA starts to degrade around its melt temperature (170 to 200 °C). However, this temperature is required for melt based processing techniques such as extrusion.[12] These properties make PHA difficult to process.

An alternative methodology, avoiding processing issues, is converting PHA into drop-in chemicals with known and established applications and markets. One promising route is the formation of crotonic acid (CA) from PHA with a high 3-hydroxybutyrate content. For example, thermal degradation or pyrolysis of 3-hydroxybutyrate containing PHAs to CA has been thoroughly investigated and the mechanism clarified.[13] The pyrolysis is performed at high temperatures of 310 °C, reaching a CA yield of 63%.[14] The pyrolysis temperature can be decreased by using a catalyst such as $Mg(OH)_2$ to reach CA yields of 84% at 220 °C to 270 °C [15] or concentrated sulphuric acid to reach a CA yield of 90% at 100 °C.[16] Further conversion of CA to butanol, maleic anhydride, propylene or acrylic acid has been proposed by Metabolix.[17-19]

In chapter 2, the direct conversion of 3-hydroxybutyrate containing PHAs to methyl crotonate (MC) is described as a first step to obtain biobased acrylates and propylene. MC has the advantage that it is immiscible with water, which improves separation from an aqueous environment. Moreover, MC can be produced at lower temperatures compared to CA from pyrolysis without the use of a catalyst. This conversion proceeds *via* thermolysis of PHA, where the 3-hydroxybutyrate is converted to CA followed by an esterification to MC. As side product methyl 3-hydroxybutyrate (M3HB) is formed by transesterification (Figure 3.1). In this catalyst free, one pot reaction, using methanol at 18 bar, 200 °C for 6 hours, 70% crotonates could be obtained.[20]
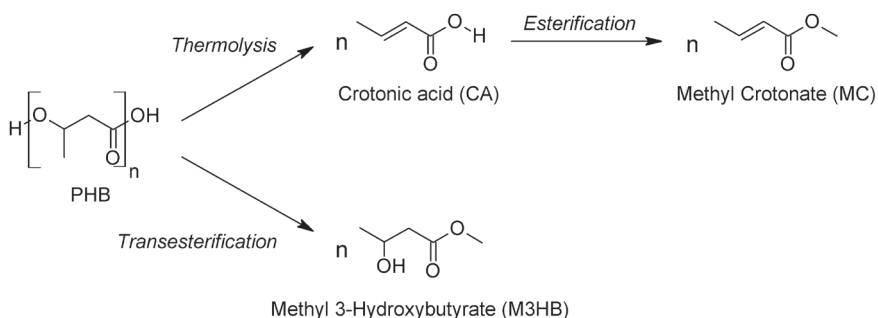
Figure 3.1. Pathway of polyhydroxybutyrate (PHB) to methyl crotonate (MC) via crotonic acid (CA) and the formation of methyl 3-hydroxybutyrate (M3HB) as side product.[20]

Although this route circumvents the processing and application issues related to the use of PHA as a polymer, the proposed route still needs to be improved with regards to the isolation of PHA and its economic impact. Unpurified PHAs from fermentation contain a wide range of other components that can potentially influence conversion of the 3-hydroxybutyrate in PHA to CA. For example, the pyrolysis of polyhydroxybutyrate (PHB) in switchgrass at 375 °C yielded 45 wt% CA, [21] while pyrolysis of isolated PHB at 310°C reaches 63% CA.[14] Farid et al. showed that pyrolysis of PHB from *Cupriavidus necator* to CA can be carried out without isolation, yielding CA in low purity.[22] In these examples, unpurified PHB leads to lower conversions to the desired product, however it was not clear which components from the biomass cause the lower yields. Impurities can also lead to increased yields, for example, a modified pre-treatment to isolate PHB from biomass using NaOH instead of chloroform for the purification of PHB, resulted in an increased conversion to a CA yield of 80% with 89% purity. The influence of this pre-treatment and its residual components was explained by a positive influence of crotonyl end groups formed during the pre-treatment, the presence of residual Na⁺ ions and the lowering of the molar mass of the treated PHB.[22]

Though it is known that unpurified PHB generally results in lower pyrolysis yields, the impact of the impurities on the reaction following the chemical route as depicted in Figure 3.1 is not known yet. Here, the influence of residues from the fermentation broth on the conversion of the 3-hydroxybutyrate in the PHA to MC in methanol is investigated by using freeze-dried cells

obtained from a pilot scale PHB production.[7] The influence of various 3-hydroxybutyrate and 3-hydroxyvalerate compositions, residual salts and water were investigated in order to obtain an insight in the desired PHA composition and purity before conversion to biobased chemicals. This could lead to an economically feasible pathway from waste based PHA to MC.

3.2 Experimental

Nitrogen gas (Nitrogen 3.0, purity 99.9%) was supplied by Linde Gas Benelux. Methanol (HPLC gradient) was purchased from Actu-All Chemicals, CA (98%), methyl crotonate (98%), methyl (R)-(-)3-hydroxybutyrate (99%), and DL 3-hydroxybutyric acid (as sodium salt) were purchased from Sigma-Aldrich; PHB was kindly provided by Technical University Eindhoven (98 mol% butyrate and 2 mol% 3-hydroxyvalerate, Mn 5450 kDa and Mw/Mn 51.3); PHBV (80 mol% butyrate, 20 mol% 3-hydroxyvalerate) was obtained from Tianan Biopolymer; PHA rich cells of varying 3-hydroxybutyrate and 3-hydroxyvalerate composition from pilot plant using *P. acidivorans* were kindly provided by Delft University. The biomass samples were freeze dried to a water content of 3 to 5% and stored at -20 °C. All other chemicals were used as received. Data visualization was aided by Daniel's XL Toolbox addin for Excel, version 6.60.

High-Performance Liquid Chromatography (HPLC) was performed on an UltiMate 3000 from Thermo Scientific with a Rezex ROA Organic acid H+ (8%) column (7.8 × 150 mm, column temp 40 °C) from Phenomenex. 12 mM H_2SO_4 (aq) (0.6 mL/min) was used as eluent. The reaction mixture (injection volume 0.5 µL) was analysed using a UV-detector (210 nm). Quantification was performed by calibration from pure products. Product elution times are: 3HB, 7.25 min; M3HB, 10.84 min; CA, 14.89 min; MC 29.63 min.

All experiments were performed in duplicates in 75 mL Parr pressure reactors (Parr multiple reactor system series 5000, 6 × 75 mL, Hastelloy C-276) equipped with glass liners and glass coated stirring bars. 0.6 g PHA was loaded in the glass liner which was subsequently placed in the Parr reactor. 10 mL Methanol was added and the reactor was closed, flushed with nitrogen and pressurized with nitrogen to the desired pressure at room temperature before the heating (ramp 12 °C/min) was started. The heating caused the pressure in the closed reactor to increase to the reported reaction pressure. The start of the reaction (t=0) was defined at the time at which the reactor reached 200 °C. After finishing the reaction the reactor was allowed to cool to room temperature before being opened. The dark brown solution was passed through a 0.20 µm single use filter unit and the liquid was analysed by HPLC. The presented conversions of PHA that contains 3-hydroxyvalerate are based on the conversion of the 3-hydroxybutyrate fraction, where a 100% conversion represents a full conversion of the 3-hydroxybutyrate fraction of PHA to the C4 compound, since 3-hydroxyvalerate will not result in C4 compounds. No remaining PHA could be observed after the reactions.

3.3 Results and Discussion

3.3.1 INFLUENCE OF 3-HYDROXYVALERATE CONTENT

PHA originating from waste stream fermentation exists as a copolymer consisting of 3-hydroxy-butyrate and 3-hydroxyvalerate monomers. The copolymer will have a fluctuating 3-hydroxy-valerate content and in the case of PHA from volatile fatty acids, this value is between 10% and 15%.[7] To investigate the influence of the 3-hydroxyvalerate content on the conversion of the 3-hydroxybutyrate fraction in the PHA copolymer, PHA with a low 3-hydroxyvalerate content (2 mol% 3-hydroxyvalerate, labelled pure PHB) and with a high 3-hydroxyvalerate content (20 mol% 3-hydroxyvalerate, labelled PHBV) were compared. Both PHAs were converted to methyl crotonate (MC) according to the previously optimised procedure using 200 °C and 18 bar in methanol (Figure 3.2).[20]
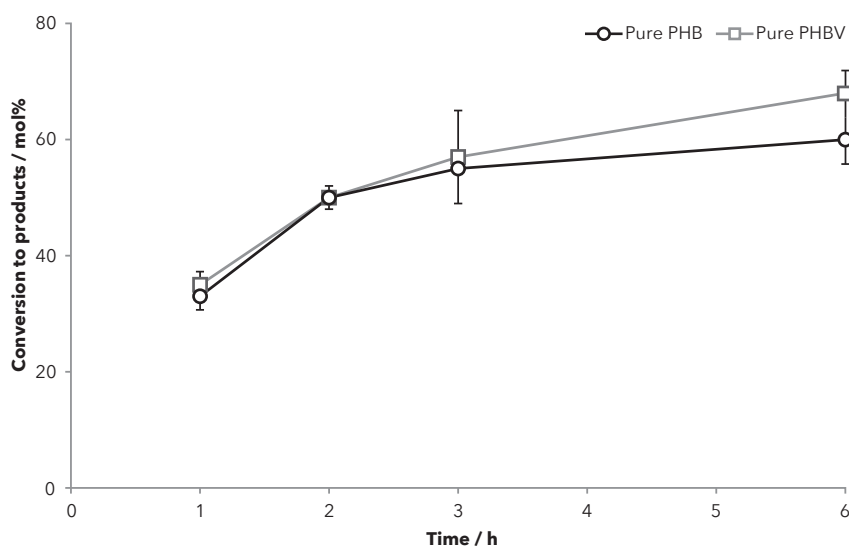
Figure 3.2. Comparison between reactivity of pure PHB (2% 3-hydroxyvalerate) and pure PHBV (20% 3-hydroxyvalerate) towards methyl crotonate (MC). Reaction conditions: Equivalent of 0.6 g PHB, P = 18 bar, T = 200 °C, 10 mL methanol. Average of duplicate experiments. Error bars show the range of results for pure PHBV. Conversion is based on the 3-hydroxybutyrate content.

The conversions presented in Figure 3.2 are based on the 3-hydroxybutyrate fraction, where a 100% conversion represents a full conversion of the 3-hydroxybutyrate fraction of PHA to MC, since the 3-hydroxyvalerate will not result in MC formation. Both PHB and PHBV followed the same conversion over time and resulted in 60 to 70% MC after 6 hours. The side product

formation (CA and M3HB, Figure 3.1) was the same for both samples as well (data not shown). The incomplete mass balance can be explained by gaseous degradation products from MC, such as propene and CO_2.[20] Therefore, it can be concluded that the selectivity towards MC formation is not influenced by the presence of 3-hydroxyvalerate in the copolymer. It is important to note that PHA containing high amounts of 3-hydroxyvalerate will still lead to less MC formation, since it contains less of the 3-hydroxybutyrate monomer. The 3-hydroxyvalerate fraction will lead to extra C5 side products such as methyl 2-pentenoate. However, the reactivity of the 3-hydroxybutyrate fraction remains unchanged.

Although it has been shown by thermogravimetric analysis (TGA) that a higher 3-hydroxyvalerate content increases the thermal stability of PHAs,[15, 23, 24] no impact on the conversion to MC from the higher 3-hydroxyvalerate content was observed in this study. This implies that PHAs from wastewater that contain a higher 3-hydroxyvalerate fraction should be equally suitable for the formation of MC as the commercial PHAs with low 3-hydroxyvalerate content.

3.3.2 INFLUENCE OF MAGNESIUM SALTS

The next parameter that could potentially alter the reactivity of PHA from fermentations are residual salts. Magnesium salts are known to catalyse the conversion of the 3-hydroxybutyrate in PHAs to CA,[15] and therefore the influence of magnesium salts on the conversion to MC and M3HB was studied.
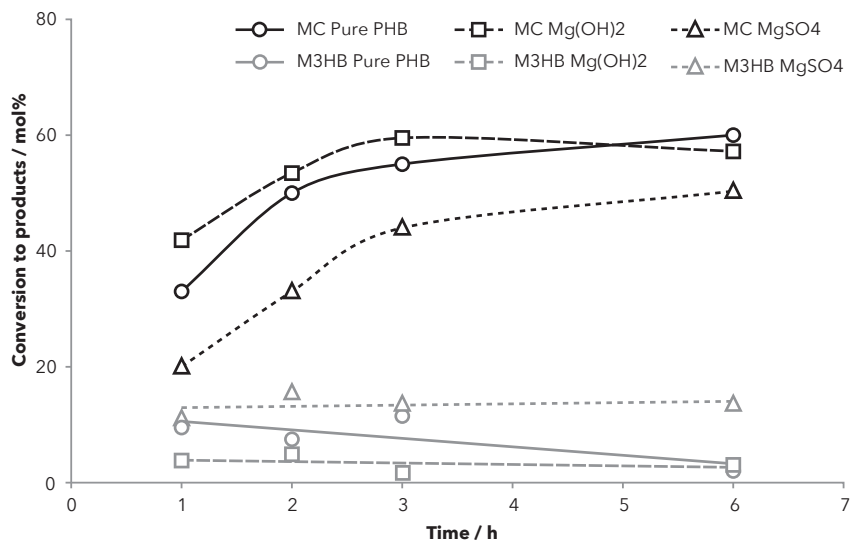
Figure 3.3. Influence of magnesium salts on the conversion of PHB to methyl crotonate (MC) and methyl 3-hydroxybutyrate (M3HB). Reaction conditions: 0.6 g PHB, P = 18 bar, T = 200 °C, 10 mL methanol. Average of duplicate experiments.

Figure 3.3 shows the effect of addition of magnesium salts on the conversion of PHB to MC and M3HB. The conversion to MC after 6 hours was identical for PHB (60%) and PHB with added $Mg(OH)_2$ (57%). $MgSO_4$ on the other hand decreases the final conversion to MC slightly to 50% after 6 hours. The effect of $Mg(OH)_2$ on the MC formation was most pronounced after one hour, where the conversion to MC with $Mg(OH)_2$ was almost ten percent higher than without salts (42% and 33% respectively). $MgSO_4$ clearly slowed down the reaction since only 20% MC is formed after one hour. The M3HB formation showed a reversed trend compared to the MC. For $Mg(OH)_2$ the formation of M3HB was lowest (3%), where addition of $MgSO_4$ gave rise to the highest M3HB formation (14%). This formation of M3HB took place in the first hour of the reaction. It appears that $MgSO_4$ stimulates M3HB production, which reduces MC formation, whereas $Mg(OH)_2$ catalyses the formation of MC and reaches the final conversion to MC of 60% faster than when pure PHB is used.

For an explanation of the role of the magnesium salts, the mechanism of the reactions should be considered (see Figure B1 in Appendix B). M3HB is formed from PHB *via* a transesterification mechanism, where CA is formed *via* an E1cB mechanism.[25]

Since $Mg(OH)_2$ is basic this can explain the higher conversion towards CA in the presence of $Mg(OH)_2$ which is in line with earlier reports.[26, 27] Apparently, a faster thermolysis of 3-hydroxybutyrate containing PHA towards CA prevents the formation of M3HB as a side product, i.e. of the two parallel pathways the one leading to the desired CA is enhanced in the presence of $Mg(OH)_2$. The hydrolysis of PHB to 3-hydroxybutyric acid (3HB) is also known to be catalysed in alkaline conditions.[28] However, no increase in formation of 3HB or M3HB as a result of PHB hydrolysis was observed, which can be explained by the poor solubility of $Mg(OH)_2$ in methanol, preventing the formation of OH^- ions as efficient nucleophiles for ester hydrolysis.

$MgSO_4$ shows the opposite behaviour, where the transesterification is catalysed, leading to a higher M3HB formation. This lowers the thermolysis towards CA, which results in a lower formation of MC. The effect is limited since PHB is only in contact with methanol during the heating of the reactor. When the reaction temperature has been reached, methanol is refluxing in the top of the reactor, out of reach of the non volatile PHB oligomers. This explains why M3HB is only formed at the start of the reaction. Transesterification reactions that use magnesium salts for catalysis prefer to use the basicity of MgO and no reports could be found studying the effect of $MgSO_4$ on transesterification reactions.[29] The activity of the Mg2+ ion is expected to be caused by its Lewis acidity, which activates the ester group of PHB, promoting a nucleophilic attack of methanol (see Figure B1 in Appendix B). The catalytic effect of Lewis acids on transesterification reactions is well known and often applied in the synthesis of biodiesel.[30] In the case of $Mg(OH)_2$, the catalytic effect of the Lewis acid is surpassed by the effects of its basicity.

3.3.3 REACTIVITY OF WHOLE CELLS CONTAINING PHA OBTAINED FROM A PILOT PLANT

The composition of the fermentation broth and PHA cells can vary significantly with respect to 3-hydroxyvalerate to 3-hydroxybutyrate ratio, salt concentration and organic content. To examine potential influences of these fluctuations on the conversion to MC, four samples from a pilot plant that produces PHA from volatile fatty acids in a waste stream from a chocolate factory were investigated.[7] Next to PHA, these samples will contain organic matter and salts from the fermentation broth. Purified, commercial PHB and PHBV were used for comparison. The properties of the samples, such as the 3-hydroxyvalerate content (expressed as 3-hydroxy-valerate/PHA), the amount of PHA per total suspended solids and the conversion to reaction products can be seen in Table 3.1.

Table 3.1. Conversion of PHA in cells to methyl crotonate (MC) and side products. Conversion is based on the 3-hydroxybutyrate content.

Entry	Sample	3-hydroxyvalerate / PHA (mol%)	PHA / total suspended solids (mass%)	MC (mol%)	M3HB (mol%)	CA (mol%)
1	Biomass A	11	61	33	11	2
2	Biomass B	15	60	49	5	3
3	Biomass C	15	59	49	7	2
4	Biomass D	16	70	44	0	2
5	Pure PHB	2	n.a.	60	2	9
6	Pure PHBV	20	n.a.	68	8	8

Reaction conditions: Equivalent of 0.6 g PHB, P= 18 bar, t = 6h, T = 200 °C, 10 mL methanol. Average of duplicate experiments.

The biomass samples show small differences in 3-hydroxyvalerate to 3-hydroxybutyrate ratio, with a 3-hydroxyvalerate content of 11% to 16% and the total PHA amount in the samples ranging from 59% to 70% (Table 3.1, entries 1 to 4). The salt concentration of the samples was not determined.

Three of the four biomass samples showed similar reactivity, with a MC formation of 44% to 49%, <10% M3HB formation and 2-3% CA formation (Table 3.1, entries 2 to 4). Biomass sample A gave a lower conversion to MC (33%) than the other three biomass samples and a higher conversion to M3HB (Table 3.1, entry 1 compared to entries 2 to 4). The conversion of PHA in cells was slightly different from the conversion of commercial PHB and PHBV. A higher crotonate formation was observed from commercial PHA and PHBV (60% to 68% MC) as opposed to 44% to 49% MC for biomass samples. There was also a different amount of CA formed when pure PHB and pure PHBV are used (8% to 9%) compared to biomass samples (2% to 3%) (Table 3.1, entry 5 & 6 compared to Table 3.1, entries 2 to 4).

The difference in reactivity of entry 1, where only 33% MC is formed, cannot originate from the difference in 3-hydroxyvalerate content (11% compared to 15%), since Figure 3.2 shows that the 3-hydroxyvalerate content has no influence in the reactivity of PHA. Moreover, pure PHBV, which has an even higher 3-hydroxyvalerate content, results in a higher MC formation of 68% (Table 3.1, entry 6). It is therefore unclear what causes the behaviour of this sample. Further experiments were conducted with biomass sample B (Table 3.1, entry 2).

3.3.4 INFLUENCE OF REACTION TIME

In an attempt to explain the slightly lower conversion to MC of the 3-hydroxybutyrate fraction of PHA in cells compared to purified PHB, a time screening was performed to investigate whether the reaction of PHA in cells is completed after 6 hours. The results of this time screening can be found in Figure 3.4.
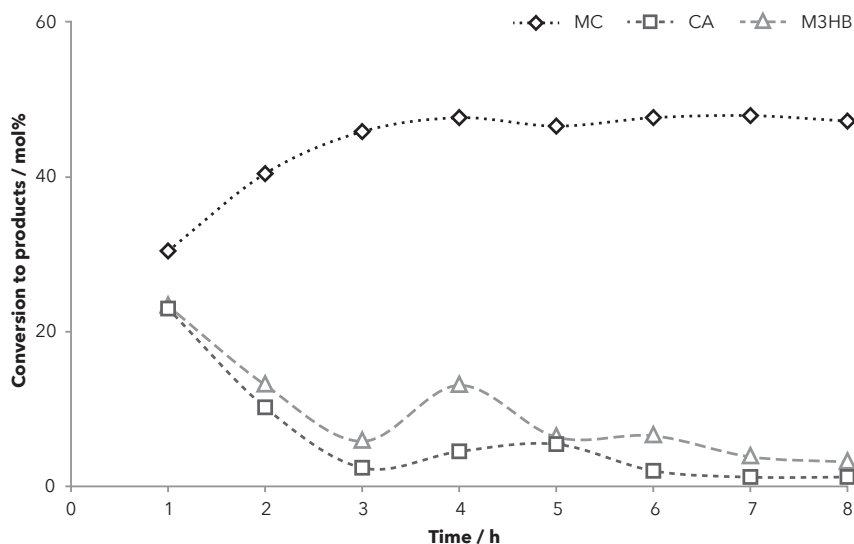
Figure 3.4. Time screening of the conversion of PHA in cells (sample B) with methanol. Reaction conditions: Equivalent of 0.6 g PHB, P = 18 bar, T = 200 °C, 10 mL methanol. Average of duplicate experiments. Conversion is based on the 3-hydroxybutyrate content.

Figure 3.4 shows that in the beginning of the reaction CA, M3HB and MC were formed. In the first three hours the amount of MC increased while the amount of CA and M3HB decreased. After three hours the reaction was completed and the amounts remained constant. This behaviour can be explained with the known reaction pathway, where CA is converted into MC (Figure 3.1). The decrease of M3HB can be explained by a degradation into C2 products *via* a cyclic intermediate.[31]

The conversion of the 3-hydroxybutyrate fraction of PHA in cells to MC was lower than the conversion of pure PHB to MC, with a maximum of 47% MC, while pure PHB reached 60% MC (Table 3.1, entry 5). From Figure 3.4 it can be concluded that the reaction has been completed after 6 hours and therefore that the lower conversion of PHA to MC in cells compared to pure PHB must originate from another factor. Since 3-hydroxyvalerate content has no influence on the conversions (Figure 3.1) we conclude that the presence of salts or biomass from the fermentation broth are the cause of a lower MC formation from PHA in cells compared to pure PHB.

3.3.5 INFLUENCE OF WATER

Currently, next to the isolation of PHA from fermentation broth residues, drying is an important step of PHA downstream processing which includes expensive techniques such as a hydrocyclone, centrifugation and air drying.[9] Since it would be beneficial when higher water contents could be used in the processing of PHA, the influence of the water/methanol ratio was investigated. Figure 3.5 shows the influence of the water content on the conversion of pure PHB to MC (Figure 3.5a) and the conversion of 3-hydroxybutyrate containing PHA in cells to MC (Figure 3.5b).
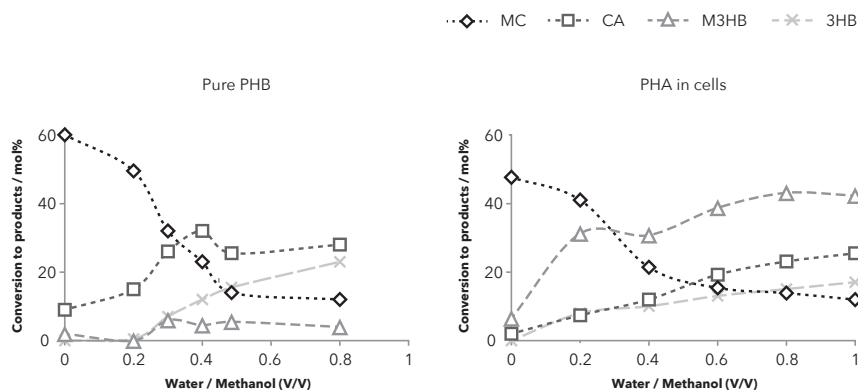
Figure 3.5. Conversion of (a) pure PHB and (b) PHA in cells (sample B) in methanol with different amounts of water to methanol. Reaction conditions: Equivalent of 0.6 g PHB, P = 18 bar, t = 6h, T = 200 °C, 10 mL methanol. Average of duplicate experiments. Conversion is based on the 3-hydroxybutyrate content.

Formation of around 50% MC for up to 0.2 V/V water/methanol (17 vol% water) was obtained from both pure PHB and PHA in cells. This dropped to 10 to 15% at 0.6 V/V water/methanol (38 vol% water) (Figure 3.5). In both samples, there was a gradual increase in both acid products (CA and 3HB) from <10% when no water is added to 25% to 28% CA and 17% to 23% 3HB with 50% water (1.0 V/V water/methanol). A difference between the two starting

materials can be found in the M3HB formation. Using pure PHB resulted in no significant amounts of M3HB independent on the water content and using PHA in cells resulted in 30% to 40% M3HB when water is present in the system.

Water appears to have two effects on the reaction pathway. First, water can hydrolyse MC into CA and M3HB into 3HB, which can lead to the observed increase in CA and a decrease in MC. Second, water can directly hydrolyse the ester bonds in PHB to form 3HB. This hydrolysis creates an extra pathway from PHB to 3HB, which could explain the increase in 3HB with a higher water content. The increased M3HB formation for PHA in cells can originate from the esterification of 3HB or the transesterification of PHB with methanol. It is unclear why PHA in cells gives rise to a large increase in M3HB formation in the presence of water compared to pure PHB. A high water/methanol ratio also shows a decreased mass loss in the conversion of PHA in cells. The mass loss is expected to originate from degradation to gaseous products.[20] However, it is at this stage unclear what mechanism prevents the formation of gaseous products.

The high formation of MC at water contents lower than 17 vol% suggest that intensive drying in the downstream processing to obtain 99.9% pure PHA[9] is not necessary when PHA is converted to chemicals and some remaining water is allowed for an efficient conversion to MC. This will lower the economic and ecological pressure of the downstream processing.

3.4 Conclusions

Water content up to 20% and 3-hydroxyvalerate content show no effect on the conversion of the 3-hydroxybutyrate fraction of PHA to MC. Depending on the counterion, magnesium salts can catalyse the production of MC or stimulate the side product formation. Without downstream processing, PHA in freeze-dried cells from a pilot plant shows a conversion to MC with a selectivity of 49%. From these results it can be concluded that the downstream processing of PHA for the production of bulk chemicals could be minimized, making intensive downstream processing of PHA unnecessary to obtain biobased chemicals from wastewater streams.

3.5 References

1.   Searchinger, T.; Edwards, R.; Mulligan, D.; Heimlich, R.; Plevin, R. *Science* **2015,** 347, (6229), 1420-1422.

2.   Laycock, B.; Halley, P.; Pratt, S.; Werker, A.; Lant, P. *Progress in Polymer Science* **2013,** 38, 536-583.

3.   Kleerebezem, R.; van Loosdrecht, M. C. *Current opinion in biotechnology* **2007,** 18, (3), 207-12.

4.   Bengtsson, S.; Werker, A.; Christensson, M.; Welander, T. *Bioresource technology* **2008,** 99, (3), 509-16.

5.   Koller, M.; Gasser, I.; Schmid, F.; Berg, G. *Engineering in Life Sciences* **2011,** 11, (3), 222-237.

6.   Morgan-Sagastume, F.; Hjort, M.; Cirne, D.; Gerardin, F.; Lacroix, S.; Gaval, G.; Karabegovic, L.; Alexandersson, T.; Johansson, P.; Karlsson, A.; Bengtsson, S.; Arcos-Hernandez, M. V.; Magnusson, P.; Werker, A. *Bioresource technology* **2015,** 181C, 78-89.

7.   Tamis, J.; Luzkov, K.; Jiang, Y.; Loosdrecht, M. C.; Kleerebezem, R. *Journal of biotechnology* **2014,** 192PA, 161-169.

8.   Madkour, M. H.; Heinrich, D.; Alghamdi, M. A.; Shabbaj, II; Steinbuchel, A. *Biomacromolecules* **2013,** 14, (9), 2963-72.

9.   Fernandez-Dacosta, C.; Posada, J. A.; Kleerebezem, R.; Cuellar, M. C.; Ramirez, A. *Bioresource technology* **2015,** 185, 368-77.

10. Wang, Y.; Yin, J.; Chen, G. Q. *Current opinion in biotechnology* **2014,** 30, 59-65.

11. Babu, R. P.; O'Connor, K.; Seeram, R. *Progress in Biomaterials* **2013,** 2, (8).

12. Grassie, N.; Murray, E. J.; Holmes, P. A. *Polymer Degradation and Stability* **1984,** 6, 95-103.

13. Ariffin, H.; Nishida, H.; Shirai, Y.; Hassan, M. A. *Polymer Degradation and Stability* **2008,** 93, (8), 1433-1439.

14. Zakaria Mamat, M. R.; Ariffin, H.; Hassan, M. A.; Mohd Zahari, M. A. K. *Journal of Cleaner Production* **2014,** 83, 463-472.

15. Ariffin, H.; Nishida, H.; Hassan, M. A.; Shirai, Y. *Biotechnology journal* **2010,** 5, (5), 484-92.

16. Yu, J.; Plackett, D.; Chen, L. X. L. *Polymer Degradation and Stability* **2005,** 89, (2), 289-299.

17. Somleva, M. N.; Peoples, O. P.; Snell, K. D. *Plant biotechnology journal* **2013,** 11, (2), 233-52.

18. Schweitzer, D.; Mullen, C. A.; Boateng, A. A.; Snell, K. D. *Organic Process Research & Development* **2014,** DOI: 10.1021/op500156b.

3

19. Schweitzer, D.; Snell, K. D. *Organic Process Research & Development* **2014**, 141124132601002.

20. Spekreijse, J.; Le Nôtre, J.; Sanders, J. P. M.; Scott, E. L. *Journal of Applied Polymer Science* **2015**, n/a-n/a.

21. Mullen, C. A.; Boateng, A. A.; Schweitzer, D.; Sparks, K.; Snell, K. D. *J Anal Appl Pyrol* **2014,** 107, 40-45.

22. Farid, N. F. S. M.; Ariffin, H.; Mamat, M. R. Z.; Mohd Zahari, M. A. K.; Hassan, M. A. *RSC Adv.* **2015,** 5, (42), 33546-33553.

23. Carrasco, F.; Dionisi, D.; Martinelli, A.; Majone, M. *Journal of Applied Polymer Science* **2006,** 100, (3), 2111-2121.

24. Li, S.-D.; He, J.-D.; Yu, P. H.; Cheung, M. K. *Journal of Applied Polymer Science* **2003,** 89, 1530-1536.

25. Kawalec, M.; Adamus, G.; Kurcok, P.; Kowalczuk, M.; Foltran, I.; Focarete, M. L.; Scandola, M. *Biomacromolecules* **2007,** 8, (4), 1053-1058.

26. kawalec, M.; Sobota, M.; Scandola, M.; Kowalczuk, M.; Kurcok, P. *Journal of Polymer Science Part A: Polymer Chemistry* **2010,** 48, (23), 5490-5497.

27. Ariffin, H.; Nishida, H.; Shirai, Y.; Hassan, M. A. *Polymer Degradation and Stability* **2010,** 95, (8), 1375-1381.

28. Chen, L. X. L.; Yu, J. *Macromolecular Symposia* **2005,** 224, (1), 35-46.

29. Lee, A. F.; Bennett, J. A.; Manayil, J. C.; Wilson, K. *Chemical Society reviews* **2014,** 43, (22), 7887-916.

30. Santacesaria, E.; Vicente, G. M.; Di Serio, M.; Tesser, R. *Catalysis Today* **2012,** 195, (1), 2-13.

31. August, R.; McEwen, I.; Taylor, R. *J. Chem. Soc., Perkin Trans. II* **1987**, 1683-1689.

3
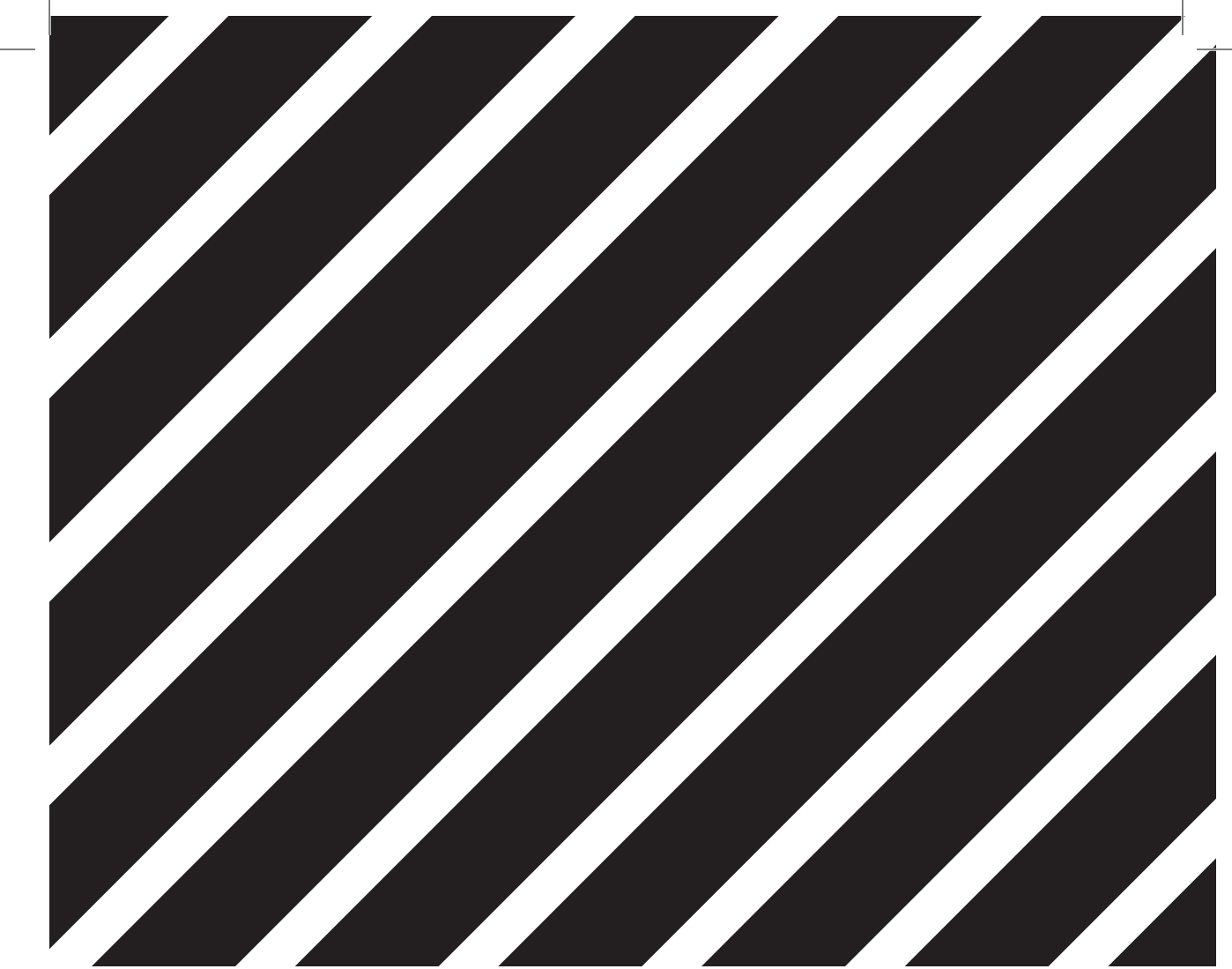
Mechanochemical immobilisation of metathesis catalysts in a metal organic framework

Abstract

A simple, one step mechanochemical immobilisation procedure for homogeneous methathesis catalysts in metal organic frameworks (MOFs) was developed. Grinding MIL-101-NH_2(Al) with a Hoveyda-Grubbs 2nd generation catalyst resulted in a heterogeneous catalyst which was active for metathesis and belongs to the most stable immobilized catalysts. During the mechanochemical immobilisation the MIL-101-NH_2(Al) structure was partially converted to MIL-53-NH_2(Al). The Hoveyda-Grubbs entrapped in the MIL-101-NH_2(Al) part is responsible for the observed catalytic activity. The developed synthesis procedure was also successful for the immobilization of a Zhan catalyst.

4.1 Introduction

The field of olefin metathesis reactions shows rapid progress, where more robust ruthenium catalysts are being developed and new, enantioselective pathways are being explored.[1] Research has reached the point where the focus is shifting towards large scale applications.[2] One of the challenges for such applications is the separation and potential reusability of the catalyst containing the noble metal ruthenium. Many examples of catalyst modification to allow recycling have been proposed, but often require complex or time consuming synthesis steps. These immobilisation strategies often involve attaching one of the ligands to an ammonium group, oligomer or insoluble material to enable separation of the catalyst after reaction.[2, 3] In these systems, the number of repeated cycles in which the catalyst can be used is still limited to five to ten cycles.[2] An example of an immobilisation on a polymer is the resin supported Zhan catalyst (Figure 4.1a), which is the only immobilised metathesis catalyst offered by chemical suppliers. However, no examples in the literature on the metathesis reactivity of this catalyst could be found.

Immobilisation without modification of the catalyst would be preferred to maintain the optimised ligand systems of the homogeneous catalysts. To successfully immobilise a catalyst without catalyst modification, the catalyst needs to be trapped inside the cavities of the material. For this purpose, the support requires to contain large pores that can be closed. Without closing the pores, the catalyst will be free to leach out of the support as has been shown by silica impregnated with Hoveyda-Grubbs 2nd generation catalyst (HG2) (Figure 4.1b). In a standard cyclization reaction of diethyl diallylmalonate (DDM), this catalyst remains active up to 9 cycles, but gradually decreases in activity with the number of cycles in which the catalyst is used. In addition, this system is limited to apolar solvents to prevent leaching of the catalyst.[4, 5] To enable reactions in polar solvents, leaching of the catalyst can be prevented by post-modification of the silica with dichlorodiphenylsilane to make the pores of the material more narrow and trap the catalyst. The resulting material can perform the conversion of DDM in dichloromethane (DCM) for 7 runs with a drop in conversion from 95% to 57% with an increasing reaction time from 1.5 to 8 hours.[6]

a) Zhan catalyst   b) Hoveyda-Grubbs 2nd generation (HG2)
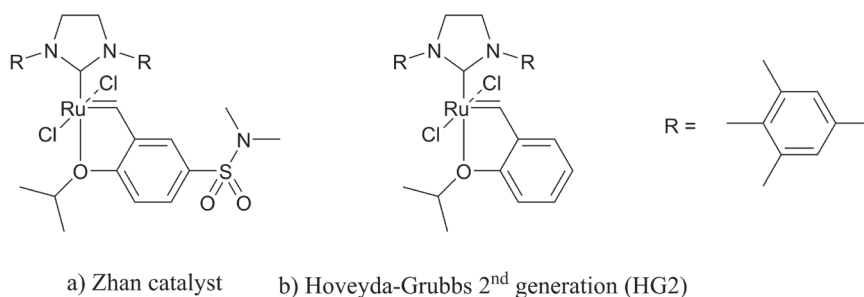
Figure 4.1. a) Zhan catalyst and b) Hoveyda-Grubbs 2nd generation (HG2)

Next to chemically modifying the support material, the support could also be synthesized around the catalyst. For this purpose, metal organic frameworks (MOFs) are suitable due to their simple synthesis procedures at low temperatures. MOFs are large, well-defined, networks consisting of mono or polynuclear coordination entities linked together by bridging organic ligands and potentially contain voids.[7] These structures are generally built from metal ions or clusters linked together by organic carboxylates or other similar organic molecules. MOFs can exhibit good chemical stability and porosity. By selecting different organic linkers and metal salts, the porosity of MOFs can be tuned. This makes them potential candidates for applications in for example gas storage, gas separation and catalysis.[8] The cavity and pore sizes of MOFs have been applied to trap various compounds for catalysis or slow drug release. For example, caffeine has been trapped in ZIF-8, a zinc based MOF, which resulted in a controlled release of caffeine over a period of 27 days.[9] Moreover, nanoparticles could be immobilised in MIL-101-NH$_2$(Cr) and used in a C-C cross coupling reaction.[10] Finally, organometallic compounds, such as positively charged polypyridyl ruthenium compounds, can be immobilised in a negatively charged manganese MOF.[11] The entrapment of catalysts in MOFs is considered to be a promising technique to reach enhanced stability of the catalyst and could also result in size selection of the substrate.[12]

For the entrapment of Zhan catalyst and HG2, MIL-101-NH$_2$(Al)(**1**) is an especially interesting MOF due to its relative simple, one step synthesis from readily available chemicals and large cavity and pore sizes. With cavity sizes of 29 and 34 Å and pore sizes of 12 and 16 Å[10], MIL-101-NH$_2$(Al)(**1**) has sufficient cavity space for the HG2 catalyst (18 x 14 x 11 Å)[6] and the pores are sufficiently small to prevent the catalyst from leaching out. During synthesis of MIL-101-NH$_2$(Al)(**1**) an intermediate structure (MIL-235) is formed first, which then proceeds to form either MIL-101-NH$_2$(Al)(**1**) or MIL-53-NH$_2$(Al)(**2**) depending on the reaction conditions. Presence of water promotes the thermodynamic product MIL-53-NH$_2$(Al)(**2**) and presence of dimethylformamide (DMF) guides the structure to form MIL-101-NH$_2$(Al)(**1**).[13, 14]

These two structures contain different secondary building units (SBUs), with the MIL-101 structure having tri-nuclear coordination entities leading to trigonal prismatic SBU's, connected by the terephthalate bridges giving a more complex topology **mtn-e**, a quadrinodal 6-c net.[15] In contrast, the MIL-53 structure is a so called rod-MOF, where there are no discrete SBUs but an infinite chain of oxygen bridged metal ions giving us the **sra** topology.[16] This difference in topology leads to a different pore structure, where the MIL-101 structure has large spherical cavities and the MIL-53 structure consists of rhombic channels as can be seen in Figure 4.2. The **sra** topology of MIL-53-NH$_2$(Al)(**2**) allows for the material to show a 'breathing' behaviour, where the pores are flexible and can widen when a guest molecule is introduced.[17, 18]
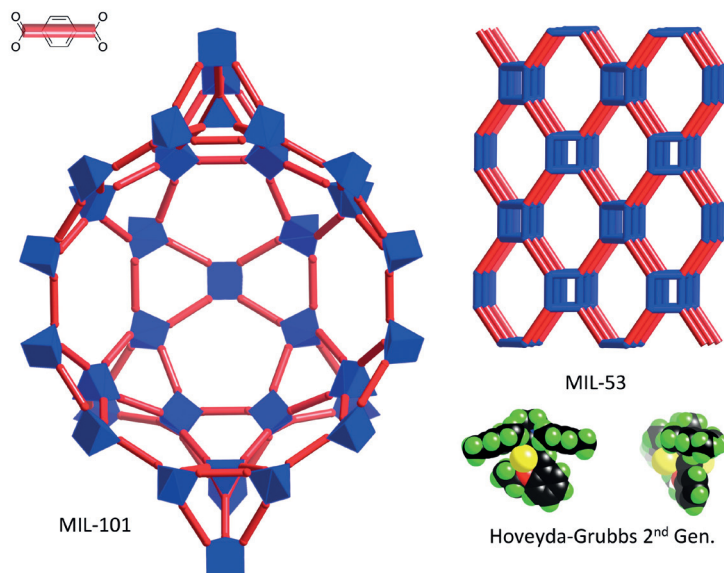
Figure 4.2. Structures drawn to scale of MIL-101 (left) with trinuclear SBUs (blue prisms) connected with the 1,4-benzenedicarboxylate ligands (red tubes) showing one of the large cavities19 and MIL-53 (right, top) with a ladder motif of interconnected metal ions in blue and again the 1,4-benzenedicarboxylate ligands (red tubes)20. These are compared to two views of the Hoveyda-Grubbs 2nd generation catalyst (HG2) drawn with the same scale (right, bottom). In the picture no allowance for the breathing behaviour of MIL-53 has been made.

To enable a catalyst to be trapped into the MOF, the catalyst can be synthesized inside the MOF *via* either a 'ship in a bottle' method or a 'bottle around ship' method.[21] An example of the former is formation of nanoparticles in a MOF, where Pd(II) was impregnated into the open MOF structure followed by reduction to form palladium nanoparticles inside the MOF structure. The resulting catalyst gave full conversion for the Suzuki-Miyaura coupling, a cross coupling forming carbon-carbon bonds, in water after 6 hours with a catalyst loading of 3 mol%, for 10 consecutive runs.[10] Bogaerts et al. showed the successful immobilisation of a palladium catalyst in MIL-101-NH$_2$(Al) (**1**) using the 'bottle around the ship' method. The resulting heterogeneous catalyst achieves a turn over number (TON) of 800 for an epoxidation reaction for each of 4 catalytic runs using 0.7 mol% catalyst in DCM for two hours.[21]

The 'ship in a bottle' method requires several synthetic steps, where the MOF is synthesized first followed by the synthesis of the catalyst inside the MOF, which requires the MOF to be stable under the synthesis conditions of the catalyst. The 'bottle around the ship' method only requires one synthesis step, where the MOF is synthesised around the catalyst. This requires the catalyst to be stable under the synthesis conditions of the MOF. In the example

of MIL-101-NH$_2$(Al) (**1**), the conditions include heating to 110 °C overnight and a build-up of acid.[14] Since the Zhan catalyst and HG2 are commercially available, the 'bottle around the ship' method is preferred.

To avoid exposing the catalyst to the solvent based synthesis conditions of the MOF, catalysts could be immobilised in MOFs by mechanochemical methods instead, for example by grinding in a ball mill. Mechanochemical reactions, performed by applying mechanical energy, have gained attention as an attractive alternative to traditional solution based thermal reactions due to their efficient use of materials and lower energy requirements.[22] The lack of mechanistic insight makes mechanochemistry less predictable and the implications for large scale use are not yet well known,[22] however, novel *in situ* monitoring techniques are being employed in the pursuit of mechanistic understanding.[23] To gain mechanistic insight, Pichon *et al.* showed the mechanochemical synthesis of many different MOF structures. Twelve different metal salts were combined with five different organic linkers in a ball mill and ground for 15 minutes. Some of the resulting compounds were sufficiently crystalline to obtain powder X-ray data.[24] This implies that the components were able to rearrange in order to form a well-defined crystalline MOF structures.

MOF structures with cavities have been also been prepared by mechanochemistry, where the presence of a small amount of solvent, such as H$_2$O, acetic acid or DMF, added or formed during the process, functioned as a template for the MOF structure and stabilised the cavities.[25] Next to solvent molecules, the Keggin anion [PMo$_{12}$O$_{40}$]$^{6-}$ was successfully encapsulated in the MOF HKUST-1 by mechanochemical means.[26] However, trapping molecules in a pre-synthesized MOF by mechanochemistry has currently not been reported.

Here we report the application of two techniques, the 'bottle around the ship' method and mechanochemical synthesis, for the immobilisation of HG2 or Zhan catalyst (Figure 4.1) MOFs. The influence of mechanochemical treatment on both MIL-53-NH$_2$(Al)(**2**) and MIL-101-NH$_2$(Al) (**1**) structure has been studied by nitrogen sorption and powder X-ray diffraction (PXRD). After successful immobilisation of these metathesis catalysts in MIL-53-NH$_2$(Al)(**2**) and MIL-101-NH$_2$(Al)(**1**) by mechanochemical methods, the catalytic activity of the immobilised catalysts were subsequently tested in the metathesis of DDM.

4.2 Experimental

Mechanochemical experiments were performed with a Fritsch planetary mill pulverisette 5. Wide angle X-ray scattering (WAXS) powder diffractograms were recorded on a Philips PC-APD diffractometer in the reflection geometry in the angular range 4-40° (2θ), with a step size of 0.02° (2θ) and an acquisition time of 4.0 s per step. The Cu Ka1 radiation from the anode, generated at 30 kV and 50 mA, was monochromatized using a 15 μm Ni foil (λ = 0.1542 nm). The diffractometer was equipped with a 1° divergence slit, a 0.2 mm receiving slit, and a 1° scatter slit. IR spectra were recorded with a Varian 1000 FT-IR, Scimitar Series. Scanning

electron microscope (SEM) images were obtained by the following procedure: Samples were mounted on sample holders by carbon adhesive tabs (EMS, Washington, USA) and subsequently sputter coated with 8 nm Iridium (MED 020, Leica, Vienna, Austria). Samples were analyzed at 2 KV at room temperature in a field emission scanning electron microscope (Magellan 400, FEI, Eindhoven, the Netherlands). EDX analyses were accomplished in the same field emission scanning electron microscope by an X-Max/AZtec X-ray analyser (Oxford Instruments Analytical, High Wycombe, England) at an acceleration voltage of 15 kV. N2-physisorption isotherms were recorded with a Micromeritics Tristar II Plus at −196°C. Both adsorption and desorption isotherms were measured. The samples (20 mg) were dried overnight at high vacuum at 200°C prior to performing the measurement. The specific surface areas were calculated according to the Brunauer-Emmett-Teller (BET) method. The total pore volume was defined as the single-point pore volume at $p/p0 = 0.95$. Ruthenium content was determined using an AAS technique by Mikroanalytisches Laboratorium Kolbe. AlCl3.6H2O, 2-aminoterephthalic acid, diethyl diallylmalonate and Hoveyda-Grubbs 2nd generation catalyst were purchased from Sigma Aldrich. Dimethyl formamide and acetone were purchased from Merck, anhydrous dichloromethane was purchased from VWR. Zhan catalyst 1B (44-0082) and hydroxyl-methyl-phenyl resin supported Zhan catalyst (44-0083) were purchased from Strem Chemicals. MIL-53-NH2(Al) was kindly provided by the catalyst engineering group of TU Delft. All chemicals were used as received. Data visualization was aided by Daniel's XL Toolbox addin for Excel, version 6.60.

4.2.1 SYNTHESIS OF MIL-101-NH2(AL) (1)

1.944 g (0.0106 mol) 2-amino terephtalic acid was dissolved in 120 mL dimethylformamide (DMF) in a 250 mL three necked flask equipped with a reflux condenser, stirring bar and two stoppers. The solution was heated to 110 °C and 2.603 g (0.0108 mol) AlCl3.6H2O was added in four portions with a twenty minutes interval while keeping the solution stirred at 110 °C. The solution changed colour from brown to bright yellow. Three hours after the last AlCl3 addition, the stirring was shut down and the solution was maintained at 110 °C for 20 hours. The product was filtered off, washed with 3 x 40 mL DMF and dried in an oven at 110 °C overnight. Yield is 3.18 g as bright yellow powder.

4.2.2 MECHANOCHEMICAL PROCEDURE.

1.2 g of MIL-101-NH2(Al) and 53 mg Hoveyda-Grubbs 2nd generation catalyst was added in a ball-mill with agate cups and balls. The seven balls used had a total mass of 9.94 g. The mill was run three times for 15 minutes at 360 RPM with 5 minutes intervals. The product was obtained as a green powder and washed with acetone using the centrifuge (15 minutes @ 3500 RPM). It should be noted that when oven drying was skipped after MIL-101-NH2(Al) synthesis, the immobilisation did not succeed. Moreover, when Teflon balls were used, small Teflon wires were observed in the product using scanning electron microscope techniques, where they could be identified by their fluorine content (SEM-EDX). No agate pollution was observed.

4.2.3 IMPREGNATION

11.0 mg Hoveyda-Grubbs 2nd generation catalyst dissolved in 0.75 mL dry DCM was added to 256.3 mg MIL-101-NH2(Al) in a centrifuge flask with septum. The moist solid was left under argon for two days before washing three times with 5 mL dry DCM using the centrifuge (15 minutes @ 3500 RPM).

4.2.4 CATALYSIS

A stock solution of 300 mg diethyl diallylmalonate (DDM) in 50 mL dry dichloromethane (DCM) was bubbled through with an argon flow for 2 hours. 250 mg loaded MOF (5 mol% HG2; 3 mol% Zhan) was put in a Schlenk tube under argon atmosphere with a stirring bar. 5 mL stock was added to the Schlenk tube and the reaction mixture was stirred for 24 hours at room temperature under argon atmosphere. The mixture was transferred to a centrifuge tube under argon flow, the centrifuge tube was equipped with a septum and centrifuged for 15 minutes at 3500 RPM. The liquid was decanted and the solid was washed twice with 5 mL dry DCM. The solid was transferred to a Schlenk tube for the next catalytic run.

4.3 Results and Discussion

The synthesis of MIL-101-NH$_2$(Al)(**1**) is well known and can be performed in an oven or under microwave irradiation.[27] This procedure was further developed to enable synthesis in standard laboratory glassware by heating 1 gram of starting materials in dimethylformamide (DMF) to 110 °C and a stepwise addition of AlCl$_3$.[28] By using this method on a larger scale we obtained 3 grams MIL-101-NH$_2$(Al)(**1**) per batch. BET surface analysis gave similar results as literature (2131 m²/g compared to 2100 m²/g)[27] and the IR spectra are identical, clearly showing the characteristic peaks for NH$_2$ around 3400 cm^{-1} (Figure C1, appendix C).[27] The Powder X-Ray Diffraction (PXRD) pattern is in correspondence to the predicted values (Figure C3, appendix C).

4.3.1 BOTTLE AROUND THE SHIP METHOD

To test the possibility of a 'bottle around the ship' method, an adapted procedure of Bogaerts *et al.* was used,[21] where Hoveyda-Grubbs 2nd generation catalyst (HG2) (Figure 4.1b) was added in the reaction mixture of MIL-101-NH$_2$(Al)(**1**). However, this leads to a rapid colour change from dark green to a bright red colour. This indicates that the dark green coloured HG2 reacted to form another ruthenium species and that HG2 is not stable under these reaction conditions. Therefore we conclude that no immobilisation of unmodified HG2 was achieved using a 'bottle around the ship' method. It has been reported that HG2 is a stable catalyst in the presence

of AlCl$_3$.[29] However, the combination of heat, acid and the AlCl$_3$ apparently causes the HG2 to react. This means that a solvent based 'bottle around the ship' approach cannot be applied when immobilising HG2 in MIL-101-NH$_2$(Al)(**1**) and a different approach is necessary.

4.3.2 MECHANOCHEMICAL IMMOBILISATION OF HG2

Mechanochemical immobilisation of HG2 in MIL-101-NH$_2$(Al)(**1**) was tested by combining HG2 and MIL-101-NH$_2$(Al)(**1**) in a ball mill. This resulted in HG2@MIL-101-NH$_2$(Al)(**3**), a green powder with a ruthenium loading of 0.25% after thorough washing with DCM, which is equivalent to 0.025 mmol HG2 per gram MOF. This is in a similar range obtained for the 'bottle around the ship' method used for the Jacobsen salen complex which resulted in 0.02 mmol catalyst per gram MOF.[21] Moreover, the percentage HG2 immobilised during this procedure is 39%, whereas 'bottle around ship' method immobilised 25% of the starting palladium catalyst,[21] although it should be noted that these procedures are not yet optimised for high catalyst uptake.

For comparison, MIL-101-NH$_2$(Al)(**1**) was also ground without catalyst present, which resulted in a decrease of BET surface from 2131 to 223 m²/g, while HG2@MIL-101-NH$_2$(Al)(**3**) has a BET surface of 347 m²/g (Table 4.1, entries 1, 2 and 3).

Table 4.1. Analysis results of loaded and unloaded MOFs

Entry	Compound	BET (m2/g)	Ruthenium loading
1	MIL-101-NH2(Al)(1)	2131	0.0049
2	Ground MIL-101-NH2(Al)	223	nd
3	HG2@MIL-101-NH2(Al)(3)	347	0.25
4	HG2@MIL-53-NH2(Al)(4)Zhan	41	0.15
5	MIL-101-NH2(Al)(5)	417	0.16

nd = not determined

4

Figure 4.3 compares the powder X-ray diffractograms (PXRD) of ground MIL-101-NH$_2$(Al)(**1**) and HG2@MIL-101-NH$_2$(Al)(**3**) with synthesized MIL-101-NH$_2$(Al)(**1**) and MIL-53-NH$_2$(Al) (**2**) from literature.[20]
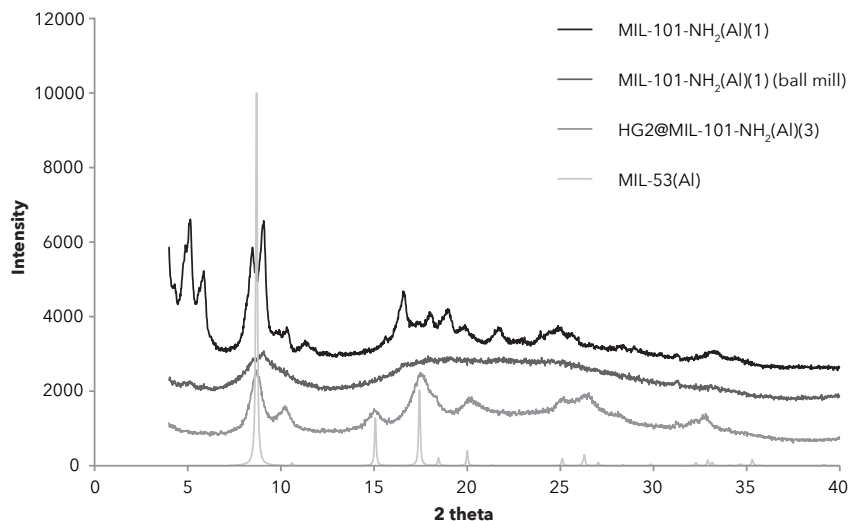
Figure 4.3. Powder X-ray Diffraction (PXRD) patterns of MIL-101-NH2(Al)(1) as synthesized, after mechanochemical treatment and after mechanochemical treatment with HG2 compared to the calculated MIL-53(Al) spectrum from literature.[20]

Figure 4.3 shows that MIL-101-NH$_2$(Al)(**1**) loses its distinctive peaks after mechanochemical treatment ("MIL-101 (ball mill)" compared to "MIL-101-NH$_2$(Al)(**1**)" in Figure 4.3. The PXRD for HG2@MIL-101-NH$_2$(Al)(**3**) shows a pattern characteristic to MIL-53-NH$_2$(Al)(**2**) rather than MIL-101-NH$_2$(Al)(**1**) (Figure 4.3). Based on these results we propose the mechanochemical conversion of MIL-101-NH$_2$(Al)(**1**) to MIL-53-NH$_2$(Al)(**2**), which is the thermodynamically favoured structure.[14] This conversion demonstrates that the MOF structures can break open and new bonds can form during mechanochemical procedures. Interestingly, the introduction of HG2 promotes the conversion of MIL-101-NH$_2$(Al)(**1**) to MIL-53-NH$_2$(Al)(**2**), where MIL-101-NH$_2$(Al)(**1**) without added catalyst does not show a clear transition. It is unclear what causes this effect, since a templating effect is unlikely considering that the size of HG2 (18 x 14 x 11 Å)[6] does not match the pore size of MIL-53-NH$_2$(Al)(**2**)(7.5 Å).[30]

The pore distribution obtained from nitrogen sorption is shown in Figure 4.4, where the pore distribution of ground MIL-101-NH$_2$(Al)(**1**) is compared to MIL-101-NH$_2$(Al)(**1**) and MIL-53-NH$_2$(Al)(**2**).
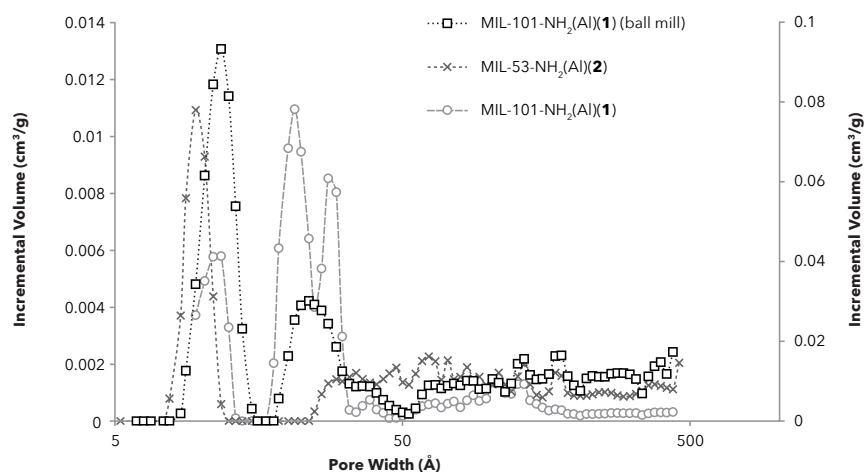
Figure 4.4. Pore distribution of MIL-53-NH2(Al)(2), MIL-101-NH2(Al)(1) and ground MIL-101-NH2(Al)(1).

Figure 4.4 reveals a similar pattern between MIL-101-NH$_2$(Al)(**1**) and ground MIL-101-NH$_2$(Al)(**1**), especially for the larger pores, which are absent in a MIL-53 structure. This indicates that some of the MIL-101 structure may still be intact and provide the cavities for the HG2 catalyst.

To further study the mechanochemical conversion of MIL-101-NH$_2$(Al)(**1**) to MIL-53-NH$_2$(Al)(**2**), the stability of MIL-53-NH$_2$(Al)(**2**) in a ball mill was investigated. Introducing MIL-53-NH$_2$(Al)(**2**) to a ball mill with or without HG2 results in a MIL-53 structure with a less defined PXRD pattern. Pore distribution is similar to MIL-53-NH$_2$(Al)(**2**) and the grinding of the material leads to a wider pore distribution. No evidence of the presence of a MIL-101 structure was observed, which can be explained by MIL-53 being the thermodynamic favoured structure.[14]

Starting from MIL-53-NH$_2$(Al)(**2**) for the immobilisation of HG2 resulted in a ruthenium loading of 0.15% in HG2@MIL-53-NH$_2$(Al)(**4**), slightly lower than for HG2@MIL-101-NH$_2$(Al)(**3**) (0.25%) (Table 4.1, entries 3 and 4). The entrapment of HG2 in MIL-53-NH$_2$(Al)(**2**) shows that the structure is capable of opening and closing *via* the mechanochemical procedure, which allows for the catalyst to enter into the structure. The lower loading of HG2@MIL-53-NH$_2$(Al)(**4**) compared to HG2@MIL-101-NH$_2$(Al)(**3**) could arise from the thermodynamic stability of MIL-53-NH$_2$(Al)(**2**), making it less reactive and therefore more difficult for the catalyst to enter the structure. Another explanation is the lack of large cavities, such as those present in MIL-101-NH$_2$(Al)(**1**), prevent higher catalyst loadings. BET surface for HG2@MIL-53-NH$_2$(Al)(**4**) is 41 m²/g, which is significantly lower than HG2@MIL-101-NH$_2$(Al)(**3**) (347 m²/g) (Table 4.1, entries 3 and 4).

In short, the mechanochemical treatment of MIL-101-NH$_2$(Al)(**1**) leads to a partial conversion to the thermodynamic product MIL-53-NH$_2$(Al)(**2**). When HG2 is introduced in the mechanochemical treatment of the MOF structures, this conversion is more evident in PXRD. HG2 can also be immobilised in MIL-53-NH$_2$(Al)(**2**) using this method, but this leads to a lower ruthenium loading (0.15% compared to 0.25%).

4.3.3 REACTIVITY OF IMMOBILISED CATALYSTS

With the successful entrapment of HG2 into the MOF structures, the activity of the trapped HG2 catalyst was investigated. It was observed that HG2@MIL-101-NH$_2$(Al)(**3**) is active in a cyclization of diethyl diallylmalonate (DDM) (Scheme 4.1), which was used as a way to determine metathesis activity of the loaded MOF. To determine reusability, the same catalyst sample was used for a series of consecutive runs (Figure 4.5). For consecutive runs the reaction mixture was centrifuged and, after separation of the liquid, the catalyst was washed three times with DCM.
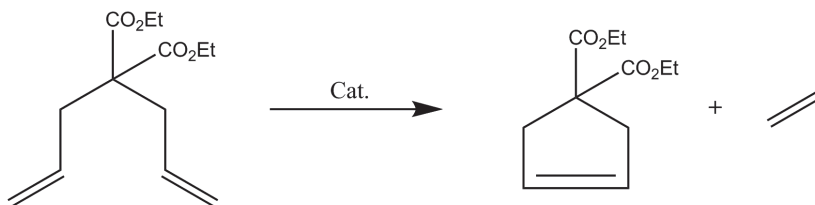
diethyl diallylmalonate (DDM)

Scheme 4.1. Cyclization of diethyl diallylmalonate (DDM), a standard reaction to test olefin metathesis activity.

The first run gives an almost full conversion with full selectivity (Figure 4.5). In the consecutive runs the activity steadily decreases. High initial conversion indicates that the catalyst in HG2@MIL-101-NH$_2$(Al)(**3**) remains active after immobilisation. Leaching of the catalyst is ruled out as a reason for the following deactivation, since the ruthenium content remains stable (0.25% at the end of 8 runs). Moreover, a leaching experiment, where the MOF was separated from the reaction mixture and the filtrate was allowed to stir for 24 hours showed no conversion, demonstrating that the reactivity does not come from traces of leached ruthenium. Therefore the deactivation must originate from a deactivation of the metathesis catalyst itself. Inherent catalyst deactivation has been observed before when HG2 molecules are immobilised with low loadings.[5]
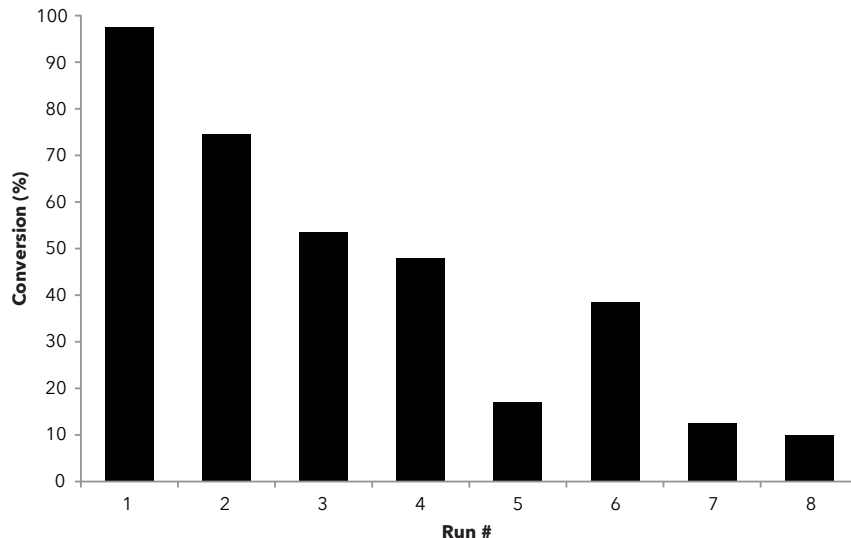
Figure 4.5. The metathesis of diethyl diallylmalonate (DDM) using HG2@MIL-101-NH2(Al) (3). Reaction conditions: equivalent of 5 mol% HG2 catalyst, RT, 24 hours, 0.05M DDM, 5 mL DCM. All reactions show full selectivity. Average of duplicate experiments.

In a system where HG2 is encapsulated in silica, a similar initial conversion could be obtained (95%) with the same catalyst loading (5 mol%) and a shorter reaction time (1h).[6] This catalyst was more stable than the immobilised catalyst reported here, where the conversion remained 57% after 7 cycles in 8 hours, compared to 13% conversion after 7 cycles in 24 hours. The authors contribute their catalyst deactivation by the inherent deactivation of HG2 as well.[6] Since we observe no leaching of ruthenium, the faster deactivation we observe is likely to originate from traces of oxygen entering the system when the reaction mixture is transferred to centrifuge tubes.

To further test the hypothesis that mechanochemistry enables the structure of a MOF to form around the catalyst and that reactivity can not originate from catalyst adsorbtion on the MOF, an impregnation experiment was performed. Here MIL-101-NH$_2$(Al)(**1**) was impregnated with HG2 in anhydrous DCM, resulting in a green powder. However, the green colour was removed by washing with DCM and the resultant yellow powder showed no activity during a reaction with DDM. This confirms that the mechanochemical method allows for immobilisations that cannot be obtained by standard impregnation techniques. The difference most likely results from mechanochemistry enabling the catalyst to be trapped inside the structure of the MOF, whereas impregnation only allows the catalyst to adsorb on the outer walls of the MOF structure. This adsorption to MOFs is not strong enough to prevent washing off by DCM. This effect has been observed before with the adsorption of HG2 to silica, where leaching of HG2 is observed using polar solvents.[31]

In the cyclization of DDM, HG2@MIL-53-NH$_2$(Al)(**4**) showed no significant catalytic activity in identical conditions as Figure 4.5 (<0.5% conversion). The different behaviour of the two materials lead us to conclude that some of the original MIL-101 structure is still intact after mechanochemical immobilisation of HG2 in MIL-101-NH$_2$(Al)(**1**). There is no MIL-101 structure present after mechanochemical treatment of MIL-53-NH$_2$(Al)(**2**). This remaining MIL-101 structure apparently fulfils an important role during catalysis. The large cavities of MIL-101 may provide enough room to accommodate the HG2 catalyst and enable catalytic activity in HG2@MIL-101-NH$_2$(Al)(**3**), where this space is not available in MIL-53-NH$_2$(Al) (**2**) and therefore also not in HG2@MIL-53-NH$_2$(Al)(**4**)(Figure 4.6). This hypothesis is supported by the preservation of larger pores in the pore distribution of ground MIL-101-NH$_2$(Al) (**1**), which are absent in a MIL-53 structure (Figure 4.4).
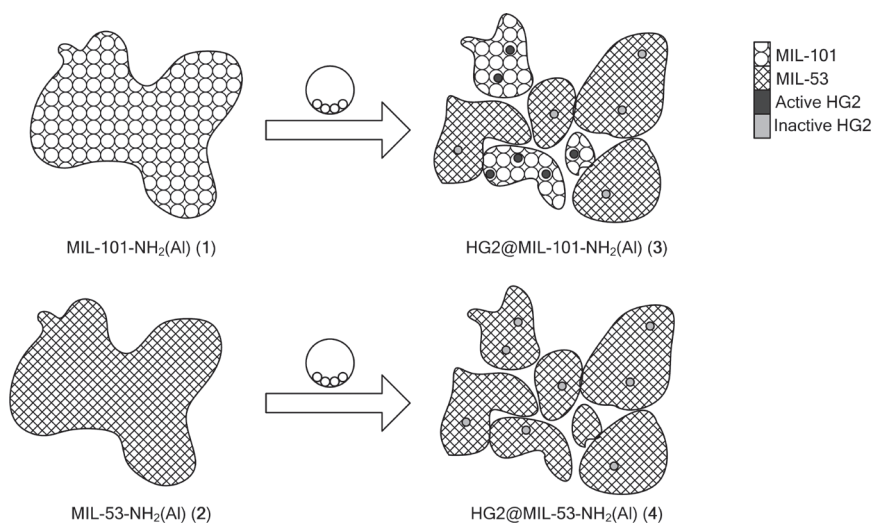
Figure 4.6. Proposed mechanochemical immobilisation, using a ball mill, of Hoveyda-Grubbs 2nd generation catalyst (HG2) starting from MIL-101-NH2(Al)(1) and MIL-52-NH2(Al)(2) resulting in the active HG2@MIL-101-NH2(Al)(3) and the inactive HG2@MIL-53-NH2(Al)(4).

4.3.4 IMMOBILISATION OF ZHAN CATALYST

To explore the versatility of the mechanochemical immobilisation method, Zhan catalyst (Figure 4.1a) was immobilised in MIL-101-NH$_2$(Al)(**1**) to obtain Zhan@MIL-101-NH$_2$(Al)(**5**). Similar results are obtained as for HG2@MIL-101-NH$_2$(Al)(**3**) when immobilising Zhan catalyst, where a dark green powder was obtained from ball-milling the catalyst with MIL-101-NH$_2$(Al)(**1**). This catalyst has a slightly lower ruthenium loading of 0.16% compared to 0.25% (Table 4.1, entries 5 and 3), which could be explained by the larger size of Zhan catalyst compared to HG2. The IR spectrum was identical to MIL-101-NH$_2$(Al)(**1**) and the BET surface comparable to

that of HG2@MIL-101-NH$_2$(Al)(**3**) (417 m²/g for Zhan@MIL-101-NH$_2$(Al)(**5**) and 347 m²/g for HG2@MIL-101-NH$_2$(Al)(**3**), Table 4.1, entries 5 and 3). The activity Zhan@MIL-101-NH$_2$(Al) (**5**) was also explored using the conversion of DDM (Scheme 4.1).
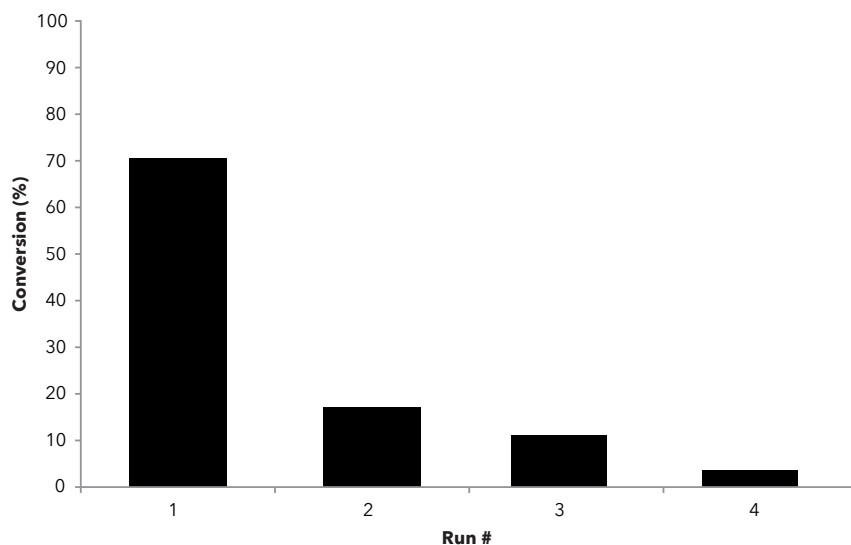

Figure 4.7. The metathesis of diethyl diallylmalonate (DDM) using Zhan@MIL-101-NH2(Al) (5). Reaction conditions: equivalent of 3 mol% catalyst, RT, 24 hours, 0.05M DDM, 5 mL DCM. All reactions show full selectivity. Average of duplicate experiments.

A lower conversion in the first run is obtained using Zhan@MIL-101-NH$_2$(Al)(**5**) compared to HG2@MIL-101-NH$_2$(Al)(**3**) (71% for Zhan@MIL-101-NH$_2$(Al)(**5**) and 98% for HG2@ MIL-101-NH$_2$(Al)(**3**)), followed by a similar decline in activity (Figure 4.7). The ruthenium content did not decrease and went from 0.16% after synthesis to 0.21% after the four catalytic runs. This increase could originate from small MOF particles being washed away after centrifugation, leaving the larger particles with catalyst behind, effectively increasing the catalyst loading. The decrease in activity is expected to originate from the same catalyst deactivation as observed for HG2@MIL-101-NH$_2$(Al)(**3**) (Figure 4.5).

The resin supported Zhan catalyst, which is the only commercially available immobilised metathesis catalyst, shows a lower conversion than the two ruthenium catalysts in MOFs, HG2@MIL-101-NH$_2$(Al)(**3**) and Zhan@MIL-101-NH$_2$(Al)(**5**). At similar conditions the resin supported catalyst shows an initial conversion of 57%, significantly lower than the 98% and 71% for the catalysts immobilised in MOFs. Moreover, no activity was observed after the first run of the resin supported catalyst, probably due to the immobilisation site of the resin supported catalyst, which is anchored on the activation site and after activation the catalyst will freely dissolve in DCM.

4.3.5 OUTLOOK

More control over the atmosphere during separation and recycling of the catalyst will likely improve catalyst activity for consecutive runs. With further understanding of the reactivity of MIL-101-NH$_2$(Al)(**1**) in mechanochemical conditions combined with higher catalyst stability, this would lead to a simple one step immobilisation of ruthenium metathesis catalysts in a MOF, available in a single step from commercial starting materials.

While it is difficult to separate decreasing particle size from the onset of a transition to an amorphous phase, we note that amorphous MOFs are attracting interest[32] and our compounds are possibly on the borderline to this interesting sub-class of MOFs.

This is the first example of using mechanochemistry to immobilise catalysts in MOFs. With a wide variety of MOFs available and their relative unknown reactivity in mechanochemical conditions, this technique could be further explored to obtain an immobilisation method for homogeneous catalysts that does not require catalyst modification. We suggest the method may indeed be quite general, as the initial cavities on MIL-101 are large enough for most homogeneous catalysts to enter and be immobilised just as these metathesis catalysts.

4.4 Conclusions

A simple, one step mechanochemical procedure was developed to immobilise ruthenium based metathesis catalysts inside metal organic frameworks (MOFs). Using a solution based 'bottle around the ship' method did not result in immobilisation of Hoveyda-Grubbs 2nd generation catalyst (HG2) in MIL-101-NH$_2$(Al). The successful immobilisation was achieved by grinding MIL-101-NH$_2$(Al) with Hoveyda-Grubbs 2nd generation or Zhan catalyst. Both MIL-101 based catalysts show metathesis activity. The highest activity in the metathesis of diethyl diallylmalonate was obtained using HG2@MIL-101-NH$_2$(Al), which showed an initial conversion of 98% and shows activity over 8 consecutive runs. The mechanochemical preparation of the immobilised catalysts modified the structure of the MOF and converted the MIL-101 structure partially to a MIL-53 structure. The Hoveyda-Grubbs entrapped in the MIL-101 part is responsible for the observed catalytic activity. This is the first report of a mechanochemical immobilisation of an active catalyst in a MOF and given the wide variety of catalysts and known MOF structures available, a new immobilisation technique for homogeneous catalysts is suggested.

4.5 References

1.   Deraedt, C.; d'Halluin, M.; Astruc, D. *European Journal of Inorganic Chemistry* **2013**, 4881 - 4908.

2.   Szczepaniak, G.; Kosiński, K.; Grela, K. *Green Chem*. **2014,** 16, (10), 4474-4492.

3.   Buchmeiser, M. R. *Chemical reviews* **2009,** 109, 303-321.

4.   Yang, H.; Ma, Z.; Wang, Y.; Fang, L. *Chemical communications* **2010,** 46, (45), 8659-61.

5.   Zelin, J.; Trasarti, A. F.; Apesteguía, C. R. *Catalysis Communications* **2013,** 42, 84-88.

6.   Yang, H.; Ma, Z.; Zhou, T.; Zhang, W.; Chao, J.; Qin, Y. *ChemCatChem* **2013,** 5, (8), 2278-2287.

7.   Batten, S. R.; Champness, N. R.; Chen, X.-M.; Garcia-Martinez, J.; Kitagawa, S.; Öhrström, L.; O'Keeffe, M.; Paik Suh, M.; Reedijk, J. *Pure and Applied Chemistry* **2013,** 85, (8).

8.   Furukawa, H.; Cordova, K. E.; O'Keeffe, M.; Yaghi, O. M. *Science* **2013,** 341, (6149), 1230444.

9.   Liedana, N.; Galve, A.; Rubio, C.; Tellez, C.; Coronas, J. *ACS applied materials & interfaces* **2012,** 4, (9), 5016-21.

10. Pascanu, V.; Yao, Q.; Bermejo Gomez, A.; Gustafsson, M.; Yun, Y.; Wan, W.; Samain, L.; Zou, X.; Martin-Matute, B. *Chemistry* **2013,** 19, (51), 17483-93.

11. Sen, R.; Koner, S.; Bhattacharjee, A.; Kusz, J.; Miyashita, Y.; Okamoto, K. *Dalton transactions* **2011,** 40, (26), 6952-60.

12. Lee, J.; Farha, O. K.; Roberts, J.; Scheidt, K. A.; Nguyen, S. T.; Hupp, J. T. *Chemical Society reviews* **2009,** 38, (5), 1450-9.

13. Goesten, M. G.; Stavitski, E.; Juan-Alcañiz, J.; Martiñez-Joaristi, A.; Petukhov, A. V.; Kapteijn, F.; Gascon, J. *Catalysis Today* **2013,** 205, 120-127.

14. Goesten, M. G.; Magusin, P. C.; Pidko, E. A.; Mezari, B.; Hensen, E. J.; Kapteijn, F.; Gascon, J. *Inorganic chemistry* **2014,** 53, (2), 882-7.

15. O'Keeffe, M.; Yaghi, O. M. *Chemical reviews* **2012,** 112, (2), 675-702.

16. Stavitski, E.; Goesten, M.; Juan-Alcaniz, J.; Martinez-Joaristi, A.; Serra-Crespo, P.; Petukhov, A. V.; Gascon, J.; Kapteijn, F. *Angewandte Chemie* **2011,** 50, (41), 9624-8.

17. Boutin, A.; Couck, S.; Coudert, F.-X.; Serra-Crespo, P.; Gascon, J.; Kapteijn, F.; Fuchs, A. H.; Denayer, J. F. M. *Microporous and Mesoporous Materials* **2011,** 140, (1-3), 108-113.

18. Stavitski, E.; Pidko, E. A.; Couck, S.; Remy, T.; Hensen, E. J.; Weckhuysen, B. M.; Denayer, J.; Gascon, J.; Kapteijn, F. *Langmuir : the ACS journal of surfaces and colloids* **2011,** 27, (7), 3970-6.

19. Ferey, G.; Mellot-Draznieks, C.; Serre, C.; Millange, F.; Dutour, J.; Surble, S.; Margiolaki, I. *Science* **2005,** 309, (5743), 2040-2.

4

20. Loiseau, T.; Serre, C.; Huguenard, C.; Fink, G.; Taulelle, F.; Henry, M.; Bataille, T.; Ferey, G. *Chemistry* **2004,** 10, (6), 1373-82.

21. Bogaerts, T.; Van Yperen-De Deyne, A.; Liu, Y. Y.; Lynen, F.; Van Speybroeck, V.; Van Der Voort, P. *Chemical communications* **2013,** 49, (73), 8021-3.

22. James, S. L.; Adams, C. J.; Bolm, C.; Braga, D.; Collier, P.; Friscic, T.; Grepioni, F.; Harris, K. D.; Hyett, G.; Jones, W.; Krebs, A.; Mack, J.; Maini, L.; Orpen, A. G.; Parkin, I. P.; Shearouse, W. C.; Steed, J. W.; Waddell, D. C. *Chemical Society reviews* **2012,** 41, (1), 413-47.

23. Uzarevic, K.; Halasz, I.; Friscic, T. *J Phys Chem Lett* **2015,** 6, (20), 4129-40.

24. Pichon, A.; James, S. L. *CrystEngComm* **2008,** 10, (12), 1839.

25. Friscic, T. *Chemical Society reviews* **2012,** 41, (9), 3493-510.

26. Wilke, M.; Klimakow, M.; Rademann, K.; Emmerling, F. *CrystEngComm* **2016,** 18, (7), 1096-1100.

27. Serra-Crespo, P.; Ramos-Fernandez, E. V.; Gascon, J.; Kapteijn, F. *Chemistry of Materials* **2011,** 23, (10), 2565-2572.

28. Hartmann, M.; Fischer, M. *Microporous and Mesoporous Materials* **2012,** 164, 38-43.

29. Bentz, D.; Laschat, S. *Synthesis* **2000,** 12, 1766-1773.

30. Couck, S.; Remy, T.; Baron, G. V.; Gascon, J.; Kapteijn, F.; Denayer, J. F. *Physical chemistry chemical physics : PCCP* **2010,** 12, (32), 9413-8.

31. Van Berlo, B.; Houthoofd, K.; Sels, B. F.; Jacobs, P. A. *Advanced Synthesis & Catalysis* **2008,** 350, (13), 1949-1953.

32. Bennett, T. D.; Cheetham, A. K. *Accounts of chemical research* **2014,** 47, (5), 1555-62.

4
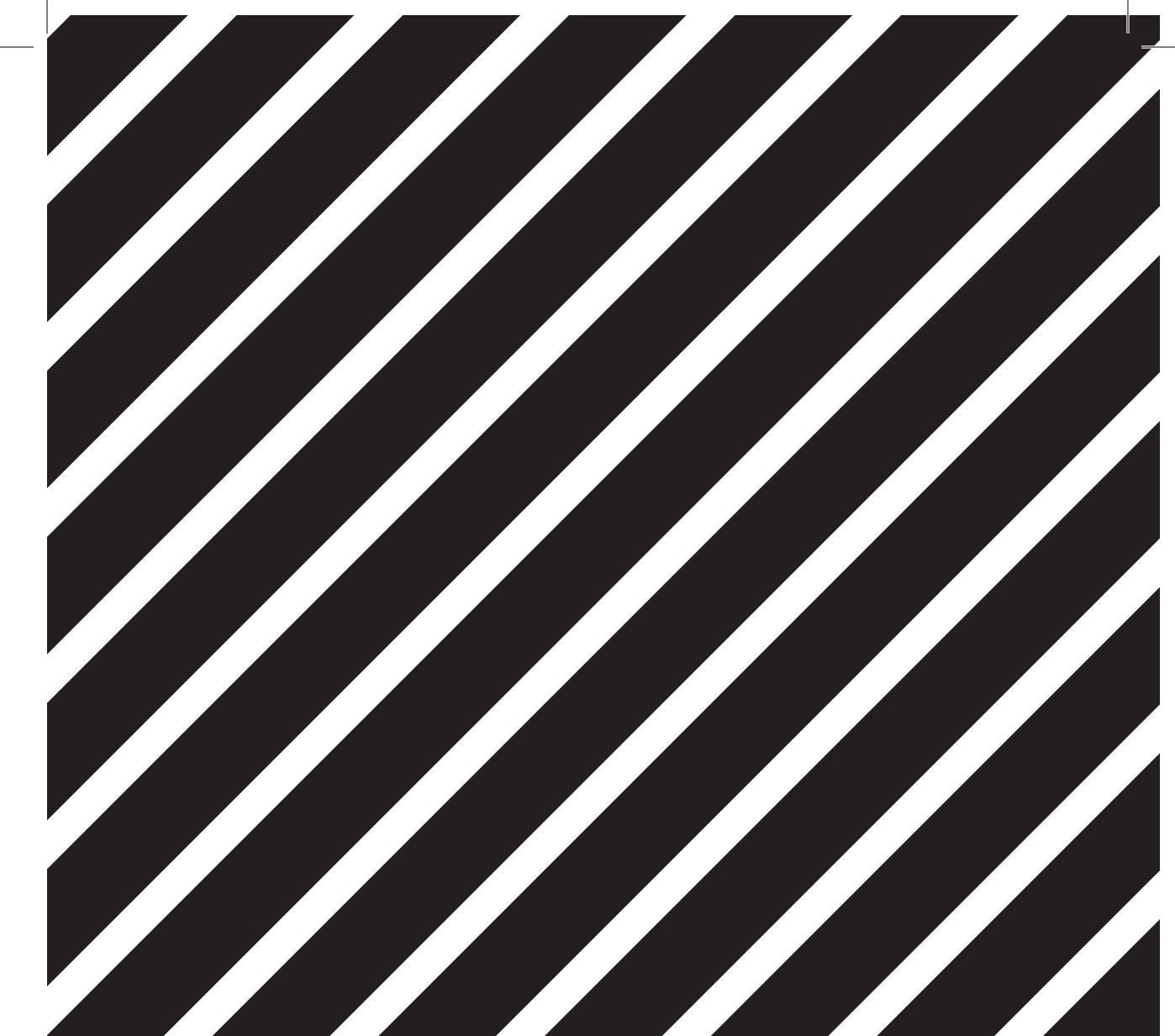
Homogeneous ethenolysis of methyl oleate and other biobased feedstocks

Co-authours for this chapter are J.P.M. Sanders, J.H. Bitter and E.L. Scott

Abstract

The desire to utilise biobased feedstocks and develop more sustainable chemistry poses new challenges in catalysis. A synthetically useful catalytic conversion is ethenolysis, a cross metathesis reaction with ethylene. In this review the state of the art in ethenolysis using methyl oleate was extensively examined and serves as a model compound for fatty acids. Associated to this, the ethenolysis of fatty acids, polymers and more challenging substrates are reviewed. The influence of reaction parameters were investigated and the limiting factors for reaching high turnover numbers identified. It was found that feedstock purity currently has a higher impact on the turnover number of the ethenolysis of methyl oleate than the development of new catalysts.

5.1 Introduction

5.1.1 CROSS METATHESIS IN BIOBASED CHEMISTRY

Due to global warming and the depletion of fossil reserves, an alternative for the use of fossil feedstocks needs to be found. Therefore, replacing fossil feedstocks with sustainable biobased resources to produce chemicals has become an important focus in chemistry. Biomass has the advantage that it can be used as a renewable feedstock and can lead to a sustainable biobased economy. Switching from fossil resources to biomass also brings new challenges for catalysis. In traditional conversions, catalysts were optimised to increase complexity in molecules by introducing functional groups starting from unfunctionalised, fossil based building blocks. Biobased molecules already possess functional groups and catalysis on biomass requires to modify or reposition the functional groups of biobased molecules.[1] A promising catalytic pathway to redistribute functional groups of biomass is olefin cross metathesis (Figure 5.1).
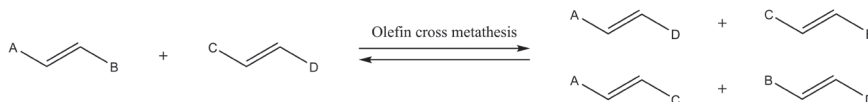
Figure 5.1. Olefin cross metathesis.

Olefin cross metathesis has become a powerful and versatile tool for generating new carbon-carbon bonds. The versatility of the catalysis is underlined by the range of topics in recent reviews. In the field of polymer chemistry, metathesis plays an important role in the synthesis of polymers and is also applied to analyse polymers by breaking the polymer down to small, soluble parts.[2] Metathesis catalysts have been developed to also enable the selective formation of Z-olefins *via* cross metathesis. Moreover, E-olefins are accessible by Z-selective ethenolysis, leaving the E-olefin intact.[3]

Catalyst separation has been a major issue for the use of metathesis catalysts and many articles are published on the topic of catalyst immobilisation, which can be found in a review from 2009.[4] Next to immobilisation, catalyst separation might be achieved by other means. An example is the combination of fluorine chemistry with metathesis. The use of fluorinated solvents might aid in catalyst separation.[5]

Previous reviews on the metathesis of biobased resources focused on rhenium and molybdenum based heterogeneous catalysis on unsaturated fatty acids. The catalysis was shown to be limited by the presence of carbonyl groups in biomass due to interactions with precursors or cocatalysts and coordination to the active site.[6, 7] However, remarkable progress have been made since then, especially with ruthenium based homogeneous catalysts that are tolerant to a broad range of functional groups, such as alcohols, amides, aldehydes and carboxylic acids.[8] With the metathesis catalysts being tolerant to functional groups, the cross metathesis

of fatty acids with ethylene became an attractive process. Fatty acids are usually obtained from transesterification of fats and oils, which are available at a low price due to their large global production volume of 103 million ton per year.[9]

5.1.2 METHYL OLEATE AS MODEL COMPOUND

To investigate the ethenolysis of fatty acids, methyl oleate (MO) is used as a model compound. The ethenolysis of MO leads to the formation of 1-nonene and methyl dec-9-enoate (Figure 5.2).
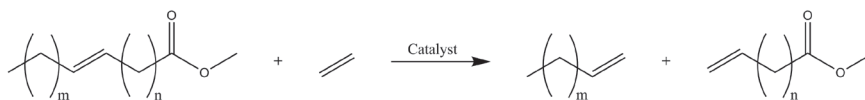
Figure 5.2. Ethenolysis of methyl oleate (MO) forming 1-nonene and methyl dec-9-enoate, m=7, n=7

The ethenolysis of MO was first published in 1981.[10] Here, heterogeneous tungsten and rhenium catalysts were used to convert 60% to 70% of the MO in 5 hours at 50 bar ethylene pressure. The interest in the reaction originated from using the product, methyl dec-9-enoate as intermediate for the synthesis of, for example, the honeybee pheromone 9-oxo-*trans*-dec-2-enoic acid.[10] However, the terminal alkenes that can be produced from fatty acids have a broad range of applications ranging from surfactants to building blocks for plant growth stimulants.[7]

To obtain an economically viable process, The Dow Chemical Company has stated that a turn over number (TON) higher than 50,000 is required for the ethenolysis of MO based on the cost of the homogeneous catalyst.[11] TON is defined as moles of ethenolysis products formed divided by moles of catalyst. Even though a calculation has not been reported, the target TON is the appropriate order of magnitude, since a minimum TON of 1,000 to 10,000 is reported for homogeneous ruthenium catalysts depending on the cost of the product.[12]

In an attempt to achieve TONs over 50,000 significant research has been carried out to develop new metathesis catalysts. An overview of the catalysts discussed in this review can be found in Figure 5.3, Figure 5.4 and an overview of results on the ethenolysis of MO in Table 5.1. Since names of the catalysts differ per paper, we labelled the catalysts Ru1 to Ru59 for ruthenium based catalyst (Figure 5.3), W1, W2 and W3 for tungsten based catalysts and Mo1 to Mo5 for molybdenum based catalysts (Figure 5.4).

In this review we will establish the current state of cross metathesis with small, terminal alkenes such as ethylene (ethenolysis) to obtain terminal alkenes from biomass and waste streams using homogeneous catalysts. Papers focusing on obtaining specific enantioselective products do not fall within the scope of this review and have been reviewed recently elsewhere.[3] To understand the obstaclestt to be overcome, the newly developed catalysts are compared with traditional catalysts Grubbs 1st generation (Ru1) and Hoveyda-Grubbs 2nd generation (Ru48). Next to investigating the type of catalyst, the influence of ethylene purity, catalyst loading, the use of solvent, temperature and pressure on the TON for the ethenolysis of MO is investigated. By understanding the limiting factors of the catalysis, recommendation is given for the direction of the field in order to obtain economically feasible TONs. As well as this, ethenolysis of other biobased materials is summarised to assess its applicability on versatile biobased substrates.

5

Ligands

NHC-Mes   NHC-Mes2   NHC-iPr   Styr   Inden

Ru1 - Ru10

Ru1: R = Styr; L_1,L_2 = PCy$_3$
Ru2: R = Styr; L_1 = NHC-Mes; L_2 = PCy$_3$
Ru3: R = Styr; L_1 = NHC-iPr; L_2 = PCy$_3$

Ru4: R = Styr; L_1,L_2 =
Ru5: R = Inden; L_1 = NHC-Mes; L_2 = PCy$_3$
Ru6: R = Inden; L_1,L_2 = PCy$_3$
Ru7: R = Inden; L_1,L_2 =

Ru8: R= Inden; L_1 = NHC-Mes; L_2 =

Ru9: L_1 = NHC-Mes; L_2 = PCy$_3$; R =

Ru10: L_1 = NHC-Mes2; L_2 = PCy$_3$; R =

Ru11 - Ru28

Ru11: R_1,R_2,R_3,R_4 = Me; R_5,R_6 = Et; R_7 = H
Ru12: R_1,R_2,R_3,R_4,R_6 = Me; R_5 = iPr; R_7 = H
Ru13: R_1,R_2,R_3,R_4 = Me; R_5,R_6 = iPr; R_7 = H
Ru14: R_1,R_2,R_3,R_4,R_5,R_6 = Me; R_7 = H
Ru15: R_1,R_2,R_3,R_4,R_6 = Me; R_5 = tBu; R_7 = H
Ru16: R_1,R_2 = Me; R_3,R_4 = Et; R_5 = iPr; R_6,R_7 = H
Ru17: R_1,R_2,R_5,R_6,R_7 = Me; R_3,R_4 = Et
Ru18: R_1,R_2,R_6 = Me; R_3,R_4 = Et; R_5 = iPr; R_7 = H
Ru19: R_1,R_2,R_5,R_6,R_7 = Me; R_3 - R_4 = (CH$_2$)$_5$
Ru20: R_1,R_2 = Me; R_5,R_6 = iPr; R_7 = H; R_3 - R_4 = (CH$_2$)$_5$
Ru21: R_1,R_2,R_4 = Me; R_3 = nPr; R_5,R_6 = iPr; R_7 = H
Ru22: R_1,R_2,R_4,R_5,R_6,R_7 = Me; R_3 = Ph
Ru23: R_1,R_2,R_3,R_6 = Me; R_4 = Ph; R_5 = Et; R_7 = H
Ru24: R_1,R_2,R_3 = Me; R_4 = Ph; R_5,R_6 = Et; R_7 = H
Ru25: R_1,R_2,R_3,R_6 = Me; R_4 = Ph; R_5 = iPr; R_7 = H
Ru26: R_1,R_2,R_3 = Me; R_4 = Ph; R_5, R_6 = iPr; R_7 = H
Ru27: R_1,R_5,R_6 = iPr; R_2,R_7 = H; R_3 - R_4 = (CH$_2$)$_5$
Ru28: R_1,R_5,R_6 = iPr; R_2,R_7 = H; R_3,R_4 = Me

Ru29 - Ru38

Ru29: R_1,R_2,R_3 = Me; R_4 = nBu

Ru30: R_1,R_2 = iPr; R_3 = H; R_4 =

Ru31: R_1,R_2 = iPr; R_3 = H; R_4 =

Ru32: R_1,R_2 = iPr; R_3 = H; R_4 =

Ru33: R_1,R_2 = iPr; R_3 = H; R_4 =

Ru34: R_1,R_2 = iPr; R_3 = H; R_4 =

Ru35: R_1,R_2 = iPr; R_3 = H; R_4 =

Ru36: R_1,R_2,R_3 = Me; R_4 =

Ru37: R_1,R_2,R_3 = Me; R_4 =

Ru38: R_1 = ^{t}Bu; R_2,R_3 = H; R_4 =

Ru39 - Ru41

Ru39: X = Cl
Ru40: X = Br
Ru41: X = I

Ru42 & Ru43

Ru42: L_1 = PCy$_3$
Ru43: L_1 = iPr

Ru44

Ru45

Ru46

[RuCl$_2$(p-cymene)]$_2$ + Cs$_2$CO$_3$ +

Ru47 - Ru51

Ru47: R = H; L_1 = PCy$_3$
Ru48: R = H; L_1 = NHC-Mes
Ru49: R = H; L_1 = NHC-iPr
Ru50: R= S(O)$_2$NMe$_2$; L_1 = NHC-Mes
Ru51: L_1 = NHC-iPr; R =

Ru52 - Ru54

Ru52: L_1 = NHC-iPr; L_2,L_3 =

Ru53: L_1 = NHC-Mes; L_2,L_3 =

Ru54: L_1 = NHC-Mes; L_2,L_3 =

Ru55 & Ru56

Ru55: L_1 = PCy$_3$ Ru56: L_1 = PCy$_3$

Ru57 - Ru59

Ru57: L_1 = PCy$_3$ Ru59: L_1 =
Ru58: L_1 = NHC-Mes

Figure 5.3. Ruthenium based metathesis catalysts discussed in this review

W1 - W3

NAr

F_3C—O—W=

CF$_3$

W1

O

CF$_3$

CF$_3$

W2

N

N—W=

OSiPh$_3$

W3: W(NAr)(C$_3$H$_6$)(Me$_2$pyr)(OBitet)

Mo1 - Mo5

Mo1: Mo(NAr)(CHCMe$_2$Ph)(Me$_2$pyr)(OBitet)
Mo2: Mo(NAr)(CHCMe$_2$Ph)[OCMe(CF$_3$)$_2$]$_2$
Mo3: Mo(NAr)(CHCMe$_2$Ph)(Me$_2$pyr)(TPP)
Mo4: Mo(NAr)(CHCMe$_2$Ph)(Me$_2$pyr)(OSiPh$_3$)
Mo5: Mo(NAd)(CHCMe$_2$Ph)(Me$_2$pyr)(OBitet)
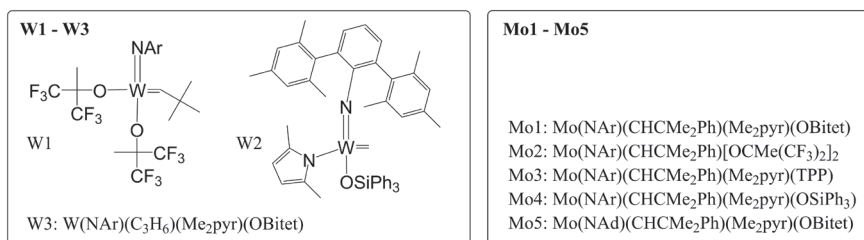
Figure 5.4. Tungsten and molybdenum based metathesis catalysts discussed in this review

5.2 Parameters that influence the turnover number of methyl oleate ethenolysis

The influence on the TON of ethylene purity, type and loading of catalyst, the use of solvent, temperature and pressure will be discussed here for the ethenolysis of MO.

5.2.1 ETHYLENE PURITY

To investigate the influence of ethylene purity, the highest reported TON for each catalyst from a number of publications was plotted against the purity of ethylene used in the ethenolysis procedure (Figure 5.5 and Table 5.1). Side reactions, such as self-metathesis, are not taken into account for the calculations of TONs.
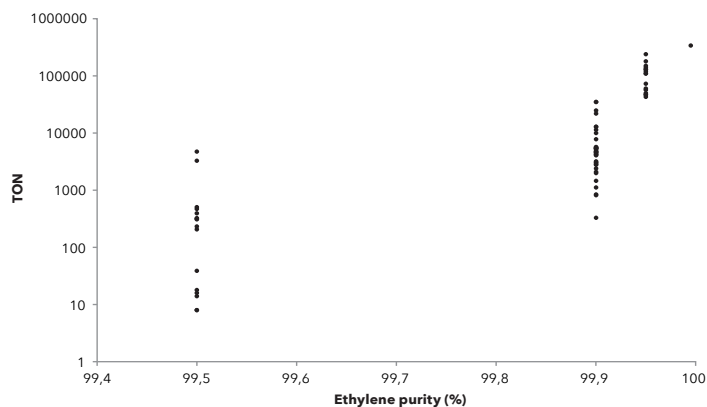
Figure 5.5. Highest TON for each catalyst per publication set out against ethylene purity reported for the ethenolysis reaction. A broad range of reaction conditions is used (See Table 5.1).

Table 5.1. Highest TON for each catalyst per publication.

Entry	TON	Ethylene purity (%)	Catalyst	Pressure (bar)	T (°C)	Time (min)	Solvent	Catalyst loading (ppm)	Reference
1	340,000	99.995	Ru12	10	40	180	neat	1	13
2	240,000	99.95	Ru12	10	40	180	neat	2	13
3	180,000	99.95	Ru25	10	40	180	neat	3	13
4	150,000	99.95	Ru26	10	40	180	neat	3	13
5	140,000	99.95	Ru24	10	40	180	neat	3	13
6	130,000	99.95	Ru23	10	40	180	neat	3	13
7	130,000	99.95	Ru18	10	40	180	neat	3	13
8	120,000	99.95	Ru11	10	40	180	neat	3	13
9	110,000	99.95	Ru14	10	40	180	neat	3	13
10	110,000	99.95	Ru22	10	40	180	neat	3	13
11	73,000	99.95	Ru17	10	40	180	neat	3	13
12	60,000	99.95	Ru13	10	40	180	neat	3	13
13	57,000	99.95	Ru15	10	40	180	neat	3	13
14	50,000	99.95	Ru21	10	40	180	neat	3	13
15	47,000	99.95	Ru16	10	40	180	neat	3	13
16	47,000	99.95	Ru19	10	40	180	neat	3	13
17	43,000	99.95	Ru20	10	40	180	neat	3	13
18	35,000	99.9	Ru11	10	40	30	neat	10	14
19	35,000	99.9	Ru11	10	40	30	neat	10	15
20	24,000	99.9	Ru1	4	30	39	neat	6	11
21	22,000	99.9	Ru3	10	40	60	neat	10	14
22	12,900	99.9	Ru1	10	40	240	neat	35	15
23	12,800	99.9	Ru49	55	25	360	neat	25	14
24	11,400	99.9	Ru13	10	40	1200	neat	50	15
25	10,000	99.9	Ru13	10	40	1200	neat	50	14
26	7,800	99.9	Ru1	10	40	240	neat	10	16
27	5,710	99.9	Ru39	12	60	390	neat	100	14
28	5,640	99.9	Ru40	10	60	180	neat	100	14
29	5,470	99.9	Ru31	10	60	240	neat	100	17
30	5,440	99.9	Ru59	10	40	1320	neat	100	14
31	5,400	99.9	Ru1	10	40	120	neat	100	14
32	5,370	99.9	Ru41	10	60	240	neat	100	14
33	5,200	99.9	Ru58	10	60	240	neat	100	14
34	4,800	99.9	Ru47	10	40	30	neat	100	14
35	4,800	99.9	Ru47	10	40	30	neat	100	15
36	4,620	99.9	Ru30	10	40	360	neat	100	18
37	4,604	99.9	Ru32	10	40	360	neat	100	18
38	4,450	99.9	Ru33	10	40	360	neat	100	18
39	4,200	99.9	Ru20	10	40	360	neat	100	14
40	4,200	99.9	Ru20	10	40	360	neat	100	15

Entry	TON	Ethylene purity (%)	Catalyst	Pressure (bar)	T (°C)	Time (min)	Solvent	Catalyst loading (ppm)	Ref.
41	4,900	99.9	Ru34	10	50	360	neat	1100	18
42	3,200	99.9	Ru48	10	60	15	neat	100	14
43	3,080	99.9	Ru29	10	40	360	neat	100	18
44	2,990	99.9	Ru44	10	60	30	neat	100	14
45	2,800	99.9	Ru2	10	60	15	neat	100	14
46	2,800	99.9	Ru2	10	40	120	neat	100	15
47	2,400	99.9	Ru9	10	60	120	neat	100	16
48	2,100	99.9	Ru52	10	40	15	neat	100	14
49	2,000	99.9	Ru48	10	40	30	neat	100	15
50	1,460	99.9	Ru35	10	40	360	neat	100	18
51	1,120	99.9	Ru37	10	40	360	neat	100	18
52	845	99.9	Ru36	10	40	360	neat	100	18
53	817	99.9	Ru38	10	40	360	neat	500	18
54	329	99.9	Ru53	10	40	15	neat	100	14
55	4,750	99.5	Mo1	10	20	900	neat	200	19
56	3,284	99.5	Ru1	20	30	1440	neat	45	20
57	508	99.5	Ru47	20	30	1440	neat	1×103	20
58	470	99.5	Mo5	4	20	1080	neat	2×103	19
59	395	99.5	Mo4	4	20	60	neat	2×103	19
60	325	99.5	Mo3	4	20	1200	neat	2×103	19
61	315	99.5	Mo2	4	20	120	neat	2×103	19
62	310	99.5	Mo6	4	20	1080	neat	2×103	19
63	233	99.5	Ru48	20	30	1440	neat	1×103	20
64	206	99.5	Ru2	20	30	1440	neat	1×103	20
65	39	99.5	Ru47	10	70	210	toluene	25×103	21
66	18	99.5	Ru56	10	20	120	[bdmim][NTf2]	50×103	21
67	16	99.5	Ru1	1	70	210	toluene	25×103	21
68	14	99.5	Ru46	1	70	210	toluene	25×103	21
69	8	99.5	Ru45	1	70	210	toluene	25×103	21
70	8	99.5	Ru55	10	20	120	[bdmim][NTf2]	50×103	21

In table 5.1 an overview is given of TONs for the ethenolysis of MO from publications where the ethylene purity was reported. This results in four categories of ethylene purity, which are ranked by TON. One experiment with an ethylene purity of 99.995% was performed (Table 5.1, entry 1), followed by a series of experiments with an ethylene purity of 99.95% by the same authors (Table 5.1, entries 2 to 17). The TONs using more common ethylene purities of 99.9% and 99.5% can be found in Table 5.1, entries 18 to 54 and Table 5.1, entries 55 to 70 respectively.

This data was used to set out the TON against the ethylene purity in Figure 5.5 to study the influence of ethylene purity on the TON. The TONs increase from 10 through 4,800 up to 300 through 35,000 when the ethylene purity is increased from 99.5% to 99.9%. This increase

continues with an increasing ethylene purity, which results in TONs of 43,000 through 240,000 at 99.95% pure ethylene. The highest TON is obtained using 99.995% pure ethylene and results in a TON of 340,000.The observation of a strong effect of the ethylene purity on the TON is in agreement with previous literature, where the influence of the ethylene purity has been investigated.[13] At 2 to 3 ppm catalyst, the authors observe little difference in the TON when different ethylene purity is used, however at 1 ppm catalyst the TON increases from 130,000 at 99.95% ethylene purity to 340,000 at 99.995% ethylene purity using neat conditions and Ru12 as catalyst (Table 5.1, entry 1). Small amounts of impurities from the ethylene, such as carbon monoxide and acetylene, are expected to poison the catalyst, which explains the more pronounced effect of ethylene purity at lower catalyst loadings.[13]

5.2.2 CATALYST

Here we compare the catalysts reported in Figures 5.3 and 5.4 for their activity towards the ethenolysis of MO, by TON, with commonly used ethylene purities (99.5% and 99.9%). The highest TON reported for each catalyst was taken from literature to assess the potential of the catalysts (Table 5.2). For clarity, only a selection of catalysts is shown in Table 5.2.

Table 5.2. Highest TON per selected catalysts reported in literature.

Entry	TON	Catalyst	Reference
1	35,000	Ru11	14, 15
2	26,000	Ru28	22
3	24,800	Ru1	11
4	22,300	Ru3	23
5	14,047	Ru4	24
6	13,500	Ru49	23
7	12,450	Ru7	25
8	11,400	Ru13	15
9	11,000	Ru48	23
10	10,000	Ru27	22
11	7,500	Ru47	23
12	7,153	Ru2	24
13	5,470	Ru31	18
14	5,200	Ru58	14
15	4,750	Mo1	19
16	4,620	Ru30	18
17	4,604	Ru32	18
18	2,400	Ru9	16

With only one exception,[13] the ethylene purities used for ethenolysis of MO in literature are 99.9% and 99.5%, therefore we assume that studies without reported ethylene purities use similar ethylene purities and that their results can be compared. Comparing these catalysts, the highest TONs are obtained by Ru11, Ru28, Ru1 and Ru3. Ru11 and Ru28 have a cyclic (alkyl)(amino) carbine (CAAC), where Ru1 and Ru3, the traditional Grubbs 1st generation catalysts, have phosphine ligands. The CAAC catalysts show the highest TONs reported with these ethylene purities, however, the margin with the Grubbs 1st generation catalysts is small with TONs of 35,000 and 26,000 for Ru11 and Ru28 (Table 5.2, entries 1 and 2)[14, 15, 22] and 24,800[11] and 22,300[23] for Ru1 and Ru3 (Table 5.2, entries 3 and 4).

The high activity of CAAC systems in ethenolysis reactions was first demonstrated in 2008,[15] where TONs of 35,000 for 10 ppm Ru11 and 11,400 for 50 ppm Ru13 were reached. Especially using low catalyst loadings proved beneficial for these catalysts. The TON of Ru1 was not influenced by this parameter, resulting in similar TONs of 12,900 and 12,700 at 35 ppm and 10 ppm, where the TON of Ru11 increased from 16,000 to 35,000 when the loading was decreased from 35 ppm to 10 ppm. The authors point out that Ru1 is limited by catalyst degradation and inhibition by the terminal alkenes that are formed by ethenolysis. However, it is not mentioned why CAAC catalysts respond different to these inhibitors.[15] A later study confirms the superior behaviour of catalysts with CAAC ligands in the ethenolysis of MO, showing the highest TONs and TOFs of the tested catalysts.[14] Ru27 and Ru28 were designed with the larger isopropyl groups on the CAAC ligand (R1, Figure 5.3). These isopropyl groups push the ortho-isopropyl on the nitrogen (R5 and R6, Figure 5.3) away. This gives the ether functionality more space to rotate, making a faster initiation possible. The highest TON reported for these bulky CAAC catalysts is 26,000 for Ru28 using 10 ppm catalyst in neat MO at 40 °C for 4h and 10 bar ethylene. This conversion has a higher selectivity (97%) than the selectivity of the system which results in a TON of 35,000 for Ru11 (83%).[22]

When the traditional catalysts are compared with each other, the diphosphine catalyst Grubbs 1st generation (Ru1) is outperforming Grubbs 2nd generation (Ru2), which has one phosphine ligand replaced by a NHC ligand, with a TON of 24,800[11] to 7,200[24] (Table 5.2, entry 3 compared to entry 12). The Hoveyda-Grubbs series (Ru47 to Ru49), which have one phosphine ligand replaced by a chelating isopropoxy group, reach TONs of 7,500 for Ru47, 11,000 for Ru48 and 13,500 for Ru49.[23] The highest reported TON for molybdenum catalysts does not surpass 4,750 using Mo1. However, the ethylene purity is lower in this example (99.5%).[19]

In order to obtain catalysts that are more stable than Ru1, Ru4 and Ru7 were synthesised by replacing the tricyclohexylphosphine ligands (PCy_3) with phoban ligands that showed success for other catalytic systems.[24, 25] The increased stability leads to a higher TON for the ethenolysis of MO compared to Ru1. At 10 bar ethylene, 60 °C and 2 hours and a catalyst loading of 25 ppm, Ru1 gives a TON of 4,247, where Ru4 gives a TON 14,047.[24] Using the same reaction conditions, but at 50 °C and 50 ppm catalyst loading, Ru7 yields a TON of 12,450 and Ru1 yields a TON of 8.[25] However, the reaction conditions for Ru1 were optimised in other studies to reach a TON of 24,800 after 39 minutes using 4 bar ethylene at 30 °C.[11]

5

The influence of bulky groups on the N-aryl of the NHC ligand was explored with the synthesis of Ru3 and Ru49.These catalysts give higher TONs, but their selectivity is still limited to 50% to 80%.[14] Even larger NHC ligands were developed to successfully increase the selectivity of the ethenolysis. Ru30, Ru31 and Ru32 showed excellent selectivity, which was confirmed by determining the steady state of the cross metathesis of 1-hexene in NMR studies. However, the activities of these catalysts are not high enough to compete for high TONs.[18]

Hoveyda-Grubbs catalysts Ru47 and Ru48, which carry a chelating isopropoxy group, are known for their high stability and activity, however, in the ethenolysis of neat MO they are more active towards self-metathesis than ethenolysis. Their low selectivity causes the productive TON to drop below the TON of Ru1. Selectivity as low as 44% for Ru47 and 33% for Ru48 have been observed in conditions were Ru1 and CAAC catalysts reached over 90% selectivity.[15] The low selectivity of Ru47 and Ru48 towards ethenolysis has been confirmed in a later report, where first generation catalysts (bearing PCy_3 ligands) give TONs of 4,800 to 5,400 and second generation catalysts (bearing a NHC ligand) give TONs of 2,800 to 3,200.[14] Moreover, when selectivity is set out against conversion of MO for a wide range of catalysts, it becomes clear that catalysts with NHC ligands first catalyse the self-metathesis reaction, where catalysts with phosphine ligands show high ethenolysis selectivity at low conversions.[26]

Most conversions are performed in neat conditions. When the ethenolysis is performed in a solvent such as toluene, Hoveyda-Grubbs type catalysts (Ru47 to Ru49) outperform Grubbs type catalysts (Ru1 to Ru3). When 0.17 M MO is converted with 2.5 mol% (25,000 ppm) catalyst, at 70 °C and 1 bar, Ru1 reaches 45% conversion where using Ru47 results in 91% conversion. In this system, where self-metathesis does not play a role, the higher activity of the Hoveyda-Grubbs type catalysts becomes more important.[21] Another way to improve the selectivity of Hoveyda-Grubbs type catalysts (Ru47, Ru48) is the use of a microchemical system to increase the contact between ethylene and the catalyst in order to decrease self-metathesis reactions. This system leads to the highest TONs reported for Ru47 and Ru48 (Table 5.2, Entries 9 and 11) using 50 to 300 ppm catalyst in neat MO, however, selectivity of these catalysts remain low in this system at around 60%.[23] Ru52 and Ru53 also have a poor stability and poor solubility in MO and therefore only reach TONs of 329 and 2,100.[14] These catalysts might also benefit from a solvent system, however no investigations were performed on these catalysts with added solvent.

Homobimetallic ruthenium complexes were synthesized as an attempt to improve on existing metathesis catalysts. The ethenolysis of methyl oleate using Ru42 and Ru43 look promising. 1 mol% (10,000 ppm) catalyst at room temperature for 12 hours and 1 bar ethylene resulted in full conversion and high selectivity for Ru1 (95%), Ru42 (97%) and Ru43 (92%). The catalysts were not tested at lower loadings and therefore could only reach TONs just below 100.[27]

Schrock type catalysts are often avoided due to the high stability of ruthenium catalysts. A report in 2009 shows that molybdenum catalysts with four ligands in a tetrahedral geometry yield superior conversions and TONs than tungsten based catalysts. The highest reported TON for the ethenolysis of MO for Schrock type catalyst remains 4,750 using Mo1. However, this study has only been performed with a low ethylene purity of 99.5%.[19]

5.2.3 CATALYST LOADING

In order to reach a high TON a low catalyst loading is necessary. However, there are reasons to consider increasing the catalyst loading if this leads to higher conversion or selectivity. For example, the loading of the more instable catalysts can be increased to ensure that the catalyst reaches the equilibrium before it is decomposed and high conversion and selectivity can be reached. Increasing the loading of the unstable Ru38 from 100 to 500 ppm increased the selectivity from 19% to 58%.[18] For the more stable Ru35 an increased loading from 100 ppm to 500 ppm resulted in a maintained selectivity of 95%, but an increased conversion from 12% to 48%.[18] However, a higher loading may also reduce selectivity as is the case for Ru10. An increase in loading from 2 ppm to 200 ppm leads to a higher amount of isomeric by-products formed. The authors describe the effect to the decomposition of the active ruthenium alkylidene complex to ruthenium hydride species, which is responsible for the double bond isomerisation reaction.[26]

Another factor that should be kept in mind is that catalyst poisoning is more evident at low catalyst loadings. This effect can be observed when Ru9 is reduced in loading from 100 ppm to 10 ppm. Instead of the expected increase in TON, the TON went down from 2,400 to 600, which suggests catalyst poisoning.[16] Catalyst poisoning will be further explored in 5.2.7 'Catalyst deactivation'.

5.2.4 SOLVENT

Using neat MO is common practice, but leads to high self-metathesis activity for Hoveyda-Grubbs type catalysts (Ru47 to Ru49).[14, 15] Adding a solvent can help prevent self-metathesis reactions. When toluene is used as a solvent, the self-metathesis reaction is successfully suppressed and both first generation catalysts, bearing phosphine ligands, and second generation catalysts, bearing NHC ligands, yield full selective ethenolysis reactions.[21] Common solvents for metathesis reactions, dichloromethane and aromatic solvents such as toluene, are harmful to the environment and toxic. For this reason, ethenolysis in dimethyl carbonate was explored and similar conversions were reached for toluene (88%) and dimethyl carbonate (82%) using 2.5 mol% (25,000 ppm) Ru47 at room temperature for 3 hours and 1 bar ethylene.[28]

Other starting materials show no conversion at all in neat conditions. For example, the ethenolysis of oleonitrile yielded no conversion with 0.25 mol% (2,500 ppm) Ru48 after 4 h at 40 °C and 15 bar ethylene, where reactions using toluene leads conversions of 50% to 90%. This peculiar behaviour of oleonitrile has not yet been explained.[29]

Solvents can also be employed to enable recycling of the catalyst. Ionic liquids have been tested for this purpose as a solvent for ethenolysis and with a modified ruthenium catalyst the ethenolysis leads to 95% conversion of 0.5 M MO and 5 mol% (50,000 ppm) catalyst. The reactants can be extracted with heptane and the ionic liquid with catalyst can be reused.[21] Using ionic liquids creates a mass transfer issue that can be avoided using a thin layer of ionic

5

liquid on silica. This increases the TON to 491 from 117 that is obtained from biphasic systems with similar conditions. The highest TON reported for this system is 2,350 for 45 ppm catalyst and has a conversion of 11%.[20]

5.2.5 TEMPERATURE

The increased catalyst decomposition at higher temperature and the reduced selectivity can completely counteract the increased reactivity of the catalyst. Therefore, an increased temperature is often counterproductive. For example, the ethenolysis of MO using Ru34 has an optimal temperature of 40 °C.[18] Robust catalysts have been developed that will remain stable and active above 100 °C to enable reactions at higher temperatures. 2 ppm Ru10 shows 50% yield and full selectivity at 150 °C, where Ru2 decomposes quickly at these temperatures.[26]

For the ethenolysis of viscous compounds, such as methyl ricinoleate, a higher temperature can be applied to reduce the viscosity and improve the ethylene solubility. For this reason the optimal temperature for methyl ricinoleate ethenolysis is 80 °C.[30] Moreover, for the ethenolysis of polymeric materials, a higher temperature may be needed to dissolve the polymer. For example, the branched copolymer of ethylene, 1-octene and butadiene fully dissolves in toluene at 70 °C.[31]

5.2.6 PRESSURE

The initial rate of the catalysis is unaffected by an increased ethylene pressure, however, the selectivity towards ethenolysis products is increased with increasing ethylene pressure. This leads to an overall increase in conversion of MO from 56% to 82% when the ethylene pressure is increased from 1 bar to 16.5 bar using 200 ppm Ru1.[11]

CO_2 can also be added to the ethenolysis reaction for an increased reactivity and pressure becomes a crucial factor in this system. Between 50 and 82 bar the added CO_2 decreases the viscosity of ethyl oleate, which increases the mass transfer and therefore the reaction speed. Moreover, the products are extracted from the liquid to the vapour phase, resulting in a more beneficial equilibrium. When the pressure is increased to 120 bar, ethyl oleate itself is extracted into the vapour phase. Since the catalyst does not dissolve well in the vapour phase, the reaction is slowed down significantly.[32]

5.2.7 CATALYST DEACTIVATION

Catalyst deactivation can occur from poisons such as carbon monoxide and acetylene from the ethylene feed as discussed in more detail in section 2.1. However, there are multiple pathways towards catalyst deactivation and a short overview of the most important pathways for ethenolysis reactions is given here.

5.2.7.1 CATALYST DEACTIVATION BY ETHYLENE

The Ru1 catalyst shows a high initial activity in the first two hours of the ethenolysis of MO, but then the selectivity and activity go down. Selectivity decreases due to the reaction mixture proceeding towards a thermodynamic equilibrium and activity decreases due to catalyst degradation and product inhibition.[11] Degradation of ruthenium metathesis catalysts is proposed to involve a ruthenium alkylidene species (Figure 5.6), which is sensitive towards decomposing pathways such as alcoholysis.[33] Moreover, it is well known that the presence of ethylene in metathesis reactions leads to the unstable ruthenium alkylidene. Next to finding catalysts that have a more stable alkylidene species to increase catalyst lifetimes, alkylidene formation can be circumvented by the use of longer terminal alkenes.
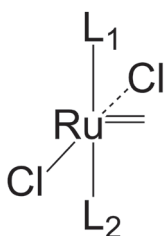
Figure 5.6. Ruthenium alkylidene species.

5.2.7.2 PRODUCT INHIBITION

Next to the degradation pathway opened by the use of ethylene, the terminal olefins produced in the ethenolysis also cause the reaction to slow down. The observed decrease in activity can not be explained by an increase in the speed of the return reaction, but a decay of the catalyst activity is needed to find a model that is in agreement to the data. The half-life from this result is 10 min, where no olefinic substrates were taken into account. Control reactions starting with a mixture of starting material and products show that it is not the catalyst lifetime that is responsible for the loss in activity, but the presence of terminal olefin products. The terminal olefins slow down the catalytic cycle by inhibition of the active catalyst. With two terminal olefins produced per MO molecule, this is a significant effect, which becomes even bigger when low catalyst loadings are used.[11]

Product inhibition can be prevented when the products are reacted further in a subsequent, one-pot reaction. An example is following the ethenolysis with a ene-yne cross-metathesis. After 3 hours in dimethyl carbonate and 2.5 mol% (25,000 ppm) Ru47, an ene-yne active ruthenium catalyst and a slight excess of but-1-yn-3-yl carbonate is added to generate dienes.[34, 35]

5.2.7.3 HYDROXYPEROXIDES

Hydroxyperoxides are formed gradually over time in oils and could poison the ruthenium catalysts. Examples where the hydroxyperoxides were removed to successfully increase metathesis reactivity includes the treatment of soy FAME with magnesium silicate. The reactivity of the propenolysis of neat soy FAME with 2.5 ppm Ru9 and 9 bar propylene for 4h at 60 °C can be improved from a TON of 1,080 without treatment to a TON of 80,320 after treatment.[16] Another example can be found in the ethenolysis of oleonitrile in toluene with 625 ppm Ru51 at 120 °C and 16h under 20 bar of ethylene. Untreated oleonitrile, with 230 meq/kg peroxides, yields a TON of 284. This number goes up with more efficient treatments as the peroxide content decreases. The highest TON of 1,239 is obtained after treatment with Al_2O_3 at 200 °C, which resulted in a peroxide content of 6 meq/kg. This effect is contributed to the removal of peroxides, however, this treatment also results in the removal of volatile compounds and water.[29]

5.2.7.4 LONGER ALKENES

To avoid degradation *via* ruthenium methylidene species, longer alkenes such as propylene, 1-butene and 1-octene could be used to obtain terminal alkenes. This will lead to fewer desirable end products per turn over, but with a substantial increased TON the productivity may still be increased. Moreover, it circumvents issues with low solubility of ethylene in MO. A higher productivity has been observed when ethylene is replaced by 1-octene for the conversion of MO. Where 10 ppm Ru9 in 4 hours at 40 °C converts 0.6% of neat MO to the desired terminal alkene, replacing the 10 bar ethylene with 3 equivalents of 1-octene leads to 23% terminal alkenes. This is an increase in TON of 600 to 23,000.[16] For electron deficient starting materials as crotonates, a switch from ethylene to the less reactive propylene only lowers the activity of the reaction leading to four times lower TONs.[36]

5.3 Ethenolysis of biomass

5.3.1 FATTY ACIDS

Methyl oleate has been studied as a model compound for fatty acids methyl esters (FAME). Another model compound, which is closer to using actual biomass is olive oil. Even though the conversion of olive oil may not be desired due to its use as food, it serves well as a model compound due to its high oleic acid content. After purification with activated carbon, 70% conversion was obtained from olive oil using 0.3 mol% (3,000 ppm) Ru1. The resulting terminal olefins were successfully transesterified and hydrogenated for biofuel production.[37]

Rapeseed oil can be transesterified with methanol and acid to obtain a mixture of methyl esters with 16, 18 and 20 carbons. A following ethenolysis using 1 mol% (10,000 ppm) Ru1, 1 bar ethylene at 70 °C for 4 hours in toluene results in 99% conversion and 93% selectivity. However, at 25 °C, the conversion drops to 82%. Using 1 mol% (10,000 ppm) Ru42 instead of Ru1 improves the ethenolysis to 99% conversion and 96% selectivity at 25 °C. Since no loading below 1 mol% were reported, highest TONs are just below 100.[27] Next to rapeseed oil, sunflower oil, waste coffee oil and a wide range of microbial oils are interesting ethenolysis substrates. The ethenolysis of these substrates was examined for fuel applications using 5.1 mol% (51,000 ppm) Ru48 in DCM with 10 bar ethylene for 1 hour at 60 °C resulted in a mixture with high C_{10} content. High amounts of self-metathesis and isomerisation products were observed, which originate from the ruthenium hydride that forms from Ru48 degradation. However, these side products did not influence the fuel properties and the resulting mixture could be separated in two different fuel classes and a polymer precursors fraction.[38]

Cacao butter is a triglyceride that is discarded after the food process and could be used as a biobased starting material that does not compete with food. Ethenolysis of cocoa butter proved most successful using biphosphine catalyst in THF at room temperature. These results were translated to a continuous flow setup with 1 mol% (10,000 ppm) catalyst. This lead to conversions up to 40% with a retention time of 60 minutes and 6 bar ethylene.[39]

Transesterified soy bean oil (Soy FAME) is another fatty acid based feedstock and is therefore expected to behave similar to methyl oleate. The conversion of soy FAME proceeds similar as MO, but with lower TONs. Where MO is converted with a TON of 7,800, similar conditions result in a TON of 1,985 for soy FAME. To prevent catalyst poisoning, the process is optimised towards propenolysis of soy FAME, which increases the TON to 20,134 at 10 ppm Ru9 after 4 h at 60 °C with 9 bar propylene. Further lowering the catalyst loading did not directly result in an increased TON, which suggest catalyst poisoning. To remove any potential organic hydroperoxides, the soy FAME was treated with magnesium silicate, which is used to regenerate aged oils. This pre-treatment allowed a catalyst loading as low as 1 ppm and resulted in a TON of 192,200 for the propenolysis of soy FAME.[16]

A second route from oleic acid to high value products is found in the decarboxylation of oleic acid followed by an ethenolysis of the resulting 8-heptadecene. This route prevents the formation of the less desirable methyl-9-decenoate. Ru48 was chosen as catalyst, due to its high activity and selectivity in the solvent system and hexane proved to be the best performing solvent. Full conversion and 96% selectivity can be achieved, however, TONs were not optimised and the highest TON achieved is 298.[40]

A third pathway to biobased chemicals from oleic acids is to obtain its corresponding nitrile from an amination reaction of oleic acid. The nitrile product of an ethenolysis of the oleonitrile could be used as a biobased jet fuel additive. After removal of peroxides using Al_2O_3 at 200 °C, ethenolysis in toluene with 625 ppm Ru51 and 20 bar ethylene resulted in a TON of 1,239 after 16 h at 120 °C.[29]

5.3.2 CASTOR OIL

Castor oil is unsuitable for food and can be extracted from the seeds of the castor plant. It has a high amount of ricinoleic acid, a fatty acid with a hydroxyl group at the C12 position (Figure 5.7), which gives it a specific boiling point, density and viscosity. The hydroxyl group also influences its reactivity in ethenolysis conversions. After transesterification with methanol to produce methyl ricinoleate, the ethenolysis products could find applications in odours, flavours, lubricants and the polymer industry.[30]
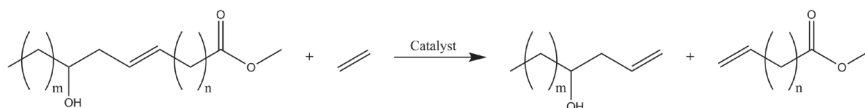
Figure 5.7. Ethenolysis of castor oil, m=5, n=7

In a catalyst screening for the ethenolysis of 0.24 M methyl ricinoleate in toluene and 20 bar ethylene, Ru5 shows highest conversion, with 98% conversion and 72% selectivity, where Ru1 only reaches 26% conversion and 67% selectivity and Ru2 reaches 98% conversion with only 66% selectivity. Toluene was found to be the optimal solvent, which is required to enhance the solubility of ethylene in the viscous methyl ricinoleate. The optimised system reached a TON of 1,780 and 96% conversion with 500 ppm Ru5 and 20 bar ethylene. Unpurified ricinoleic acid (80% pure) and castor oil reached a conversion of 87%.[30]

Methyl ricinoleate can also be converted with an ethenolysis followed by ene-yne cross-metathesis in a one-pot reaction. The ethenolysis reaction is performed with 1 mol% (10,000 ppm) Ru48 and, together with the subsequent ene-yne cross-metathesis, yields 70% conversion. Catalyst decomposition from the allylic alcohol is likely the limiting factor in the conversion. [35]

5.3.3 CASHEW NUT

Cashew nut shell liquid consists of three major compounds: cardanol, cardol and anacardic acid. The compounds exist of a meta-substituted phenol ring with a C15 group containing zero to three double bonds at the C8, C11 and C14 position. They differ in extra substituents on the benzene ring (Figure 5.8).[41] These compounds can lead to a wide variety of target products, for example cardanol could be converted to detergents, tsetse fly attractant and polymer additives. Ethenolysis of cardanol gives rise to 1-octene and 3-(non-8-enyl)phenol, which can be used as detergent precursor (Figure 5.8). Initial attempts gave 65% to 76% yield of the products with Ru48 at room temperature, 20 bar ethylene after 24 hours. Yields were limited due to incomplete conversion and side product formation from isomerisation reactions.[42]
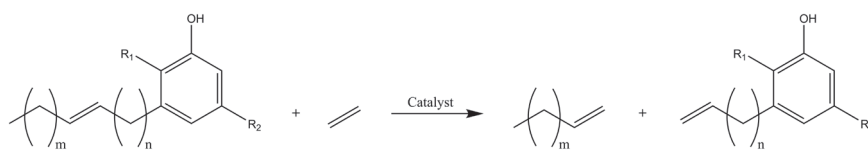
Cardanol: R_1, R_2 = H;   Cardol: R_1 = H, R_2 = OH;   Anacardic acid: R_1 = COOH, R_2 = H

Figure 5.8. Ethenolysis of cardanol, m=5, n=7

In a study where several catalysts were tested at several temperatures it was found that Ru6 and Ru1 were the most potent catalysts for this transformation. 500 ppm Ru6 in dichlorometh-ane at 20 °C for 6 h with 8 bar ethylene resulted in 95% conversion and 94% selectivity. Hoveyda-Grubbs type catalysts (Ru47 to Ru49) showed lower conversions and selectivity and more side products were observed in these reactions, especially in the form of isomerisation products. By etherification of the phenol group the authors showed that the phenolic OH-group of cardanol has a positive effect of the conversion, moreover the multiple double bonds in the starting material gives rise to 1,4-cyclohexadiene, which appears to be crucial for the activity of Ru6 on the ethenolysis of cardanol. It was even shown that addition of 1,4-cyclohexadiene increases the conversion of MO using Ru6 and potentially that 1,4-cyclohexadiene plays a role in the stabilisation of Ru6 in ethenolysis reactions.[41] Immobilised catalysts have also been tested on cardanal and both Ru2 and Ru50 give similar conversion in homogeneous conditions as immobilised on SBA-15. Immobilised Ru50 reached the highest TON at 630 when 0.1 mol% (1,000 ppm) catalyst was applied.[43]

Anacardic acid can be converted to 3-non-8-enylphenol *via* ethenolysis. Several catalysts have been tested and Ru47 appears to be most suitable for this conversion, leading to 98% conversion and 92% selectivity after 6 hours using 0.5 mol% (5,000 ppm) catalyst in 25 °C DCM and 8 bar ethylene.[41] The loading of Ru47 could even be brought down to 0.05 mol% (500 ppm), reaching a TON of 1,221. After a thermal decarboxylation, the resulting product could be isolated and converted with a one-pot isomerisation and ethenolysis. After a final hydration step, kairomone, a tsetse fly attractant, was obtained in 78% yield.[44]

5.4 Ethenolysis of polymers

Metathesis can play many roles in the field of polymer chemistry and a recent review discusses all these facets.[2] Here we focus on using end alkenes to recycle polymers and obtain useful end products. Recycling of plastics can help to minimise the need for fossil feedstock. How-ever, for a replacement of fossil feedstock by renewable resources, the use of natural rubber could be explored. Due to its highly regular stereochemistry it makes an interesting substrate for ethenolysis.[45] This conversion, and the conversion of polymers to terminal alkenes for the purpose of recycling are discussed here.

5.4.1 POLYBUTADIENE AND POLYISOPRENE

Many polymers exhibit double bonds and could therefore be an interesting starting material for ethenolysis. First attempts on depolymerisation using metathesis reactions were called degradations instead because no useful products would be formed. However, when polybutadiene was subjected to ethylene with 5 mol% (50,000 ppm) W1, monomers and small oligomers were obtained. These products could be used to generate new polymers and opened a pathway to polymer recycling.[46] From calculation it was found that the ethenolysis of polybutadiene will reach 46% 1,5-hexadiene at equilibrium and 1,4-polyisoprene will result in 90% 2-methyl-1,5-hexadiene when equilibrium is reached.[47] This conversion is increased when Ru1 is used as a catalyst instead. With 27.5 bar ethylene, 82% 1,5-hexadiene was obtained. With lower ethylene pressures self-metathesis reactions become more dominant and a higher ethylene pressure causes an unproductive self-metathesis of ethylene. Some side product formation from isomerisation of the ruthenium hydride species has also been observed.[48]

To obtain polyisoprene blocks in the range of 10,000 g/mol, the conditions can be tuned using 1 mol% (10,000 ppm) Ru1 or Ru47 catalyst at 60 °C and 1 bar ethylene. Some isomerisation has been observed and can be suppressed when 1-octene is used instead of ethylene. The products could be used to synthesize block copolymers.[49] Another method to obtain starting materials for block copolymers is starting from a polymer made from ethylene, 1-octene and butadiene. The double bonds can be broken with ethenolysis at 90 °C, after 2 hours in toluene and 1.7 bar ethylene using 2.2 mol% (22,000 ppm) Ru5.[31]

5.4.2 POLYNORBORNENE

The equilibrium of the metathesis of polynorbornene was determined using molecular modelling and found to depend on the chain-transfer agent and olefin used. Ethylene resulted in no significant formation of the monomer unit 1,3-divinyl cyclopentane, much lower than for polybutadiene. This result was explained by the fact that polymerisation of the norbornene monomers happens more readily than for polybutadiene.[50]

5.4.3 SQUALENE AND NATURAL RUBBER

Squalene was chosen as a model substrate to optimise the ethenolysis on natural rubber. Squalene is a linear molecule of 30 carbons that resembles rubber in structure (Figure 5.9). After optimisation it was found that 100 ppm Ru8 in toluene for 3 hours at 120 °C at 7 bar ethylene gave 75% conversion of squalene. The lessons learned from the optimisation could be applied to natural rubber. It was found a higher catalyst loading is needed for natural rubber to prevent catalyst poisoning by impurities. Moreover, more side reactions take place when natural rubber is used as substrate. Using the optimised conditions from squalene on natural rubber, a yield of 65% oligoisoprenes (n = 1 to 10) was obtained.[45]
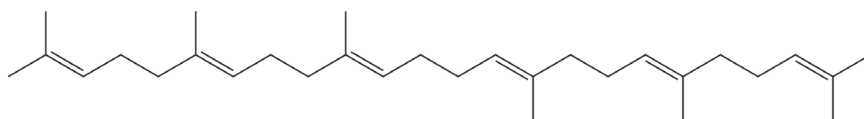
Figure 5.9. Structure of squalene (C30H50)

The optimised system of natural rubber could also be applied to end of life tyres. These tyres consist of multiple components such as sulphur cross linked polymers, mainly polyisoprene, and inorganic fillers. An additional challenge for converting tyres with ethenolysis is that they are not soluble in organic solvents. 50% of the mass of small end of life tyre granules could successfully be converted to soluble organics using 7 bar ethylene, 80 °C and 20 hours in toluene. The main components were oligoisoprenes and some products from polybutadiene were observed.[51]

5.5 Ethenolysis of other substrates

The ethenolysis of other biobased substrates can often be challenging due to the vicinity of steric or electron withdrawing groups to the double bond. This can lead to a different reactivity and a different optimal catalyst system. The conversion of these substrates are discussed here.

5.5.1 NORBORNENES

Functionalised norbornenes can be used as a starting material to obtain vinylcyclopentanes. These pentanes can be applied as cross linking agents or chemical building blocks. However, it is important that during the ethenolysis of these compounds, polymerisation is prevented. The ethenolysis of silicon substituted norbornenes (Figure 5.10) proceeded with full conversion using 250 ppm Ru1 as catalyst at 20 °C, 24 h in toluene with 4 bar ethylene. The sequence in which the compounds are added to the reaction mixture are found to play a crucial role, where the catalyst and ethylene have to be premixed before the substrate is added to prevent polymerisation.[52] Without self-metathesis occurring, the TOF of the reaction can directly be deduced from the ethylene uptake and a peak activity is seen in the first 15 minutes of the reaction.[53]
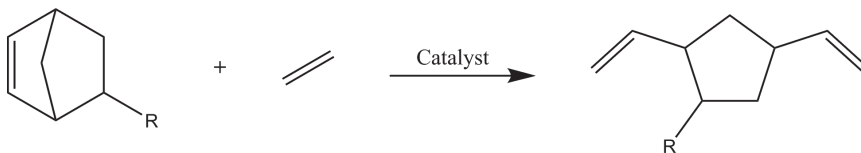
Figure 5.10. Ethenolysis of substituted norbornenes

Tungsten based catalysts have been designed with bulky ligands to be able to react with norbornenes and are then, after the first insertion, more reactive towards ethylene. In this manner the ethenolysis of norbornenes can be performed with high selectivity using 1 bar ethylene, 60 °C in toluene and 2 mol% (20,000 ppm) W2 after 24 hours.[54]

5.5.2 ELECTRON POOR SUBSTRATES

Next to the degradation pathway of ruthenium alkylidene species, the introduction of ethylene to ruthenium catalysts opens another deactivation pathway. When an excess of ethylene is available, or when the substrate is sufficiently electron poor[55], ethylene can inhibit the ruthenium catalyst an form a stable and dormant species. This inhibition is reversible, however it reduces the amount of available active catalyst for the metathesis reaction.[56]

Cinnamic acid can be obtained from the conversion of phenylalanine and makes an interesting target for ethenolysis. The ethenolysis of cinnamic acid yields both styrene and acrylic acid (Figure 5.11). The target double bond in cinnamic acid is electron poor, since both the acid group and phenylring are in conjugation with the double bond. This makes the double bond only active to the highly active Ru48 and Ru54. Catalysts with phosphine ligands show no activity at all in this conversion. Since the double bond is electron poor, a low pressure of ethylene is required for the reaction. High pressures of ethylene result in the catalyst primarily being present in the dormant species. However, the highly electron poor double bond also leads to very low TONs, with the highest TON reported of 12.[55]
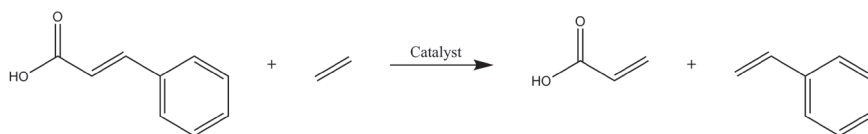
Figure 5.11. Ethenolysis of cinnamic acid

To develop new synthetic routes to vitamin A, the ethenolysis of β-carotene was investigated. Due to the unique conjugated system of 11 double bonds, β-carotene is a challenging substrate and therefore 20 mol% (200,000 ppm) of Ru48 was needed for conversion. Other catalysts were unable to catalyse this substrate. A full analysis of the reaction products was not published.[57]

To obtain functionalised styrenes from biobased starting materials, the ethenolysis of isoeuginol was studied (Figure 5.12). This electron poor double bond, which is in conjugation with a phenyl ring shows full conversion and 96% selectivity in tetrahydrofuran (THF) with 3 mol% (30,000 ppm) Ru48 catalyst at 60 °C and 10 bar ethylene. When this reactionsystem is combined with an palladium based isomerisation catalyst, natural products as eugenol, safrol, estragol and methyleugenol can be converted to their corresponding functionalised styrene with yields over 90%.[58]
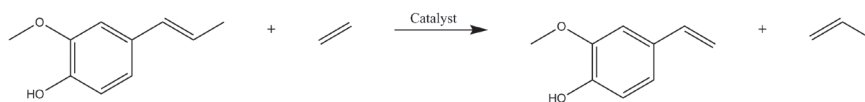
Figure 5.12. Ethenolysis of isoeuginol

Ethenolysis of biobased crotonates, which could be obtained from the conversion of polyhydroxybutyrate, leads to biobased propylene and acrylates, important monomers for the polymer industry (Figure 5.13). The acid of crotonic acid is in conjugation with the double bond, leading to another electron deficient starting material. Again, Ru48 shows to be the optimal catalyst for this electron deficient substrate. Using neat crotonate, 500 ppm Ru48 and 25 °C, TON of 300 to 500 are achieved for ethyl and butyl crotonate. Interestingly, a high pressure of ethylene leads to a higher conversion which is contrary to previous reports on electron deficient substrates. A possible explanation could be the high loading of neat starting material (0.35 mol) compared to the available ethylene (0.3 mol).[36]
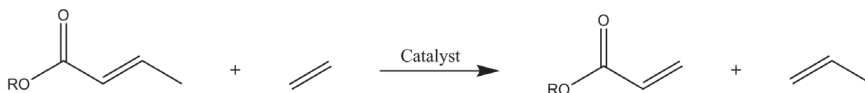
Figure 5.13. Ethenolysis of Crotonates

5.6 Perspectives

To justify an ethenolysis reaction using a precious metal in a homogeneous ruthenium catalysts, TONs over 50,000 must be reached.[11] Many parameters can be varied to obtain optimal conversion and selectivity to achieve these TONs, such as the use of solvent, ethylene pressure and temperature and many catalysts have been developed to obtain optimal results for each system.

When similar conditions for the ethenolysis of methyl oleate (MO) are compared using Figure 5.5 and Table 5.1, it becomes clear that the ethylene purity has a bigger influence on the TON than the catalyst used. For example, Table 5.1, entries 1 and 2, show that the TON achieved by Ru12 increases from 240,000 to 340,000 when the ethylene purity is increased from 99.95% to 99.995% using identical reaction conditions (10 bar ethylene, 40 °C, 180 minutes) and a slightly different loading (2 ppm and 1 ppm respectively). Similar observations can be made with Ru11, which shows an increase in TON of 120,000 from 35,000 when 99.95% pure ethylene is used instead of 99.9% purity (Table 5.1, entry 8 compared to entries 18 and 19). However, the reaction conditions differ in this case from 180 minutes to 30 minutes and a loading of 3 ppm and 10 ppm. These increases in TON are significantly larger than the increases obtained

by novel catalysts. Using 99.9% pure ethylene Ru11 obtains a TON of 35,000 (Table 5.1, entry 19)[15], which is only slightly higher than the TON of 24,800 obtained with the traditional Grubbs 1st generation catalyst, Ru1 (Table 5.1, entry 20).[11]

From these examples it becomes clear that ethylene purity is the most important factor that influences the TON. The lowering in TON by lower purity ethylene likely originates from catalyst poisoning. Removal of poisons such as carbon monoxide and acetylene from the substrate and ethylene streams is therefore a crucial way to achieve TONs above 50,000. Unfortunately, there is only one paper so far that uses ethylene purities above 99.9%.[13]

Removal of peroxides from the substrate by a treatment of Al_2O_3 at 200 °C leads to an increase in TON by a factor 8. An increase in ethylene purity from the commonly used 99.9% to 99.995% leads to an increase of TON by a factor ten to reach the highest reported TON so far of 340,000.[13] Removing specifically the compounds that are harmful for metathesis catalysts could improve TONs without the need of intensive purification of substrates. Ensuring that no poisons are introduced *via* the ethylene stream will enable high TONs, far above the threshold of 50,000.

The type of catalyst has a much smaller impact on the TONs of ethenolysis. This is illustrated by the fact that Grubbs 1st generation (Ru1) is still among the best performing catalysts. Next to the traditional catalysts that bear phosphine ligands, the catalysts with a cyclic (alkyl)(amino) carbine (CAAC) ligand reach high TONs. Within the bracket of 99.9% pure ethylene, a CAAC catalyst Ru11 and the traditional Grubbs 1st generation Ru1 show highest activity with TONs of 35,000[14, 15] and 24,800[11] respectively. Hoveyday-Grubbs catalysts Ru47, Ru48 and Ru49, which carry a chelating isopropoxy group, show high activity, but their TON is limited by a loss in selectivity due to a competing isomerisation reaction. Moreover, their unstable ruthenium alkylidene species decomposes to ruthenium hydride, which catalyses isomerisation reactions. These catalysts are best used in solvent systems or with electron poor substrates, where self-metathesis and isomerisation is not an issue.

Electron poor substrates are still challenging for ethenolysis reactions. The highly active Hoveyda-Grubbs 2nd generation catalyst (Ru48) is often used due to its high activity and the fact that self-metathesis and isomerisation of the starting material is often not an issue. Catalytic systems for these type of ethenolysis substrate still need to be further developed in order to reach economically feasible TONs. However, no ethenolysis of electron poor substrates were published with high purity ethylene and especially the sensitive Ru48 might benefit remarkably from poison removal.

With the broad range of biobased molecules with double bonds that could be selectively cleaved using ethenolysis, the development where TONs above 50,000 are achieved is very promising. Currently, the purity of the substrates has a larger impact on the TON for the ethenolysis of MO than the type of catalyst used. In order to assess which catalyst would be preferred, the most promising catalysts should be tested for the ethenolysis of MO using high purity ethylene and with the removal of peroxides. A full understanding of the influence of the purity of the feeds on the catalyst poisoning is crucial in order to obtain high TONs, which are required for the application of ethenolysis on biobased feedstocks.

5.7 References

1. Deuss, P. J.; Barta, K.; de Vries, J. G. *Catalysis Science & Technology* **2014,** 4, (5), 1174.

2. Leimgruber, S.; Trimmel, G. *Monatshefte für Chemie - Chemical Monthly* **2015,** 146, (7), 1081-1097.

3. Herbert, M. B.; Grubbs, R. H. *Angew Chem Int Ed* **2015,** 54, 5018-5024.

4. Buchmeiser, M. R. *Chemical reviews* **2009,** 109, 303-321.

5. Fustero, S.; Simon-Fuentes, A.; Barrio, P.; Haufe, G. *Chemical reviews* **2015,** 115, (2), 871-930.

6. Mol, J. C. *Journal of Molecular Catalysis* **1994,** 90, 185-199.

7. Mol, J. C.; Buffon, R. *J. Braz. Chem. Soc.* **1998,** 9, (1), 1-11.

8. Trnka, T. M.; Grubbs, R. H. *Acc. Chem. Res.* **2001,** 34, 18-29.

9. Mol, J. C. *Green Chemistry* **2002,** 4, (1), 5-13.

10. Bosma, R. H. A.; Aardweg, F. V. d.; Mol, J. C. *J.C.S. Chem Comm* **1981**, (21), 1132-1133.

11. Burdett, K. A.; Harris, L. D.; Margl, P.; Maughon, B. R.; Mokhtar-Zadeh, T.; Saucier, P. C.; Wasserman, E. P. *Organometallics* **2004,** 23, 2027-2047.

12. Chapuis, C.; Jacoby, D. *Applied Catalysis A: General* **2001,** 221, 93-117.

13. Marx, V. M.; Sullivan, A. H.; Melaimi, M.; Virgil, S. C.; Keitz, B. K.; Weinberger, D. S.; Bertrand, G.; Grubbs, R. H. *Angewandte Chemie* **2015,** 54, (6), 1919-23.

14. Schrodi, Y.; Ung, T.; Vargas, A.; Mkrtumyan, G.; Lee, C. W.; Champagne, T. M.; Pederson, R. L.; Hong, S. H. *CLEAN - Soil, Air, Water* **2008,** 36, (8), 669-673.

15. Anderson, D. R.; Ung, T.; Mkrtumyan, G.; Bertrand, G.; Grubbs, R. H.; Schrodi, Y. *Organometallics* **2008,** 27, 563-566.

16. Nickel, A.; Ung, T.; Mkrtumyan, G.; Uy, J.; Lee, C. W.; Stoianova, D.; Papazian, J.; Wei, W.-H.; Mallari, A.; Schrodi, Y.; Pederson, R. L. *Topics in Catalysis* **2012,** 55, (7-10), 518-523.

17. Thomas, R. M.; Keitz, B. K.; Champagne, T. M.; Grubbs, R. H. *Journal of the American Chemical Society* **2011**.

5

18. Thomas, R. M.; Keitz, B. K.; Champagne, T. M.; Grubbs, R. H. *Journal of the American Chemical Society* **2011,** 133, (19), 7490-6.

19. Marinescu, S., C.; Schrock, R. R.; Müller, P.; Hoveyda, A. H. *Journal of the American Chemical Society* **2009,** 131, 10840-10841.

20. Aydos, G. L. P.; Leal, B. C.; Perez-Lopez, O. W.; Dupont, J. *Catalysis Communications* **2014,** 53, 57-61.

21. Thurier, C.; Fischmeister, C.; Bruneau, C.; Olivier-Bourbigou, H.; Dixneuf, P. H. *ChemSusChem* **2008,** 1, (1-2), 118-122.

22. Zhang, J.; Song, S.; Wang, X.; Jiao, J.; Shi, M. *Chemical communications* **2013,** 49, (82), 9491-3.

23. Park, C. P.; Van Wingerden, M. M.; Han, S.-Y.; Kim, D.-P.; Grubbs, R. H. *Organic Letters* **2011,** 13, (9), 2398-2401.

24. Forman, G. S.; McConnell, A. E.; Hanton, M. J.; Slawin, A. M. Z.; Tooze, R. P.; van Rensburg, W. J.; Meyer, W. H.; Dwyer, C.; Kirk, M. M.; Serfontein, D. W. *Organometallics* **2004,** 23, 4824-4827.

25. Forman, G. S.; Bellabarba, R. M.; Tooze, R. P.; Slawin, A. M. Z.; Karch, R.; Winde, R. *Journal of Organometallic Chemistry* **2006,** 691, (24-25), 5513-5516.

26. Kadyrov, R.; Azap, C.; Weidlich, S.; Wolf, D. *Topics in Catalysis* **2012,** 55, (7-10), 538-542.

27. Öztürk, B. Ö.; Topoğlu, B.; Karabulut Şehitoğlu, S. *European Journal of Lipid Science and Technology* **2015,** 117, (2), 200-208.

28. Miao, X.; Fischmeister, C.; Bruneau, C.; Dixneuf, P. H. *ChemSusChem* **2008,** 1, (10), 813-6.

29. Bidange, J.; Dubois, J.-L.; Couturier, J.-L.; Fischmeister, C.; Bruneau, C. *European Journal of Lipid Science and Technology* **2014**, n/a-n/a.

30. Behr, A.; Krema, S.; Kämper, A. *RSC Advances* **2012,** 2, (33), 12775.

31. Patil, V. B.; Saliu, K. O.; Jenkins, R. M.; Carnahan, E. M.; Kramer, E. J.; Fredrickson, G. H.; Bazan, G. C. *Macromolecular Chemistry and Physics* **2014,** 215, (11), 1140-1145.

32. Song, J.; Hou, M.; Liu, G.; Zhang, J.; Han, B.; Yang, G. *J. Phys. Chem. B* **2009,** 113, 2810-2814.

33. Manzini, S.; Poater, A.; Nelson, D. J.; Cavallo, L.; Slawin, A. M.; Nolan, S. P. *Angewandte Chemie* **2014,** 53, (34), 8995-9.

34. Le Ravalec, V.; Fischmeister, C.; Bruneau, C. *Advanced Synthesis & Catalysis* **2009,** 351, (7-8), 1115-1122.

35. Le Ravalec, V.; Dupe, A.; Fischmeister, C.; Bruneau, C. *ChemSusChem* **2010,** 3, (11), 1291-7.

36. Schweitzer, D.; Snell, K. D. *Organic Process Research & Development* **2014**, 141124132601002.

37. Lima, P. S.; Ferreira, L. A.; Freitas, L. H.; Rheinheimer, M. W.; Sokolovicz, Y. C. A.; Schrekker, H. S. *Journal of the Brazilian Chemical Society* **2014**.

38. Jenkins, R. W.; Sargeant, L. A.; Whiffin, F. M.; Santomauro, F.; Kaloudis, D.; Mozzanega, P.; Bannister, C. D.; Baena, S.; Chuck, C. J. *ACS Sustainable Chemistry & Engineering* **2015,** 3, (7), 1526-1535.

39. Schotten, C.; Plaza, D.; Manzini, S.; Nolan, S.; Ley, S. V.; Browne, D. L.; Lapkin, A. *Sustainable Chemistry and Engineering* **2015**.

40. van der Klis, F.; Le Nôtre, J.; Blaauw, R.; van Haveren, J.; van Es, D. S. *European Journal of Lipid Science and Technology* **2012,** 114, (8), 911-918.

41. Julis, J.; Bartlett, S. A.; Baader, S.; Beresford, N.; Routledge, E. J.; Cazin, C. S. J.; Cole-Hamilton, D. J. *Green Chemistry* **2014,** 16, (5), 2846.

42. Mmongoyo, J. A.; Mgani, Q. A.; Mdachi, S. J. M.; Pogorzelec, P. J.; Cole-Hamilton, D. J. *European Journal of Lipid Science and Technology* **2012,** 114, (10), 1183-1192.

43. Shinde, T.; Varga, V.; Polášek, M.; Horá ek, M.; Žilková, N.; Balcar, H. *Applied Catalysis A: General* **2014,** 478, 138-145.

44. Baader, S.; Podsiadly, P. E.; Cole-Hamilton, D. J.; Goossen, L. J. *Green Chem.* **2014,** 16, (12), 4885-4890.

45. Wolf, S.; Plenio, H. *Green Chemistry* **2011,** 13, (8), 2008.

46. Wagener, K. B.; Puts, R. D.; Smith, D. W. J. *Makromol. Chem., Rapid Commun.* **1991,** 12, 419-425.

47. Gutierras, S.; Vargas, S. M.; Tlenkopatchev, M. A. *Polymer Degradation and Stability* **2004,** 83, (1), 149-156.

48. Watson, M. D.; Wagener, K. B. *Journal of Polymer Science Part A: Polymer Chemistry* **1999,** 37, 1857-1861.

49. Ouardad, S.; Peruch, F. *Polymer Degradation and Stability* **2014,** 99, 249-253.

50. Ortega, J. V.; Fomine, S.; Tlenkopatchev, M. A. *Polymer Degradation and Stability* **2004,** 86, (1), 85-93.

51. Wolf, S.; Plenio, H. *Green Chem.* **2013,** 15, (2), 315-319.

52. Karlou-Eyrisch, K.; Müller, B. K. M.; Herzig, C.; Nuyken, O. *Journal of Organometallic Chemistry* **2000,** 606, 3-7.

53. Eyrisch, K. K.; Müller, B. K. M.; Herzig, C.; Nuyken, O. *Designed Monomers & Polymers* **2004,** 7, (6), 661-676.

54. Gerber, L. C. H.; Schrock, R. R. *Organometallics* **2013,** 32, (19), 5573-5580.

55. Spekreijse, J.; Le Nôtre, J.; van Haveren, J.; Scott, E. L.; Sanders, J. P. M. *Green Chemistry* **2012,** 14, 2747-2751.

56. Scholz, J.; Loekman, S.; Szesni, N.; Hieringer, W.; Görling, A.; Haumann, M.; Wasserscheid, P. *Advanced Synthesis & Catalysis* **2011,** 353, 2701-2707.

5

57. Jermacz, I.; Maj, J.; Morzycki, J. W.; Wojtkielewicz, A. *Toxicology mechanisms and methods* **2008,** 18, (6), 469-471.

58. Baader, S.; Ohlmann, D. M.; Goossen, L. J. *Chemistry* **2013,** 19, (30), 9807-10.

5
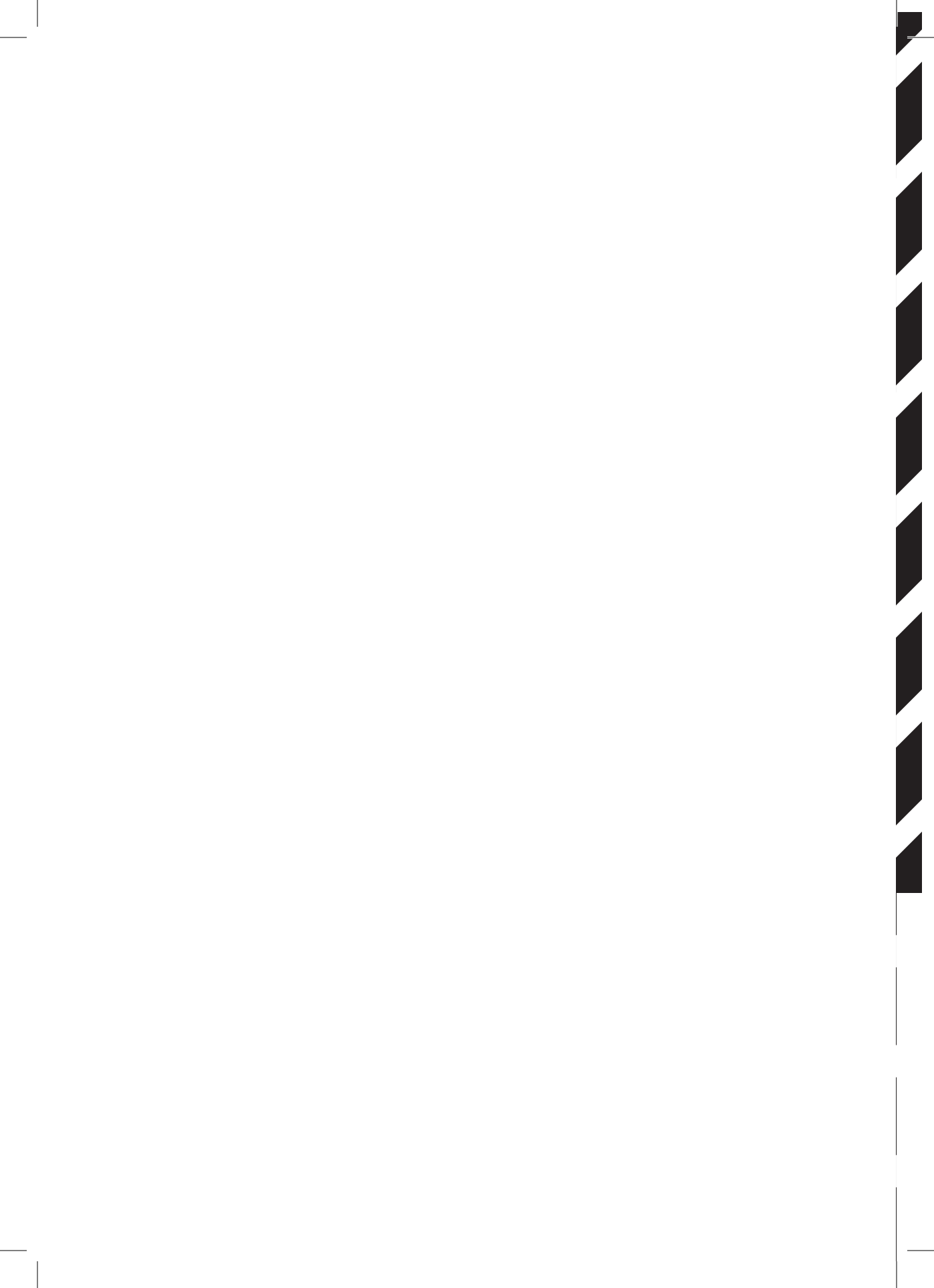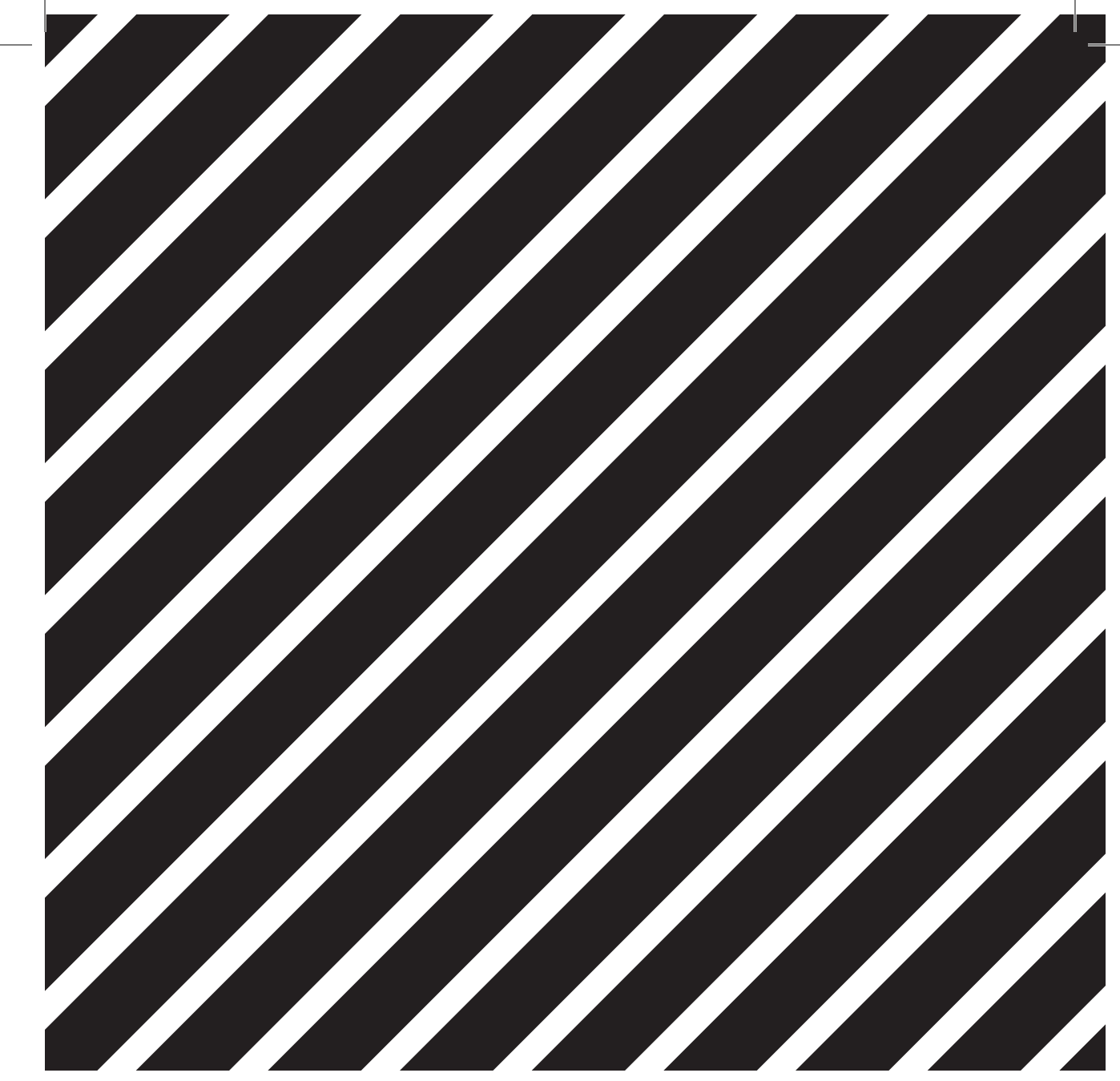
General discussion and recommendations

6.1 Introduction

Within the concept of a biorefinery, wastewater streams containing organic compounds can be used as a resource for chemicals. The organic compounds can be converted to polyhydroxy-alkanoate (PHA) using microorganisms. PHA is produced in a fermentation process which simultaneously cleans the wastewater. The most common form of PHA is polyhydroxybutyrate (PHB). However, the implementation of PHB from wastewater as a material poses several challenges, such as the fluctuating amount of valerate in the polymer chain, which causes fluctuating material properties.[1] Additionally, PHB is difficult to melt process due to its decomposition temperature. Moreover, it does not age well as a material, which leads to stiffness and brittleness.[2] To overcome the challenges of applying PHB as a plastic, the potential use of PHB as intermediate towards biobased building blocks is explored in this thesis (Figure 6.1).

In a wastewater treatment plant, PHB can be produced while cleaning wastewater (Figure 6.1, left). The PHB can either be isolated from the microorganisms and converted to methyl croto-nate (MC) (**chapter 2**) or the PHB rich cells can directly be converted to MC circumventing the need of a downstream processing (DSP) (**chapter 3**). In chapter 2, the reaction pathway of the conversion of PHB to MC is elucidated and the conditions are optimised using purified PHB. In chapter 3, the purified PHB is replaced by PHB rich cells and the effects of fermentation residues are investigated. The resulting MC could be used in an ethenolysis to obtain methyl acrylate and propylene. This reaction requires the use of an expensive homogeneous ruthenium-based catalyst. In order to improve the economic aspect of this conversion, the metathesis catalyst is immobilised in a metal organic framework (MOF) (**chapter 4**). Here a mechanochemical approach is used and its effects on immobilisation and stability are explored. In **chapter 5**, the application of ethenolysis on biomass in general is discussed as well as the importance of the purity of substrates in order to reach high turnover numbers (TONs). In this chapter (**chapter 6**) the results are summarised and suggestions for further research and development are discussed.
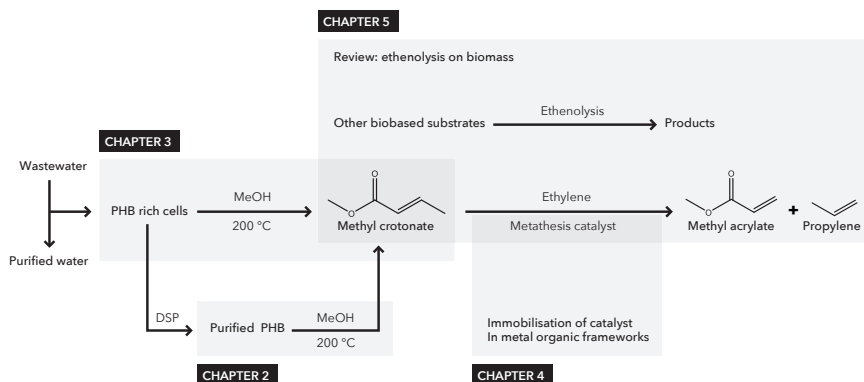
Figure 6.1. Thesis outline.

6.2 Conversion of PHB to methyl crotonate

In chapter 2, the conversion of commercial, purified PHB to MC is discussed. The conversion of PHB to crotonic acid (CA) as a biobased building block has been reported by a number of authors.[3-6] However, MC has an advantage due to its immiscibility with water, which can aid the separation of the product. It has been shown that MC can be obtained in a single, catalyst free reaction, using methanol at 200 °C and 18 bar. Under these conditions methanol refluxes in the cooled reactor head, while the bottom of the reactor has a temperature of 200 °C. Thus, facilitating conditions for thermolysis followed by esterification and full conversion with a 70% selectivity towards crotonates (MC and CA) is obtained (Figure 6.2). Depending on the reaction conditions, a side reaction may occur where PHB undergoes a transesterification reaction to form methyl 3-hydroxybutyrate (M3HB) (Figure 6.2). It was also observed that below 18 bar, the esterification is the rate determining step, while at conditions above 18 bar the thermal conversion of PHB to CA is the rate determining step.
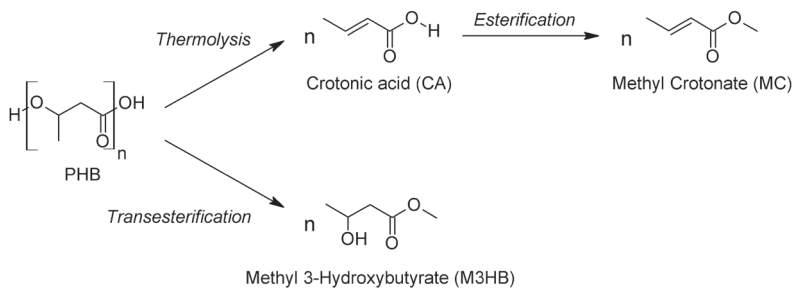
Figure 6.2. Reaction pathway of PHB to MC and the side reaction forming M3HB.

6.2.1 REACTOR DESIGN

For an optimal process it is important to obtain a high selectivity. In the conversion of PHB to MC one of the factors that limit the selectivity towards crotonates to 70% is the side product formation of M3HB. This side product formation could be avoided by changing the reaction set up. The reaction is performed in a closed reactor in a heating mantle. The temperature is measured near the bottom of the reactor, while the top of the reactor is cooled to 20 °C to prevent damage to the pressure sensor. This set up results in an unusual system where a temperature gradient is formed over the reactor. Since 10 mL gaseous methanol at 200 °C in a volume of 75 mL would reach a pressure of 130 bar, we concluded that the methanol is present in liquid state. This can only be explained by a reflux system, where the methanol condenses at the top of the reactor and flows down *via* the reactor wall over a temperature gradient where it evaporates again (Figure 6.3).
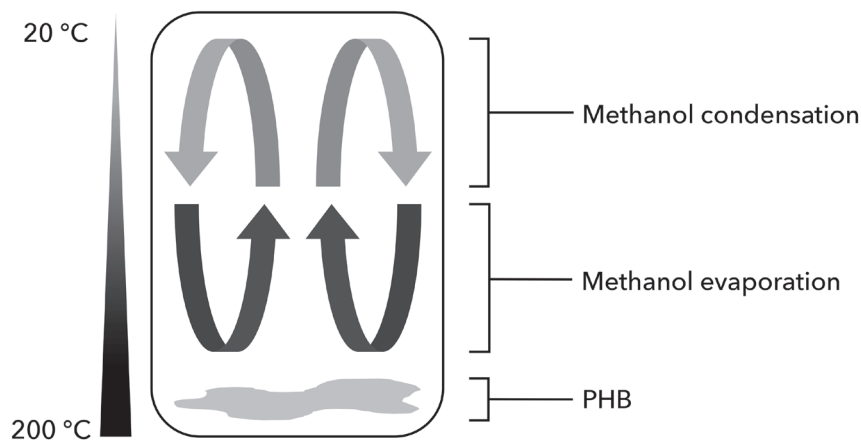
Figure 6.3. Scheme of the reactor with methanol refluxing in the top.

The reflux system causes the PHB at the bottom of the reactor to first undergo thermal conversion to CA, which at 200 °C is in gaseous state and then comes into contact with the methanol in the top of the reactor to form MC. When the reactor is heated up, the methanol is still at the bottom of the reactor and may already start reacting with the PHB to form M3HB as a side product before the desired reflux system is reached.

In order to overcome this initial M3HB formation a continuous system where PHB is allowed to thermally convert to CA followed by a direct conversion of CA with methanol to MC could be used. A continuous system, where the methanol is not in contact with the PHB would prevent M3HB formation and result in a higher MC formation. Therefore, a continuous reactor system should be designed to increase the selectivity of the conversion. In this system a pressure range of 18 to 30 bars becomes viable and the prevention of M3HB formation could increase the MC formation by 10% to 20%.

6.2.2 DEGRADATION PRODUCTS

Another factor that limits the selectivity of the conversion is the degradation to gaseous products. At high temperatures, M3HB, CA and MC degrade into CO_2 and other small, gaseous compounds. These gases were detected and identified as ethylene and propylene by sampling gas from the reactor headspace and analysing the sample using gas chromatography. A nitrogen flow was used to obtain a sample of the reactor headspace, therefore only an identification of the components could be obtained and no quantitative analysis was achieved.

From these qualitative measurements, it can be concluded that the greatest contribution to the formation of gaseous compounds is the degradation of MC and M3HB. MC shows a significant mass loss of 15% at 200 °C (Figure 2.5, chapter 2), where M3HB leads to 30% gaseous products

at this temperature (Figure 2.3, chapter 2). Degradation of MC could arise from hydrolysis followed by a decarboxylation leading to propylene. The degradation of M3HB to C2 compounds at high temperatures is known.[7] Due to the lack of quantitative data on the gaseous products, it is unclear which pathway is the main contributor to the formation of gaseous side products. When the gases are quantified, the origin of the gases as either crotonates or 3-hydroxybutyrates (3-hydroxybutyric acid (3HB) and M3HB) could be identified, which gives more information about the initial selectivity of the conversion of PHB.

The formation of gaseous side products could be overcome by lowering the reaction temperature. A lower reaction temperature can be made feasible by using a catalytic system. For example, conjugated bases of weak Brønsted-Lowry acids show a decrease in the degradation temperature of PHB by promoting the E1cB mechanism.[8] The stimulation of the E1cB mechanism will enable the formation of CA from PHB at lower temperatures. However, the temperature should be kept above 150 °C, since the conversion of CA to MC does not proceed below 150 °C (Figure 2.2, chapter 2).

6.3 Conversion of PHB in cells to methyl crotonate

The downstream processing of PHB costs, depending on the method used, between €1.40 and €1.95 per kg PHB, which constitutes of 70% to 80% of the total cost of the PHB production.[9] It is therefore desirable to minimise the downstream processing and use unpurified biomass. In order to enable the conversion of PHB to MC on biomass directly, the knowledge obtained in chapter 2 on the reaction pathway was applied in chapter 3, where PHB rich biomass samples from a PHB production pilot plant at a chocolate factory wastewater outlet were used. In a wastewater treatment plant, PHA is produced as a copolymer of 3-hydroxybutyrate and 3-hydroxyvalerate. It was found that a water content of up to 20% and the incorporation of 3-hydroxyvalerate monomers have no influence on the conversion of the 3-hydroxybutyrate fraction of PHA to MC. However, residual magnesium salts from the fermentation broth are capable of catalysing the reaction to MC or, depending on the counter ion, catalyse the side reaction to M3HB. The conversion was directly measured in the reaction mixture by High Pressure Liquid Chromatography (HPLC) and no purification was performed.

6.3.1 OPTIMISING PHB DOWNSTREAM PROCESSING

In order to enable a direct conversion of PHB rich biomass, it is of importance to understand the influence of fermentation residues. In this regard, two magnesium salts were tested on their influence on the conversion of PHB to MC, which showed that the type of salt is an important factor on the conversion. To achieve full understanding of the influence of residual fermentation components, an extensive screening of common fermentation salts and organic components should be performed. This will give a better understanding in how the different salts influence

the reaction and which type of DSP is needed before the PHB rich biomass is converted to MC. It has been found that monovalent metal ions, such as potassium ions, have a bigger influence on the E1cB mechanism than the bivalent magnesium ions tested in chapter 3.[8] Therefore, we expect that the influence of salts containing monovalent metal ions is more pronounced than the influence of magnesium ions.

The influence of water on the conversion is not yet well understood. When water is added to the reaction, the selectivity of the reaction for pure PHB and PHB in cells is different, where pure PHB forms high amounts of CA and 3HB and PHB in cells forms mostly M3HB. The cause of this different reactivity is still unknown. It is possible that the encapsulation of PHB in cells prevents a fast heating of the PHB granules, while it forms a poor barrier against methanol, favouring a transesterification reaction to M3HB over a thermal conversion to CA. With a better understanding of the influence of cells and fermentation residues on the reactivity of PHB in the presence of water, a system could be developed where the products formed are controlled by modifications in the DSP.

Overall, the results indicate that a full purification of PHB before conversion to MC is not required. Without the requirement to isolate the PHB from within the cells, the DSP can be significantly reduced. A disruption of the cell walls and a subsequent extraction of PHB is no longer required. A washing to remove salts and drying to a water content of 20% will be sufficient to obtain a conversion to MC of 50%, which is close to the 60% MC obtained for pure PHB.

6.3.2 METHYL CROTONATE PURIFICATION

The MC formed during the reaction must also undergo a DSP before it can be used as a commodity chemical. The isolation of MC, and therefore the optimal DSP of MC, was not determined. In both chapter 2 and chapter 3, the conversion of PHB to MC was determined by HPLC on the reaction mixture without purification. MC could be isolated using distillation due to its volatile nature. The immiscibility of MC with water could also be used in the separation since most side products are soluble in water, whereas MC is not. This means that a system where water is added to the methanol could be used to isolate MC from the reaction mixture. This would remove the need of a distillation tower and reduce the energy needed for the purification. However, an additional cleaning of the resulting water would be required and further analysis of the purification of MC is needed in order to study whether this route or a distillation of the reaction mixture is preferred.

By using PHB rich cells instead of purified PHB, a large part of the production costs of PHB is avoided and the DSP is minimised to a drying step. However, the fermentation residues and products formed from the biomass present in the reaction have to be taken into account for the DSP of MC. It can be postulated that the additional purification of MC that is presented by the fermentation residues is more straightforward than the isolation of PHB from within the cells. It is therefore likely that the additional purification of MC is less expensive than the isolation of PHB and that a direct conversion of PHB rich cells is favoured over the conversion of purified PHB. However, a cost analysis should be performed to confirm this hypothesis.

6.3.3 LARGE SCALE IMPLEMENTATION OF THE CONVERSION OF PHB RICH CELLS TO METHYL CROTONATE

With a simple, one step conversion without the use of catalyst, the conversion of PHB rich cells to MC is a promising technique. However, the implementation of this new technique on a large scale has several challenges to overcome. For example, new techniques require investments and the wastewater streams are very dilute which make them unsuitable for transport. To prevent transport of wastewater, there is a possibility of converting carbon rich wastewater streams to MC on site at a small scale due to a limited DSP of PHB. This allows for water to be recycled and gives room for innovations to the new technique without large investments.[10]

Another method to minimise investment costs is to adapt current systems to enable the conversion of PHB. Currently, a common treatment of the resulting sludge from wastewater treatment plants of pulp and paper industry is a mechanical dewatering followed by incineration. The dewatering leads to a dry content of 20 to 50%, which can be increased to 68% by using thermal drying instead.[11] When the current biomass is replaced by PHB rich biomass, the same equipment could be used for drying. Instead of an incineration to obtain energy from the dried PHB rich cells, it will then be heated in the presence of methanol to obtain the more valuable MC. Further research should be aimed at calculating the feasibility of this small scale conversion using carbon rich wastewater examples together with testing the conversion on pilot scale using existing equipment.

6.4 Immobilisation of Hoveyda-Grubbs 2nd generation catalyst

In order to convert MC to methyl acrylate and propylene, two important monomers for the plastics industry, a metathesis reaction can be used. This conversion is performed using ethylene and a homogeneous ruthenium catalyst. However, as discussed in chapter 5, this conversion suffers from low TONs. An immobilisation of the ruthenium catalyst would help towards economically feasible TONs. In chapter 4, a method to immobilise the catalyst in a MOF is discussed using Hoveyda-Grubbs 2nd generation (HG2). The MOF of choice, MIL-101-NH_2(Al) has three distinct advantages. First, it is easily synthesised from commercially available building blocks. Second, it has a large cage structure with cavities big enough to hold the HG2 catalyst linked with pores that are too small for the catalyst to leach out. Third, the MOF is stable at higher temperatures and in most solvents, making it possible to perform a range of metathesis reactions with the material. Initial attempts using a bottle around the ship method proved unsuccessful due to the instability of the HG2 catalyst in these reaction conditions. However, a mechanochemical method, where the MOF and HG2 catalysts are ground in a ball-mill resulted in an immobilised catalyst with a ruthenium loading of 0.25%. In this chapter, the catalyst and the resulting MOF structure are analysed. The structure is shown to partially convert from a MIL-101 structure to a MIL-53 structure. The immobilised catalyst remained active for several runs

without leaching, however, the activity dropped significantly from 98% conversion in the first run to 10% conversion in the eighth run. The procedure could be repeated with Zhan catalyst, a second ruthenium metathesis catalyst.

6.4.1 THE INFLUENCE OF THE MOF ON CATALYST ACTIVITY

The activity of Grubbs catalysts in MOFs and the influence of the MOF on the activity is not yet well understood. The resulting MOF structure proved difficult to analyse and several pieces of information lead us to believe that the structure changed from MIL-101 to MIL-53 with small amounts of the MIL-101 structure still intact. First, powder X-ray diffraction showed a clear MIL-53 structure, which indicates that the major part of the compound exists as a MIL-53 structure. However, N_2-sorption experiments show the existence of pores that are in similar size to MIL-101 pores. Moreover, when MIL-53 is used as a starting material, the resulting immo-bilised HG2 is not active in catalysis. Therefore the active, immobilised HG2 that is obtained when MIL-101 is used as a starting material must have a different structure. This leads to the hypothesis that small areas of MIL-101 still exist after the conversion of MIL-101 to MIL-53. A better understanding on the conversion of MIL-101 to MIL-53 by mechanochemical means is needed for a better understanding of the activity of Grubbs catalysts in these structures.

The presence of catalytic activity of immobilised HG2 and Zhan catalysts inside the MOF struc-ture has been shown. However, the influence of the MOF on the TON and turnover frequency (TOF) was not studied. The immobilisation may have an effect on the rate of the catalysis due to mass transfer limitation. On the other hand, the stability of the catalyst may be enhanced due to the lack of catalysts interacting with each other and forming an inactive ruthenium dimer species.[12] Further studies, where other conditions such as reaction time of the catalysis are studied will be needed to understand the influence of the MOF structure on the catalysis.

6.4.2 IMPROVING THE CATALYST STABILITY AND ACTIVITY

The TONs of the immobilised catalyst remained low, with a total TON of 70, which is too low for an economical feasible route. The TON needs to exceed 10.000 before applications could be investigated.[13] The lifetime of the metathesis catalyst needs to be improved, which could be achieved by performing all operations under a protective atmosphere. A continuous flow system, where the catalyst does not need to be isolated and washed, would prevent exposure to air. This would increase the catalyst lifetime and thereby increase the TONs.

Another method to improve the catalytic performance is to prevent the presence of inactive catalyst. The inactive catalyst present decrease both TOF and TON, since it has no catalytic activity. Catalyst deactivation occurs from catalyst being entrapped in the MIL-53 part of the MOF. To increase the performance of the catalyst, the amount of MIL-53 formed should be minimised. The mechanochemical procedure has not been optimised and the influence of factors such as time and speed of the ball mill procedure could have a pronounced effect on the product. The conversion of MIL-101 structure into MIL-53 could be followed over time

and, using this data, the amount of immobilised HG2 in MIL-101 cavities could be improved. Another method to decrease the amount of MIL-53 structure formed is the use of DMF during the mechanochemical procedure. It is known that DMF promotes the formation of MIL-101 over MIL-53.[14] Therefore, addition of DMF during the mechanochemical procedure could impact the MIL-101 conversion as well, which would enable a higher loading of active catalyst in the MOF structure.

6.4.3 RUTHENIUM LEACHING

A direct leaching experiment for ruthenium could not be performed due to small MOF particles that could not be fully separated by centrifugation. These small MOF particles present in the product would give a false positive reading for ruthenium leaching. However, no loss of ruthenium from the MOF was observed after the reactions. Moreover, an experiment where the reaction was stopped and the reaction mixture was left to stir showed no conversion, indicating that the conversion did not originate from leached catalyst. The ruthenium content in the product should be analysed to really ensure no ruthenium leached from the immobilised catalyst. This is could potentially be achieved by a microfiltration to filter off the small MOF particles.

6.4.4 SCOPE OF MECHANOCHEMICAL IMMOBILISATION METHOD

The immobilisation of homogeneous catalysts in MOFs using mechanochemistry has not been studied before. To test the scope of an immobilisation method using mechanochemistry, different catalysts could be trapped in the MIL-101 structure. These catalysts need to be stable under air or a mechanochemical setup under a protective atmosphere would be needed. Moreover, the MOF could be varied, where the influence of different metal centres within a MIL-101 structure could be tested. Different porous MOFs, which may not undergo a change in morphology could also be explored for the immobilisation of catalysts. For example, the zinc-based MOF ZIF-8 has been shown to be able to trap caffeine.[15] Mechanochemical entrapment of catalysts in MOFs could lead to simple method where homogeneous catalysts can be immobilised using a standard procedure.

6

6.5 Homogeneous ethenolysis of biobased feedstocks

In chapter 5, the current state of the ethenolysis reaction in literature is studied by using the ethenolysis of methyl oleate (MO) as an example. Many catalysts have been developed to optimise different classes of metathesis reactions or to learn more on how the catalyst behaves. However, the highest improvements on TONs for ethenolysis reactions are obtained when the purity of the starting materials are improved. A higher purity of ethylene of 99.995% from 99.95% leads to an increase in TON of 340.000 from 240.000 in similar conditions for the conversion of MO.[16] Moreover, the removal of peroxides from the substrate lead to an increase in TON from 284 to 1.239 in the ethenolysis of oleonitrile.[17] A dedicated research paper on the influence of potential poisons and optimal removal of these compounds is needed to further the field and to be able to assess the plausibility of an economically viable ethenolysis of biomass. When the ethenolysis is optimised in terms of TONs by selective removal of catalyst poisons, immobilised catalysts could be explored to further increase the TON of the expensive ruthenium catalysts.

6.5.1 APPLICATIONS OF THE CONVERSION OF METHYL CROTONATE TO PROPYLENE AND METHYL ACRYLATE

The ethenolysis of MC to propylene and methyl acrylate has been shown to be a challenging reaction due to the vicinity of an ester group to the double bond. This leads to low conversions, where TONs of 300 to 500 are achieved.[18] To achieve TONs above 10.000, which is needed for an economically feasible pathway,[13] the TON needs to be improved by a factor 20. Using high purity ethylene will be the first step towards reaching high TONs. With an increased catalyst lifetime from less catalyst poisoning, the immobilisation of the homogeneous catalyst in a MOF could be sufficient to increase the total TON of the catalyst above the threshold of 10.000.

6.6 Outlook

The conversion of PHB to CA has been suggested in a range of publications. For example, this conversion can be performed using concentrated acid at 100 °C,[4] or using $Mg(OH)_2$ at 260 to 320 °C.[6] When the PHB purification is optimised, PHB rich cells can be used without the need of a catalyst. This pyrolysis uses temperatures around 310 °C.[3] Compared to the direct conversion using MeOH, similar results are obtained using PHB rich cells, where 50% MC is obtained. However, a lower temperature of 200 °C can be used. Moreover, due to its immiscibility with water, a DSP of MC will be more straightforward than the DSP of CA.

Next to obtaining acrylic acid and propylene from PHB *via* MC, nitrogen containing chemicals could be obtained from PHB by reacting PHB with ammonia *via* an amidation pathway. The resulting crotonamide could then undergo ethenolysis to obtain acrylamide and propylene (Figure 6.4).
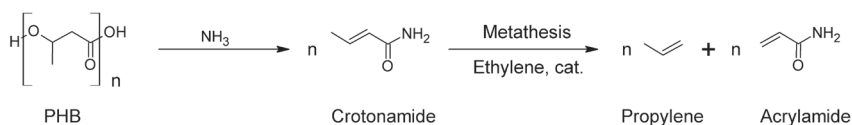

**Figure 6.4. Conversion of PHB to propylene and acrylamide via crotonamide.**

Unfortunately, initial results using ammonia showed very low selectivity towards the amidation reaction of PHB and even with a full conversion of PHB no crotonamide formation was observed. A method using a Lewis acid to catalyse the reaction could be developed to obtain a selective amidation.[19] Even when crotonamide could efficiently be obtained from PHB, a route towards nitrogen containing chemicals from biomass might be more efficient when amino acids are used as starting materials to prevent the high energy use of the production of ammonia.[20]

Due to its simplicity and cheap starting materials, the conversion of PHB to MC can be promising even with low conversions. The ethenolysis, however, requires a ruthenium catalyst and ethylene. TONs over 10.000 need to be achieved to make this route economically feasible.[13] Even when such TONs could be reached in the conversion of MC to propylene and methyl acrylate, it is likely that a conversion of PHB to MC is economically more attractive. Moreover, many pathways to obtain biobased acrylic acid have emerged, including fermentation from starch and glucose and the conversion of glutamic acid and glycerol.[21] For crotonates, there are few biobased routes available next to the conversion of PHB. Biobased CA can be obtained from bacterial fermentation. The purification of CA from water, however, is a challenging task that includes an inefficient crystallisation step. The fossil route to CA is long and results in low yields (30%) and a more efficient biobased route to crotonates may enable the emergence of CA and MC as platform chemicals.[22]

6

6.7 References

1. Tamis, J.; Luzkov, K.; Jiang, Y.; Loosdrecht, M. C.; Kleerebezem, R. *Journal of biotechnology* **2014,** 192PA, 161-169.

2. Bugnicourt, E. *Express Polymer Letters* **2014,** 8, (11), 791-808.

3. Zakaria Mamat, M. R.; Ariffin, H.; Hassan, M. A.; Mohd Zahari, M. A. K. *Journal of Cleaner Production* **2014,** 83, 463-472.

4. Chen, L. X. L.; Yu, J. *Macromolecular Symposia* **2005,** 224, (1), 35-46.

5. Ariffin, H.; Nishida, H.; Shirai, Y.; Hassan, M. A. *Polymer Degradation and Stability* **2010,** 95, (8), 1375-1381.

6. Ariffin, H.; Nishida, H.; Hassan, M. A.; Shirai, Y. *Biotechnology journal* **2010,** 5, (5), 484-92.

7. August, R.; McEwen, I.; Taylor, R. *J. Chem. Soc., Perkin Trans. II* **1987**, 1683-1689.

8. kawalec, M.; Sobota, M.; Scandola, M.; Kowalczuk, M.; Kurcok, P. *Journal of Polymer Science Part A: Polymer Chemistry* **2010,** 48, (23), 5490-5497.

9. Fernandez-Dacosta, C.; Posada, J. A.; Kleerebezem, R.; Cuellar, M. C.; Ramirez, A. *Bioresource technology* **2015,** 185, 368-77.

10. Bruins, M. E.; Sanders, J. P. M. *Biofuels, Bioproducts and Biorefining* **2012,** 6, 135-145.

11. Stoica, A.; Sandberg, M.; Holby, O. *Bioresource technology* **2009,** 100, (14), 3497-505.

12. Leitao, E. M.; Dubberley, S. R.; Piers, W. E.; Wu, Q.; McDonald, R. *Chemistry* **2008,** 14, (36), 11565-72.

13. Chapuis, C.; Jacoby, D. *Applied Catalysis A: General* **2001,** 221, 93-117.

14. Goesten, M. G.; Magusin, P. C.; Pidko, E. A.; Mezari, B.; Hensen, E. J.; Kapteijn, F.; Gascon, J. *Inorganic chemistry* **2014,** 53, (2), 882-7.

15. Liedana, N.; Galve, A.; Rubio, C.; Tellez, C.; Coronas, J. *ACS applied materials & interfaces* **2012,** 4, (9), 5016-21.

16. Marx, V. M.; Sullivan, A. H.; Melaimi, M.; Virgil, S. C.; Keitz, B. K.; Weinberger, D. S.; Bertrand, G.; Grubbs, R. H. *Angewandte Chemie* **2015,** 54, (6), 1919-23.

17. Bidange, J.; Dubois, J.-L.; Couturier, J.-L.; Fischmeister, C.; Bruneau, C. *European Journal of Lipid Science and Technology* **2014**, n/a-n/a.

18. Schweitzer, D.; Snell, K. D. *Organic Process Research & Development* **2014**, 141124132601002.

19. Lundberg, H.; Tinnis, F.; Selander, N.; Adolfsson, H. *Chemical Society reviews* **2014,** 43, (8), 2714-42.

20. Scott, E.; Peter, F.; Sanders, J. *Applied microbiology and biotechnology* **2007,** 75, (4), 751-62.

21. Beerthuis, R.; Rothenberg, G.; Shiju, N. R. *Green Chem.* **2014**.

22. Farid, N. F. S. M.; Ariffin, H.; Mamat, M. R. Z.; Mohd Zahari, M. A. K.; Hassan, M. A. *RSC Adv.* **2015,** 5, (42), 33546-33553.

6
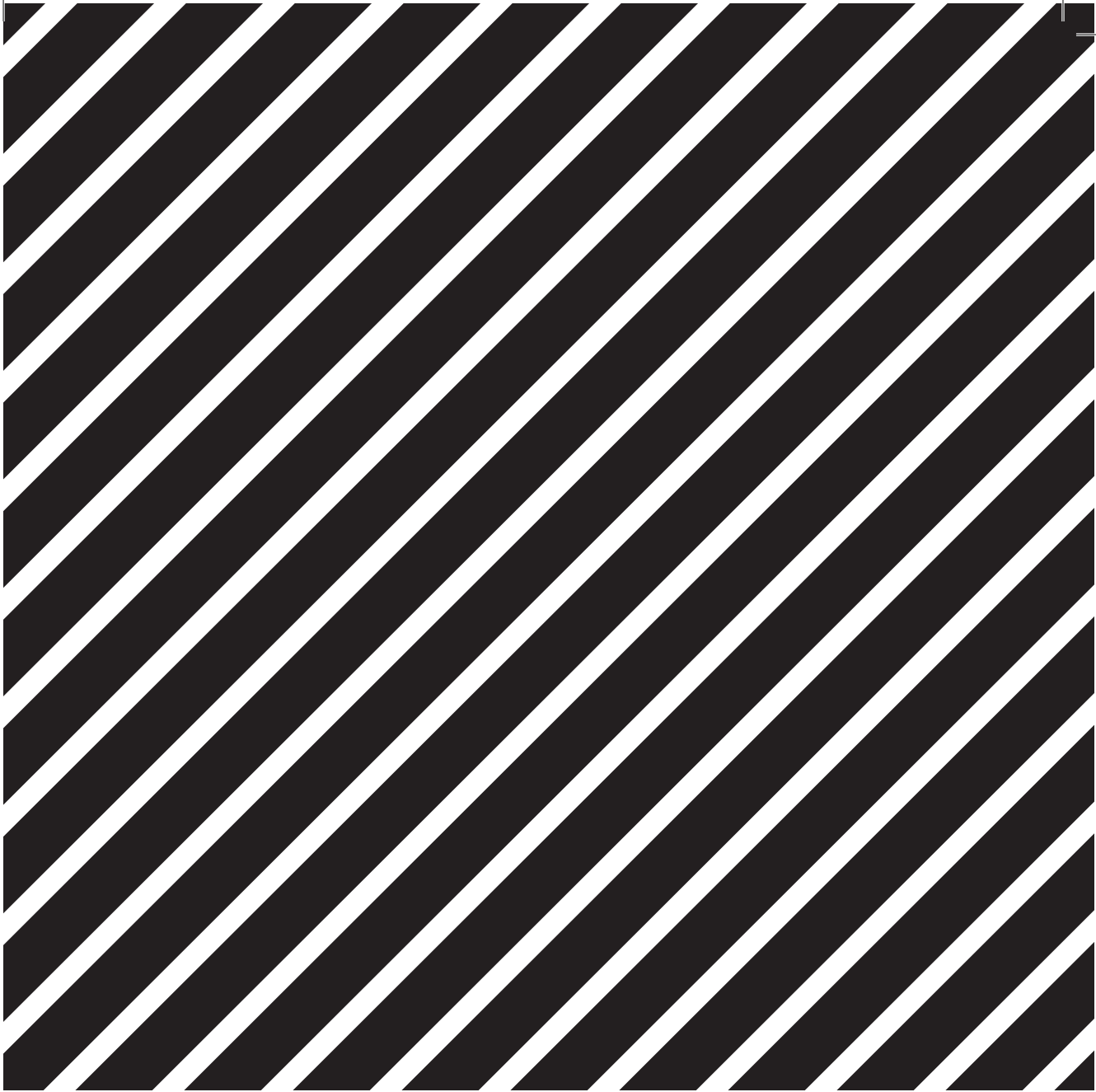
Supplementary information to the research chapters

Appendix A
Supplementary information to Chapter 2

A.1 EXPERIMENTAL

A.1.1 General

Proton nuclear magnetic resonance spectra (^{1}H NMR) were recorded on a Bruker AM-400 (400 MHz). High-Performance Liquid Chromatography (HPLC) was performed on an UltiMate 3000 from Thermo Scientific with a Rezex ROA Organic acid H+ (8%) column (7.8 × 150 mm) from Phenomenex, 12 mM H_2SO_4 (aq) as eluent at 0.6 ml/min. Column temperature was 40.0 °C, UV-detection was measured at 210 nm, 0.5 µL injection volume was used. Quantification was performed by calibration from pure products. Product elution times are: 3HB, 7.25 min; M3HB, 10.84 min; CA, 14.89 min; MC 29.63 min.

High-performance liquid chromatography-mass spectrometry (HPLC-MS) measurements were performed by connecting a LXQ linear ion trap to the ROA Organic acid 150x7.8 mm column. 3.4 M formic acid (aq) was used as eluent at room temperature. Gas chromatography-mass spectrometry (GC-MS) measurements were made using a Trace GC Ultra from Thermo Finnigan with a PolarisQ MS. GC-MS data were recorded using an initial temperature of 45°C for 1.8 min, ramping 50°/min to 250 °C.

Matrix-assisted laser desorption/ionization time-of-flight (MALDI-TOF) samples were prepared following an adapted literature procedure.[1] 10 mg dithranol was dissolved in 1 mL tetrahydrofuran (THF) as matrix and 10 mg LiBr was dissolved in 1 mL THF as ionizing agent. 10 µL from the reaction mixture, 20 µL from the matrix solution and 10 µL from the ionizing agent were mixed and 1 µL of the mixture was applied to a sample slide and air dried. Measurements were performed on an UltraFlextreme from Bruker Daltonics (Germany).

A.1.2 Pressure data
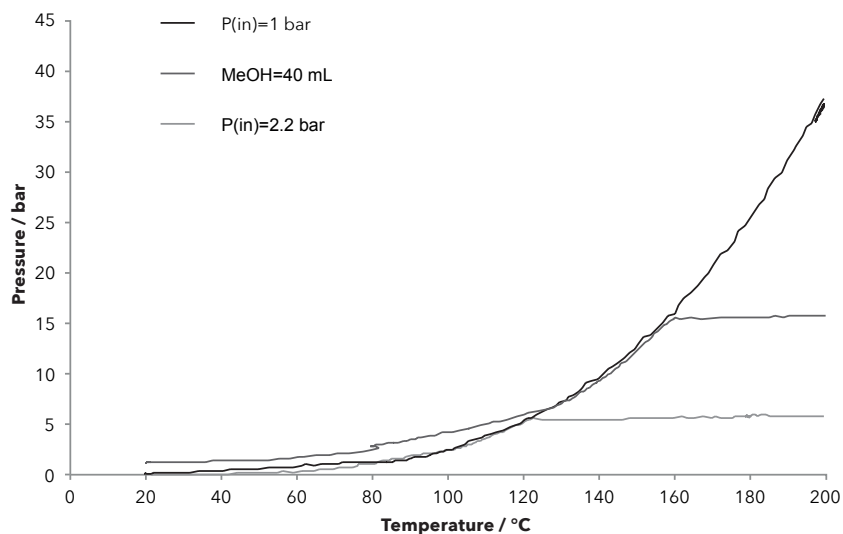
Figure A1. Pressure and temperature data from the reactors.

Comparing three different reaction set ups. One with 40 mL methanol (green) and two with 10 mL methanol (red and blue), where in the blue data set the initial pressure is increased to 2.2 bar by added nitrogen. When sufficient amounts of methanol are present, the line follows the vapour pressure of methanol (green line). When the amount of methanol is smaller at a certain point there is no more methanol present in the bottom of the reactor. Therefor heating the reactor has no further influence on the pressure of the system.

A.2 MALDI-TOF

A typical MALDI-TOF result is shown in Figure A2. As a reference, 600 mg PHB was added to 10 mL methanol and held at 100 °C for 67 hours. The remaining PHB (85% of the starting material) was filtered with a Büchner filter and the filtrate was measured by MALDI-TOF (Figure A3)
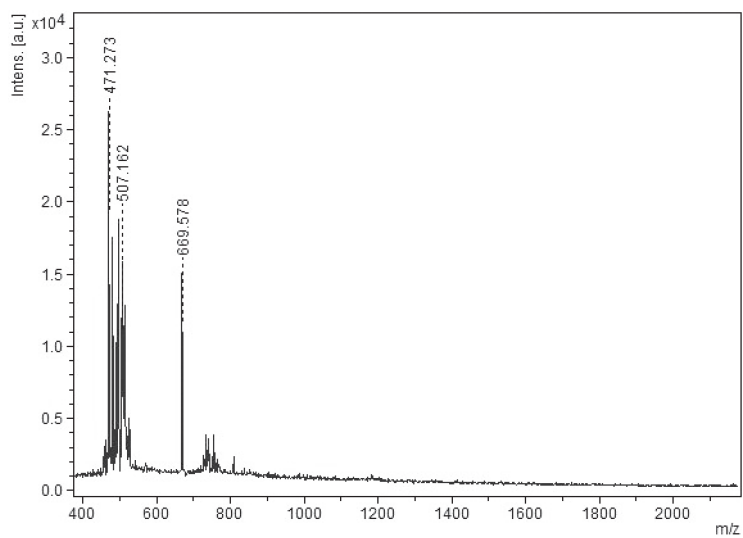
Figure A2. A typical MALDI-TOF result. Showing no indication of oligomers.
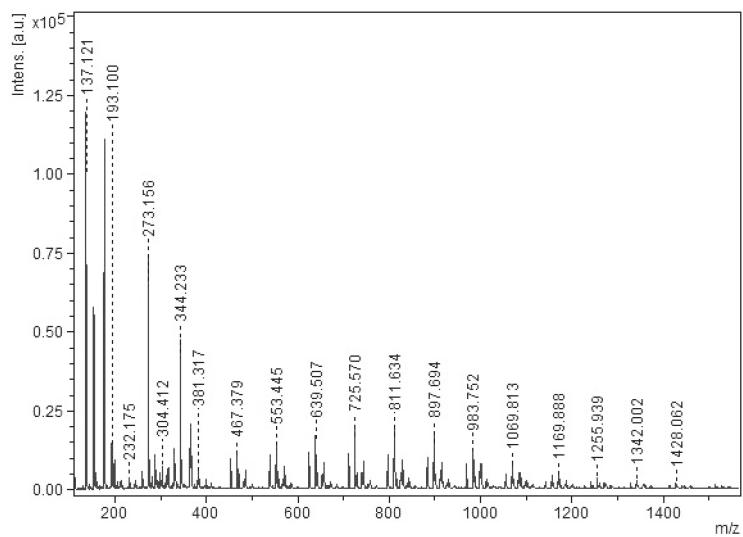
Figure A3. The MALDI-TOF result for the reference sample, showing oligomers up to n = 15.

A.3 REFERENCES

1.   Yu, G.-e.; Marchessault, R. H. *Polymer* **2000,** 41, 1087-1098.

Appendix B
Supplementary Information to Chapter 3

B.1 EXPERIMENTAL

All experiments were performed in duplicates in 75 mL Parr pressure reactors (Parr multiple reactor system series 5000, 6 X 75 mL, Hastelloy C-276) equipped with glass liners and glass-coated stirring bars. High-Performance Liquid Chromatography (HPLC) was performed on an UltiMate 3000 from Thermo Scientific with a Rezex ROA Organic acid H+ (8%) column (7.8 × 150 mm) from Phenomenex, 12 mM H2SO4 (aq) as eluent at 0.6 ml/min. Column temperature was 40.0 °C, UV-detection was measured at 210 nm, 0.5 µL injection volume was used. Quantification was performed by calibration from pure products. Product elution times are: 3HB, 7.25 min; M3HB, 10.84 min; CA, 14.89 min; MC 29.63 min. Nitrogen gas (Nitrogen 3.0, purity 99.9%) was supplied by Linde Gas Benelux. Methanol (HPLC gradient) was purchased from Actu-All Chemicals, CA (98%), methyl crotonate (98%), methyl (R)-(-)3-hydroxybutyrate (99%), and DL-3-hydroxybutyric acid (as sodium salt) were purchased from Sigma-Aldrich; PHB was kindly provided by Technical University Eindhoven (2 mol % Polyhydroxy valerate (PHV), Mn5450 kDa and Mw/Mn51.3); PHBV (20% valerate) was obtained from Tianan Biopolymer; PHB-rich cells from pilot plant, rich in *P. Acidivorans* was kindly provided by Delft University. All chemicals were used as received. Data visualization was aided by Daniel's XL Toolbox addin for Excel, version 6.60.

Starting material of 0.6 g was loaded in a glass liner with a glass-coated stirring bar. The liner was placed in a Parr reactor and methanol was added using a syringe. The reactor was closed, flushed with nitrogen and pressurized with nitrogen to the desired pressure at room temperature before heating was applied. The heating caused the pressure in the closed reactor to increase to the reported reaction pressure. Typical heating times up to 200 °C took place in 20–30 min. The reaction time started when the temperature reached 200 °C. After the allocated reaction time, the reactor was allowed to cool to room temperature before being opened. The dark brown solution was passed through a 0.20 µm single use filter unit and analysed by HPLC.

A

Table B1. Overview of detected products from PHBV:

Reaction time (h)	MC (%)	CA (%)	M3HB (%)
1	35	31	9
2	50	17	13
3	57	12	16
6	68	8	8

Reaction conditions: 0.6 g PHBV, P = 18 bar, T = 200 °C, 10 mL methanol. Average of duplicate experiments.

B.2 INFLUENCE OF MAGNESIUM
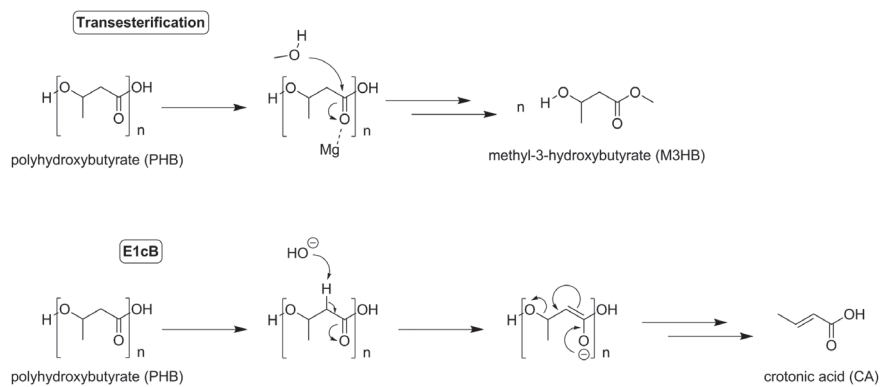
Figure B1. Influence of magnesium ion on the conversion of methyl crotonate.

# Appendix C
Supplementary Information to Chapter 4

C.1 ANALYSIS RESULTS

C.1.1 IR
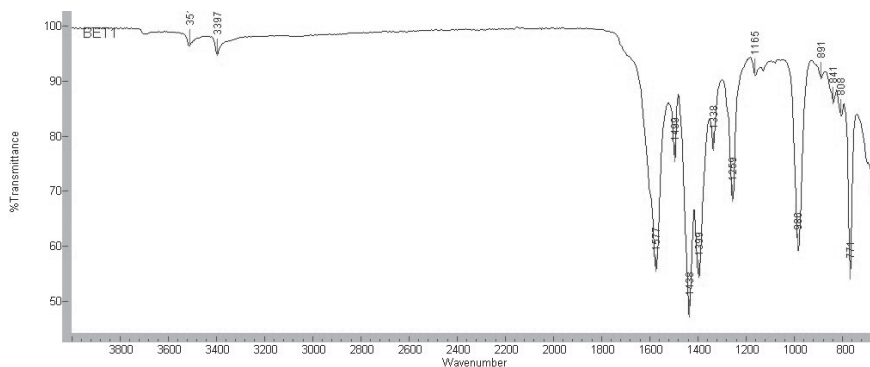
Figure C1. IR-spectrum of MIL-101-NH$_2$.
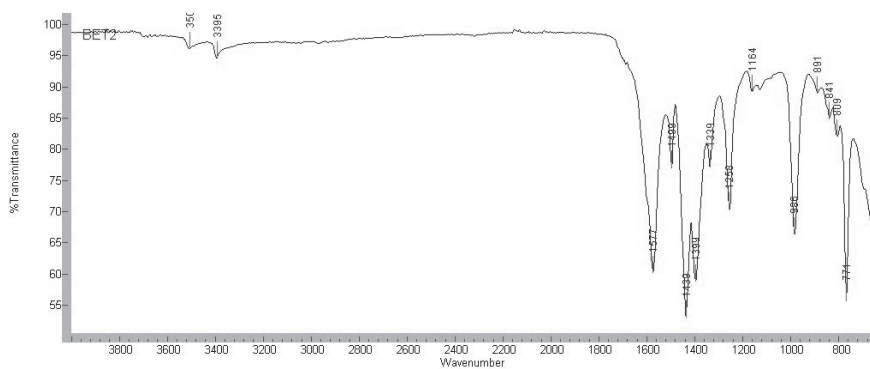
Figure C2. IR-spectrum of HG2@MIL-101-NH$_2$.

All other loaded and unloaded MOFs showed identical spectra as well.

C.1.2 PXRD
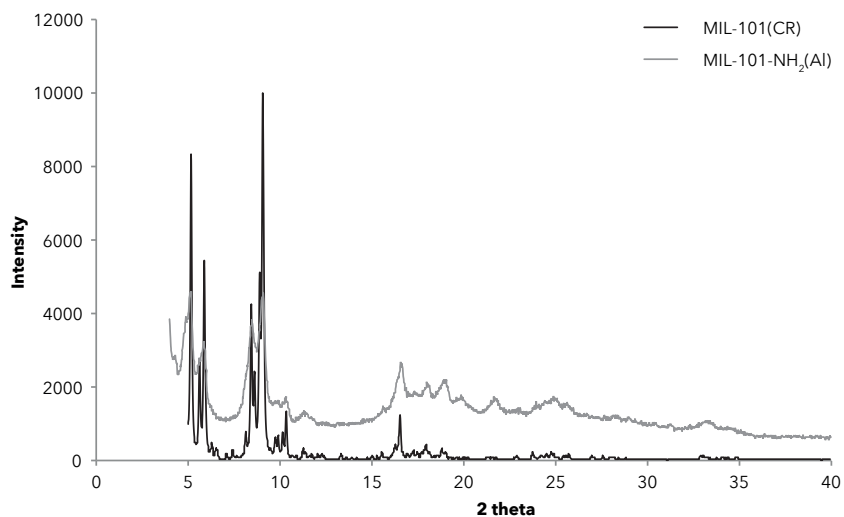
Figure C3. Calculated PXRD spectrum of MIL-101(Cr)[1] and measured spectrum of MIL-101-NH2(Al).

Table C1. Elemental analysis

Material	C (%)	H (%)	N (%)	Al (%)	Cl (%)
HG2@MIL-101-NH2(Al)(3)	39.34	3.42	5.54	9.53	1.23
Zhan@MIL-101-NH2(Al)(5)	39.61	3.44	5.66	9.86	1.81
MIL-53-NH2(Al)	41.64	3.88	5.75	11.15	0.16

C.1.4 Loading Calculation
0.25% ruthenium = 0.0025 g Ru / g MOF = 0.025 mmol Ru / g MOF.

Assuming all ruthenium originated from the HG2 catalyst, this equals 0.025 mmol HG2 / g MOF.

C.1.5 Scanning Electron Microscopy
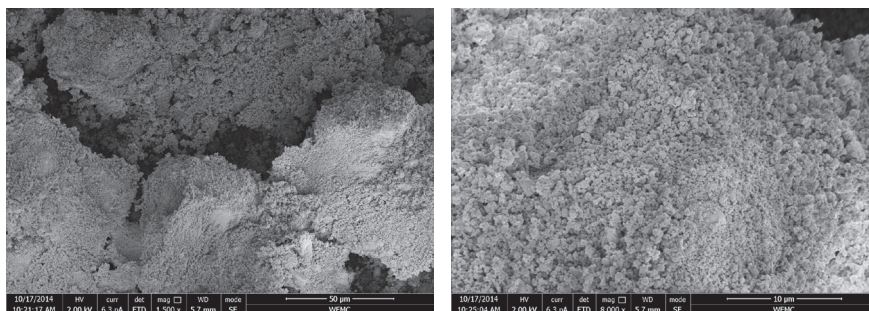
Figure C4. Scanning Electron Microscopy (SEM) images of HG2@MIL-101-NH2(Al).
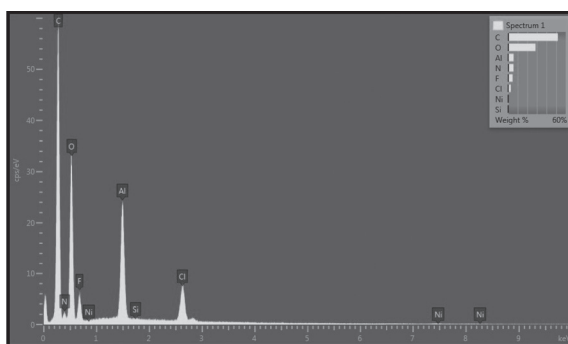
Figure C5. Backscattering pattern of HG2@MIL-101-NH2(Al). The expected ruthenium peak is overlapped by the chlorine peak and can not be observed.

C.2 REFERENCES

1.   Ferey, G.; Mellot-Draznieks, C.; Serre, C.; Millange, F.; Dutour, J.; Surble, S.; Margiolaki, I. Science 2005, 309, (5743), 2040-2.

A
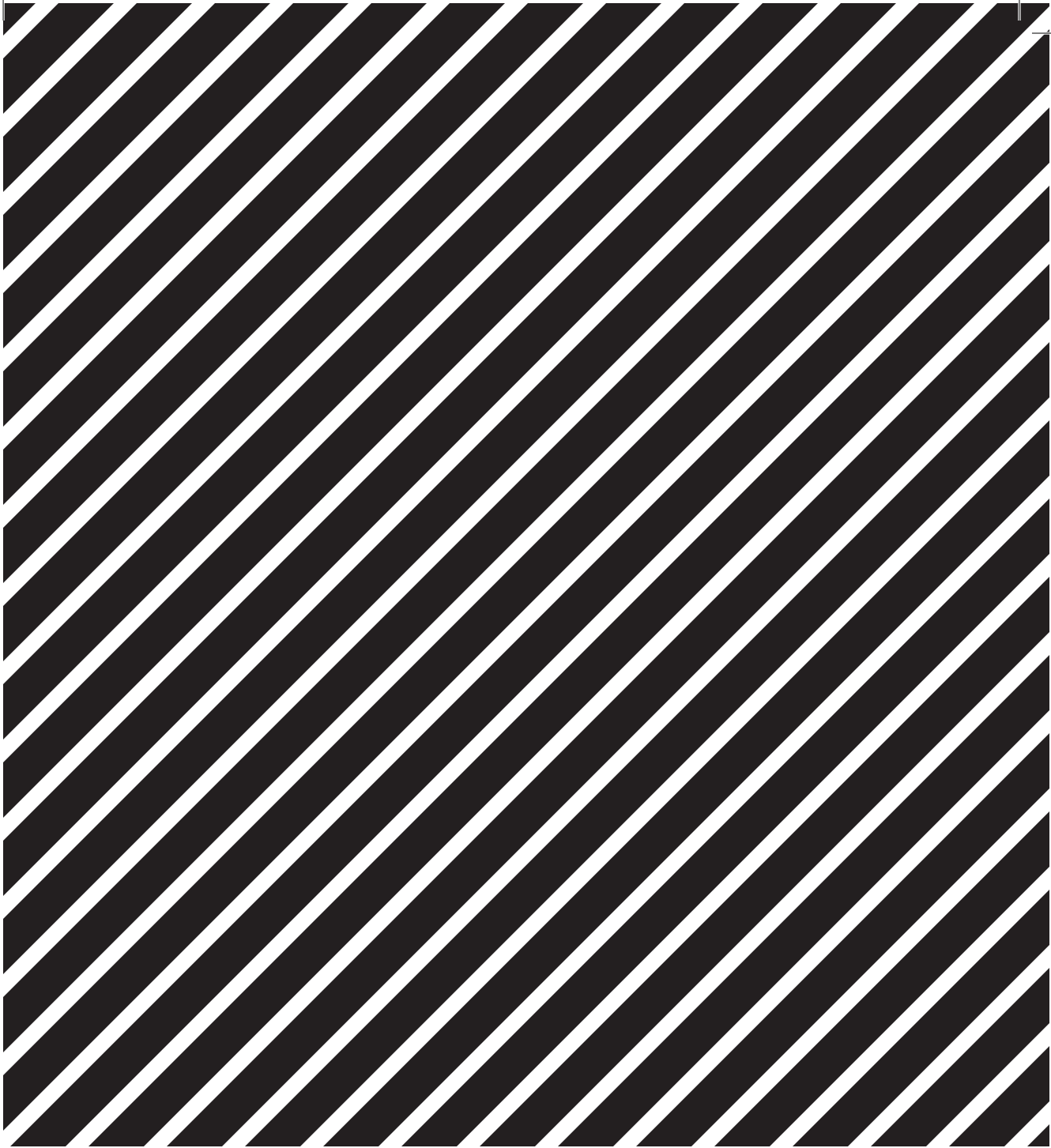
Summary

Currently, most chemicals and materials are obtained from fossil resources. After use, these chemicals and materials are converted to CO_2. As discussed in **chapter 1**, this causes a build-up of CO_2 in the atmosphere, the main driving force of global warming. In order to reach a sustainable system, biomass could be used as a resource for chemicals and materials instead. A biorefinery approach, where all parts of biomass are used to its full potential is essential. Taking this into consideration, wastewater streams of current biobased processes could be an excellent source for chemicals and materials. However, wastewater is often dilute and heterogeneous of nature. To overcome these challenges, wastewater rich in carbon can be processed by microorganisms to obtain a biodegradable polyester, polyhydroxyalkanoate (PHA). However, the mechanical properties of this polymer make it unsuitable as polymeric material. Moreover, processing of PHA is challenging. To circumvent these issues, we propose a conversion of the inferior PHA to methyl acrylate and propylene (Figure 7.1) which can be used in current processing infrastructure. PHA rich cells are obtained from the purification of wastewater. The PHA obtained can be purified and converted to methyl crotonate (MC) (Figure 7.1, chapter 2) or the PHA rich cells can be used directly (Figure 7.1, chapter 3). For the second step, the conversion of MC to methyl acrylate and propylene, the catalyst was immobilised (Figure 7.1, chapter 4). The current state of ethenolysis reaction on biomass was reviewed (Figure 7.1, chapter 5). The conversion of PHA to methyl acrylate and propylene enables the use of carbon from wastewater streams without the disadvantages related to the direct use of PHA.

In **chapter 2,** the first step of the conversion of PHA to methyl acrylate and propylene was investigated. Since PHA obtained from wastewater exists mostly as polyhydroxybutyrate (PHB), this was chosen as a starting material for our studies. It was shown that PHB could be converted to MC using methanol at 200 °C. MC has the advantage of being immiscible with water, which aids its separation. In chapter 2, the pathway of the reaction was clarified, which was subsequently used to optimise the conditions of this conversion. The conversion of PHB to MC proceeds *via* a thermolysis to crotonic acid (CA), which is followed by an esterification to MC. The formation of CA is the rate determining step below 18 bar, where above 18 bar this changes to the esterification to MC. A selectivity of 60% to MC is obtained with a full conversion of PHB with 18 bar being the optimal pressure for the conversion.

Microorganisms produce PHA within their cells, which poses challenges to the downstream processing of PHA as the material has to be isolated from within the cells and dried. The isolation and drying of PHA is costly and is responsible for a large part of the production costs of PHA. In order to reduce the costs of PHA for the production of biobased chemicals, the conversion of PHA to MC was tested using whole cells. In **chapter 3**, PHA rich cells were directly converted to MC using the optimised conditions found in chapter 2. The influence of fermentation salts, water and the presence of valerate monomers in the PHA were studied. It was found that the valerate monomers have no influence on the conversion. Fermentation salts do influence the conversion depending on the salt. Magnesium hydroxide catalyses the conversion of PHB to MC, where magnesium sulphate catalyses the formation of methyl 3-hydroxybutyrate as side product. The reaction tolerates up to 20% water, which means that the drying step in the downstream processing of PHA can be significantly reduced.

The second step of the conversion of PHA to methyl acrylate and propylene involves an ethenolysis, a cross metathesis of MC with ethylene. This ethenolysis reaction requires a homogeneous catalyst. One of the most active catalysts for this conversion is the ruthenium based Hoveyda-Grubbs 2nd generation. However, the required high loading of this catalyst makes it an expensive part of the conversion. In order to enable reusing of the catalyst, immobilisation of the Hoveyda-Grubbs catalyst was investigated in **chapter 4**. The catalyst was immobilised inside a metal organic framework (MOF). For this purpose MIL-101-NH_2(Al) was used for its large cavities connected by small openings. This allows the catalyst to reside inside the cavities, while the small openings prevent it from leaching out. The catalyst was successfully immobilised using a mechanochemical approach. This method can be applied on other catalysts as well, which was shown by the immobilisation of Zhan catalyst. Both immobilised catalysts show metathesis activity for multiple reaction cycles. It was found that the MOF, MIL-101-NH_2(Al), partially undergoes a structural change to form MIL-53-NH_2(Al). When MIL-53-NH_2(Al) was used as starting MOF the catalyst was trapped but inactive. It was concluded that when starting from MIL-101-NH_2(Al), the catalyst trapped in the parts of the material that was converted to MIL-53-NH_2(Al) are catalytically inactive.

To investigate the current state of the art of the use of ethenolysis on biomass, a literature review was performed in **chapter 5**. The results of the ethenolysis of methyl oleate (MO) were compared in order to investigate the most important parameters. It was found that the purity of the ethylene feed has the biggest influence on the turn over numbers (TONs) and that a higher purity ethylene has shown a larger impact on the ethenolysis of MO than the development of novel catalysts. When electron poor substrates are used, the highest TONs are obtained with the less stable Hoveyda-Grubbs 2nd generation. However, no studies were performed on the influence of ethylene purity on these reactions and higher TONs may be achieved using a higher purity ethylene.

In **chapter 6**, the results and conclusions of the thesis are summarised. The implications of these findings are discussed and suggestions for further research within the field are given.
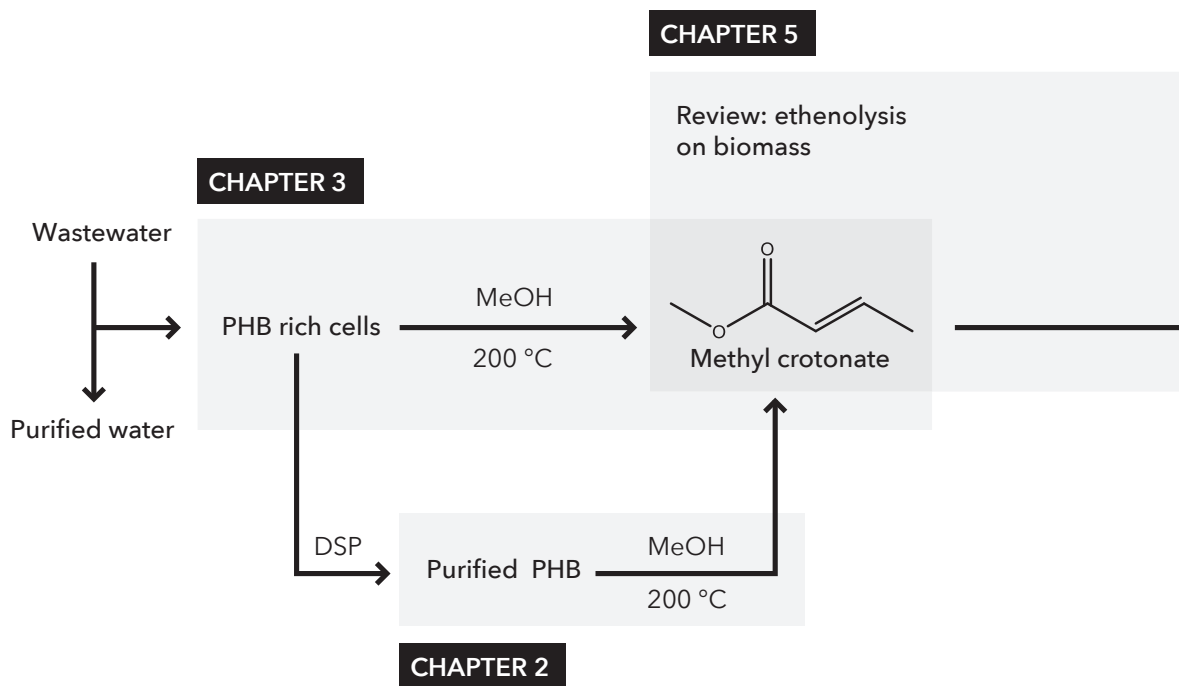
Figure 7.1. Overview of the thesis.

Other biobased substrates —————Ethenolysis————→ Products

Ethylene
————————————————————→   Methyl acrylate **+** Propylene
Metathesis catalyst
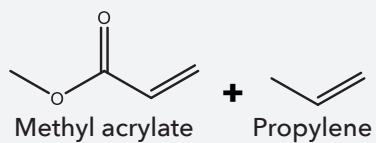
Immobilisation of catalyst
In metal organic frameworks

CHAPTER 4
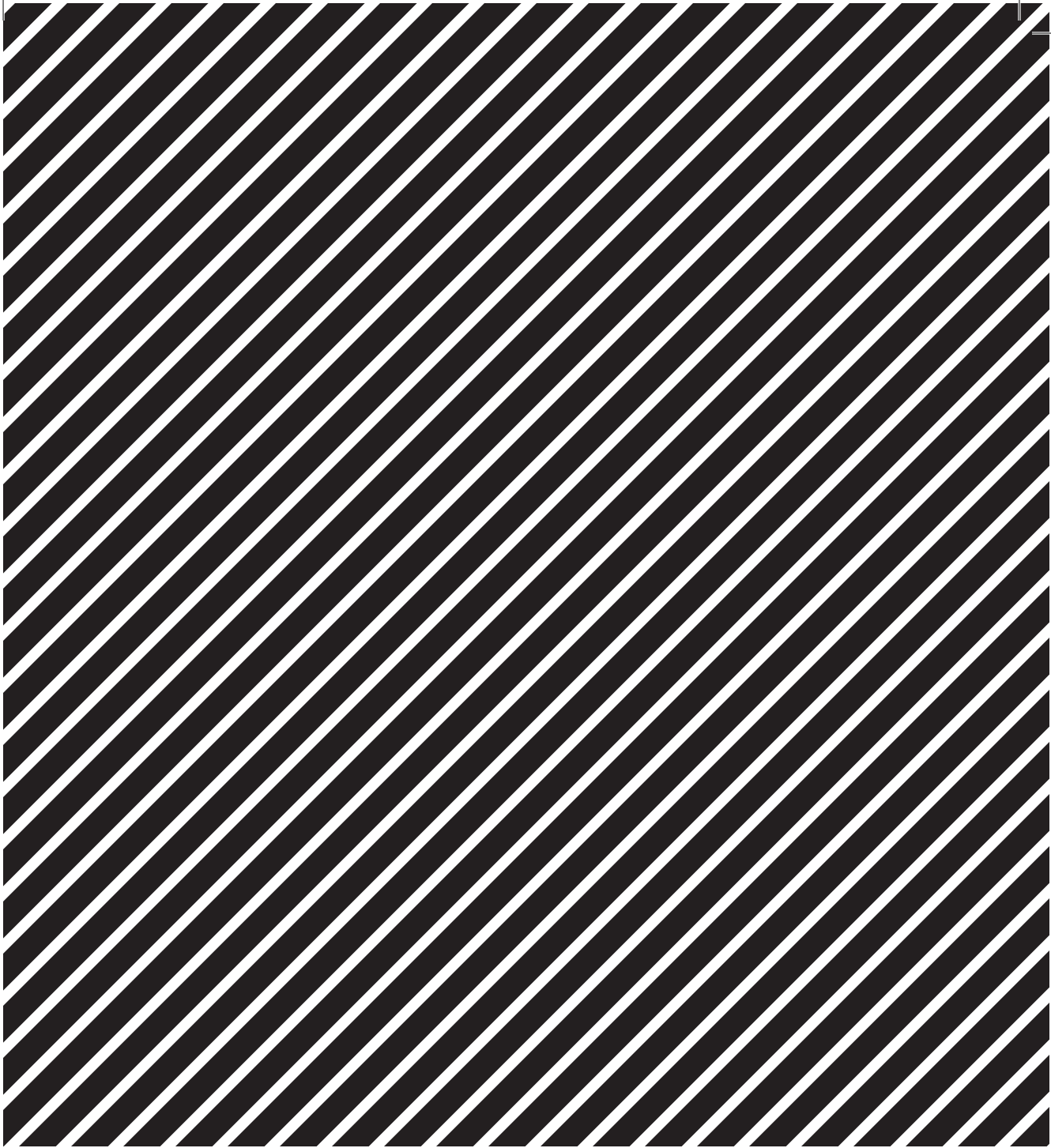
Acknowledgments

Een PhD traject doorloop je niet alleen en er zijn veel mensen die hebben bijgedragen in de totstandkoming van deze thesis. Op deze pagina's wil ik een poging doen om al deze mensen te bedanken.

Als eerst wil ik mijn promotor **Johan** bedanken. Niet alleen voor alle inzet en begeleiding, maar vooral ook voor het bodemloze geloof in mijn kunnen en voor de inspirerende visie op een duurzame toekomst, die je niet alleen verwoord, maar ook actief probeert te verwezenlijken. Vervolgens wil ook graag **Elinor** bedanken voor alle jaren samenwerken. Je hebt mij gestuurd om te ontwikkelen van student tot wetenschapper en ik heb in de afgelopen jaren veel geleerd.

I was lucky enough to have three supervisors and even more lucky that **Jérôme** was my third supervisor. I admire the way you had an open door policy and always had time for great brainstorming sessions. Next to that you proved irreplaceable in the lab and you thought me many practical tips and tricks. I noticed that when I am guiding students myself, I try to follow your example.

Als laatste begeleider wil ik **Harry** bedanken. Jouw late toevoeging aan mijn thesis had misschien weinig impact in de richting die we zijn opgegaan, maar het heeft zeker geholpen met de diepgang van de wetenschappelijke kant van mijn thesis.

I would like to thank **Lars** for his efforts during the three months of my PhD in Gothenburg and making it possible for me to experience living in Sweden during this time. Your calm way of explaining and positive approach to science contributed to a great time in Sweden during this internship, which made it an easy decision to go back for a post-doc.

Tijdens mijn PhD traject heb ik ook studenten mogen begeleiden die allebei uitstekend werk hebben verricht en daarom wil ik ook **Irene en Juan** bedanken voor het kiezen van mijn project en al het labwerk dat jullie hebben verricht.

Behalve mijn begeleiders en studenten zijn er een aantal mensen in de vakgroep die een apart dankwoord verdienen. **Susan**, met jou inzet, geduld en kennis van de analyse methoden kan ik me geen betere hulp bedenken bij het analyseren van mijn reactiemengsels. **Gerda**, jij bent de afgelopen jaren een cruciaal onderdeel van de groep gebleken. Ondanks alle taken staat jou deur nog steeds altijd open en heb je antwoord op elke vraag wat resulteert in de gezegde "Gerda weet alles". **Tomas**, jou vraag over druk opbouw bleek cruciaal en je kennis over gassen en BET oppervlakken hebben mij erg geholpen om mijn processen te begrijpen. **Annemarie**, met jou inzet, vooral bij het meten van het BET oppervlak, kon ik op tijd mijn experimenten afronden.

Everybody in VPP/BCH/BCT helped towards creating an open and pleasant working atmosphere and I enjoyed the breaks and the random chats in the hallway with all of you. **Gwen**, I enjoyed the depth of our conversations and I did not expect to learn about language and computers in that much detail. **Chen**, I have learned a lot about China during our discussions and I liked my two trips to China that you helped made possible. **Teng**, it was great to have somebody else passionate about Groningen in the group and it was a fun experience to be your paranymph.

Yessie, I also enjoyed the honour of being your paranymph and it was again a great experience. **Yu and Daniel**, it took a while to get used to sharing my office with modelers, but this lead to very interesting discussions and I even regained some of my interest for mathematics. However, part of this renewed interest is thanks to **Elvira**. I also want to thank everybody from Wageningen UR who were in some way involved in my PhD. Either helping with the science or for the social aspect of my PhD, **Marieke, Ruud, Astrid, Gerard, Karel, Kees, Piet, Rachel, Ton, Ellen, Jan-Eise, Neus, Rani, Ischa, Kiira, Pascal, Pauline, Youri, Farnoosh, Luana, Marja, Nathan, Nik, Nurul, Piet, Pom, Roxani, Sanne, Frits, Guus and Linda.** You all helped making my PhD four great years of my life.

Efter min doktorand, jag har blivit post-doc i Sverige och jag vill gärna säga tack till **alla kompisar från Chalmers**. Tack för läsa och göra bättre min avhandling och tack för en kanonbra tid. En specialt tack för **Linda** för tar min bild.

Naast iedereen op het werk wil ik ook mijn paranimfen **Jelle en Jorrit** bedanken voor hun, ongetwijfeld, geweldige inzet en hulp tijdens mijn verdediging. Bovendien wil ik **Mike** bedanken voor het schitterende ontwerp voor de omslag.

Ook wil ik al mijn vrienden en familie bedanken voor alle steun en vertrouwen, tijdens mijn PhD, maar ook vooral tijdens mijn studietraject dat tot mijn PhD leidde. Met name **Joris, Tessa, Jacobien, Finnley, Janneke, Marieke, Thomas, papa en mama**.

Și, ultimul, eu vreau să mulțumesc **Andrada**. Cu tine, tot este mai bună.
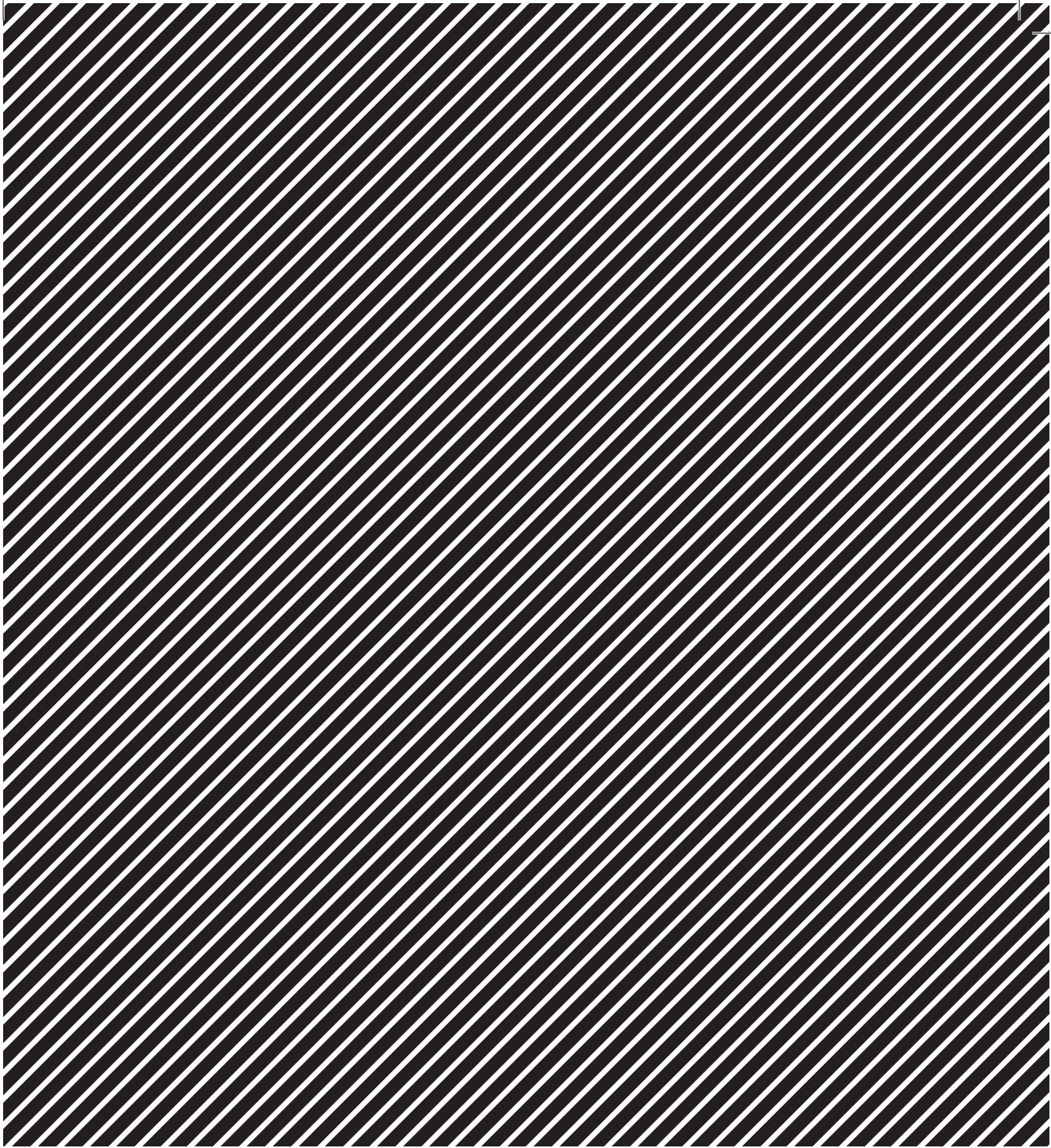
About the author

Curriculum Vitae

Jurjen Spekreijse was born on 1 March 1987 in Leeuwarden and shortly after he moved to Kûbaard. In 2005 he obtained his gymnasium degree at RSG in Sneek in order to study Chemistry at the University of Groningen. After writing a bachelor thesis on silver cyanide based metal organic frameworks, he obtaining his bachelor in chemistry in 2009. For his master thesis he investigated the ethenolysis on electron poor double bonds for the production of biobased chemicals at Wageningen University, which resulted in his Master degree in Organic and Molecular Inorganic Chemistry from the University of Groningen in 2011. The results of this study were published in *Green Chemistry*. During his master degree he became passionate about the production of biobased chemicals. This lead to a PhD position on the production of biobased chemicals from polyhydroxybutyrate and this thesis. Currently, he works as a post-doc on the synthesis of biobased metal organic frameworks at Chalmers University.

Publications

Bio-derived olefin synthesis, J.P.M. Sanders, J. Van Haveren, E. Scott, D.S. Van Es, J. Le Nôtre, J. Spekreijse, *US Patent*, 13/381,644, **2010**

Simultaneous production of biobased styrene and acrylates using ethenolysis, J. Spekreijse, J. Le Nôtre, J. Van Haveren, E.L. Scott, J.P.M. Sanders, *Green Chemistry*, 14, 10, **2012**, 2747-2751

Conversion of polyhydroxybutyrate (PHB) to methyl crotonate for the production of biobased monomers, J. Spekreijse, J. Le Nôtre, J.P.M. Sanders, E.L. Scott, *Journal of Applied Polymer Science*, 132, 35, **2015**

Conversion of polyhydroxyalkanoates to methyl crotonate using whole cells, J. Spekreijse, J.H. Ortega, J.P.M. Sanders, J.H. Bitter, E.L. Scott, *Bioresource Technology*, 211, **2016**, 267-272

Overview of completed training activities

DISCIPLINE SPECIFIC COURSES AND ACTIVITIES

Renewable Resources in Bulk Chemistry, Wageningen, **2011**

Catalysis, An Integrated Approach, Ameland, **2011**

Statistiek 2, Wageningen, **2013**

NCCC XIII, XV & XVI, Noordwijkerhout, **2012, 2014, 2015**

CCESC, Madrid, Spain, **2013**

ISOM, Nara, Japan, **2013**

Science & Technology Day, Gothenburg, Sweden, **2014**

Organikerdagarna, Stockholm, Sweden, **2014**

GENERAL COURSES

Effective behaviour, Wageningen, **2012**

Competence assessment, Wageningen, **2012**

Techniques for writing and presenting scientific papers, Wageningen, **2012**

Interpersonal communication, Wageningen, **2013**

Interdisciplinary research, Wageningen, **2013**

Didactic Skills, Wageningen, **2013**

Teaching as a profession, Wageningen, **2014**

Career Perspective, Wageningen, **2015**

OTHER

Preparation of research proposal, **2011**

Meetings VPP/BCH/BCT, **2011-2015**

STW users committee meeting, **2011-2015**

Summer school, Schiermonnikoog, **2012**

Organisation of PhD trip, Brazil, **2013**

Participant of PhD trip, China, **2015**